

NASA/TM–20230000313



Multicopter Test Bed Load and Stress Analysis

*Sarah Conley
Ames Research Center, Moffett Field, California*

February 2023

NASA STI Program ... in Profile

Since its founding, NASA has been dedicated to the advancement of aeronautics and space science. The NASA scientific and technical information (STI) program plays a key part in helping NASA maintain this important role.

The NASA STI program operates under the auspices of the Agency Chief Information Officer. It collects, organizes, provides for archiving, and disseminates NASA's STI. The NASA STI program provides access to the NTRS Registered and its public interface, the NASA Technical Reports Server, thus providing one of the largest collections of aeronautical and space science STI in the world. Results are published in both non-NASA channels and by NASA in the NASA STI Report Series, which includes the following report types:

- **TECHNICAL PUBLICATION.** Reports of completed research or a major significant phase of research that present the results of NASA Programs and include extensive data or theoretical analysis. Includes compilations of significant scientific and technical data and information deemed to be of continuing reference value. NASA counter-part of peer-reviewed formal professional papers but has less stringent limitations on manuscript length and extent of graphic presentations.
- **TECHNICAL MEMORANDUM.** Scientific and technical findings that are preliminary or of specialized interest, e.g., quick release reports, working papers, and bibliographies that contain minimal annotation. Does not contain extensive analysis.
- **CONTRACTOR REPORT.** Scientific and technical findings by NASA-sponsored contractors and grantees.

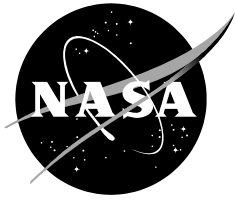
- **CONFERENCE PUBLICATION.** Collected papers from scientific and technical conferences, symposia, seminars, or other meetings sponsored or co-sponsored by NASA.
- **SPECIAL PUBLICATION.** Scientific, technical, or historical information from NASA programs, projects, and missions, often concerned with subjects having substantial public interest.
- **TECHNICAL TRANSLATION.** English-language translations of foreign scientific and technical material pertinent to NASA's mission.

Specialized services also include organizing and publishing research results, distributing specialized research announcements and feeds, providing information desk and personal search support, and enabling data exchange services.

For more information about the NASA STI program, see the following:

- Access the NASA STI program home page at <http://www.sti.nasa.gov>
- E-mail your question to help@sti.nasa.gov
- Phone the NASA STI Information Desk at 757-864-9658
- Write to:
NASA STI Information Desk
Mail Stop 148
NASA Langley Research Center
Hampton, VA 23681-2199

NASA/TM–20230000313



Multicopter Test Bed Load and Stress Analysis

*Sarah Conley
Ames Research Center, Moffett Field, California*

National Aeronautics and
Space Administration

*Ames Research Center
Moffett Field, CA 94035-1000*

February 2023

ACKNOWLEDGMENTS

The author would like to thank the following people for their contributions to this project. First, the author would like to thank the principal investigator Carl Russel for giving Sarah a challenging and rewarding project and for being an amazing mentor and project lead. Gina Willink, lead of the Ames Aeromechanics Mechanical Systems Team, helped throughout the design process, reviewed the design and analysis, and provided invaluable advice. The NASA Machine Shop Team, led by Robert Kornienko and Vincent Derilo, machined the parts of the MTB and provided guidance and helpful suggestions during the design process. Thank you to William Warmbrodt for his continued outstanding leadership and to Tom Norman for invaluable guidance and assistance. Additionally, the author would like to mention that the first wind tunnel test of the MTB would not have been a success without the many hours put in by the U.S. Army 7- by 10-ft Wind Tunnel crew, particularly Gary Fayaud, Bruce Gesek, Steve Nance, Dan Pruyn, and Jiawei Toh. This work was primarily funded by NASA's Revolutionary Vertical Lift Technology (RVLT) Project, with seed funding from the NASA Ames FY18 Internal Research and Development Fund.

Available from:

NASA STI Support Services
Mail Stop 148
NASA Langley Research Center
Hampton, VA 23681-2199
757-864-9658

National Technical Information Service
5301 Shawnee Road
Alexandria, VA 22312
webmail@ntis.gov
703-605-6000

This report is available in electronic form at

<http://ntrs.nasa.gov>

TABLE OF CONTENTS

LIST OF FIGURES.....	iv
LIST OF TABLES.....	iv
DEFINITIONS AND ACRONYMS	ix
NOMENCLATURE FOR BOLT ANALYSIS.....	x
FORMULAS FOR BOLT CALCULATIONS:.....	xi
1. PROJECT SCOPE	1
2. REQUIREMENTS	1
3. MATERIALS	1
4. SUMMARY OF RESULTS	4
5. DESIGN.....	8
OVERVIEW OF THE MTB	8
5.1 Strongback Assembly	9
5.2 Strut Assembly	10
5.3 Beam System	12
5.4 Rotor Assembly	18
5.5 Installation Assembly	22
6. LOAD AND STRESS ANALYSIS	24
6.1 Strongback Assembly Analysis.....	24
6.2 Strut Assembly Analysis	31
6.3 Beam System Analysis	59
6.4 Rotor Assembly Analysis	70
6.5 Installation Assembly	81
6.6 Blade Out FEA.....	85

LIST OF FIGURES

Figure 5.1.	MTB assembly side view.....	8
Figure 5.1.1.	Isometric view of strongback.....	9
Figure 5.2.1.	View of strut assembly.	10
Figure 5.2.2.	Close up view of top of strut assembly.....	11
Figure 5.3.1.	Isometric view of lateral beam system. (Older model).....	13
Figure 5.3.2.	Front view of small gap with 24-inch diameter propellers. (Older model).....	13
Figure 5.3.3.	Front view of large gap with 24-inch diameter propellers. (Older model).....	14
Figure 5.3.4.	View of gap between lateral support beam and vertical support beam.	14
Figure 5.3.5.	View of transparent adjusting L-bracket in shortest position. (Older model).....	15
Figure 5.3.6.	View of transparent adjusting L-bracket, fully extended. (Older model).....	15
Figure 5.3.7.	Front (right) and back (left) view of vertical beam system in medium height configuration. (Updated image).....	16
Figure 5.3.8.	Front view of front right rotor assembly at minimum height of 12.36 inches (dimensions correct, model outdated).	17
Figure 5.3.9.	Front view of front right rotor assembly at maximum height of 21.24 inches (dimensions correct, model outdated).	17
Figure 5.4.1.	View of rotor assembly.....	18
Figure 5.4.2.	Close up view of the top of the rotor assembly.	19
Figure 5.4.3.	Close up side view of bottom of rotor assembly in short (left) and tall (right) configurations.	20
Figure 5.4.4.	Motor-load cell interface.	21
Figure 5.5.1.	Installation assembly.....	22
Figure 5.5.2.	Exploded view of installation assembly.	23
Figure 6.1.1.	Strongback Study 1 – FEA stress plot.	25
Figure 6.1.2.	Strongback Study 2 – FEA stress plot.	26

Figure 6.1.3.	Strongback Study 3 – FEA stress plot.	27
Figure 6.1.4.	Strongback Study 4 – FEA stress plot.	28
Figure 6.1.5.	Strongback Study 5 – FEA stress plot.	29
Figure 6.2.1.	Strut assembly in pitched configuration when strongback rotation is 20 degrees forward without propeller load.	31
Figure 6.2.2.	Schematic of strut assembly in pitched configuration when strongback rotation is 20 degrees forward with propeller load.	32
Figures 6.2.3 and 6.2.4.	Distance from the wind tunnel ceiling for zero-degrees rotor rotation.	34
Figures 6.2.5 and 6.2.6.	Distance from the wind tunnel ceiling for 45-degrees rotor rotation. Left - strongback rotation 30 degrees forward. Right - strongback rotation 20 degrees forward.	36
Figures 6.2.7 and 6.2.8.	Distance from the wind tunnel ceiling for 90-degrees rotor rotation. Left - strongback rotation 20 degrees forward. Right - strongback rotation 30 degrees forward.	38
Figures 6.2.9 and 6.2.10.	Distance from the wind tunnel ceiling for -10-degrees rotor rotation. Left - strongback rotation 30 degrees forward. Right - strongback rotation 20 degrees forward.	39
Figure 6.2.11.	Schematic of MTB with zero-degrees strongback rotation and 90-degree rotor rotation.	40
Figure 6.2.12.	Schematic of MTB with 22-degrees strongback rotation and 90-degrees rotor rotation – Calculation 2.	41
Figure 6.2.13.	Close up schematic of MTB with 22-degrees strongback rotation and 90- degrees rotor rotation – Calculation 2.	42
Figure 6.2.14.	Schematic of MTB with zero-degrees strongback rotation and -10-degrees rotor rotation – Calculation 3.	43
Figure 6.2.15.	Schematic of MTB with -13.6-degrees strongback rotation and -10-degrees rotor rotation – Calculation 3.	44
Figures 6.2.16 and 6.2.17.	Close up schematics of MTB with -13.6-degrees strongback rotation and -10-degree rotor rotation. Left - view of pitching mechanism. Right - view of rotor.	45
Figure 6.2.18.	Strut Assembly Study 1 – strongback support interface, FEA stress plot.	47

Figure 6.2.19. Strut Assembly Study 2 – upstream stopper, FEA stress plot.	48
Figure 6.2.20. Strut Assembly Study 3 – downstream stopper, FEA stress plot.	49
Figure 6.2.21. Strut Assembly Study 4 – designed lug, FEA stress plot.	50
Figure 6.2.22. Strut Assembly Study 5 – bottom strut clevis, FEA stress plot.	51
Figure 6.2.23. Strut Assembly Study 6 – top strut clevis, FEA stress plot.	52
Figure 6.2.24. Strut Assembly Study 7 – large hinge, FEA stress plot.	53
Figure 6.2.25. Strut Assembly Study 8 – strut washer, FEA stress plot.	54
Figure 6.3.1. Beam Assembly Study 1 – adjusting L-bracket, FEA stress plot with close-up view of L-bracket on left.	60
Figure 6.3.2. Beam Assembly Study 2 – adjusting L-bracket, FEA stress plot with close-up view of L-bracket on left.	61
Figure 6.3.3. Beam Assembly Study 3 – adjusting L-bracket, FEA stress plot with close-up view of L-bracket on left.	62
Figure 6.3.4. Beam Assembly Study 4 – adjusting L-bracket, FEA stress plot with close-up view of L-bracket on left.	63
Figure 6.3.5. Beam Assembly Study 5 – vertical support beam, FEA stress plot with close-up view of beam on left.	64
Figure 6.3.6. Beam Assembly Study 6 – vertical support beam, FEA stress plot with close-up view of beam on left.	65
Figure 6.3.7. Beam Assembly Study 7 – vertical support beam, FEA stress plot with close-up view of beam on left.	66
Figure 6.3.8. Beam Assembly Study 8 – vertical support beam, FEA stress plot with close-up view of beam on left.	67
Figure 6.3.9. Beam Assembly Study 9 – lateral support beam, FEA stress plot.	68
Figure 6.3.10. Beam Assembly Study 10 – lateral support beam, FEA stress plot.	69
Figure 6.4.1. Schematic of rotor assembly – Calculation 4.	70
Figure 6.4.2. Rotor Assembly Study 1 – clevis interface, FEA stress plot.	72

Figure 6.4.3.	Rotor Assembly Study 2 – bottom prop clevis, FEA stress plot.	73
Figure 6.4.4.	Rotor Assembly Study 3 – custom linear actuator mount, right, FEA stress plot.	74
Figure 6.4.5.	Rotor Assembly Study 4 – linear actuator top clevis, FEA stress plot.	75
Figure 6.4.6.	Rotor Assembly Study 5 – bottom actuator interface, FEA stress plot.	76
Figure 6.5.1.	Installation Assembly Study 1 – gearbox-pillow block interface, FEA stress plot.	82
Figure 6.5.2.	Installation Assembly Study 2 – pillow block, FEA stress plot.	83
Figure 6.6.1.	Blade Out Study 1 – vertical support beam, helicopter, FEA stress plot.	86
Figure 6.6.2.	Blade Out Study 2 – vertical support beam, helicopter, FEA stress plot.	87
Figure 6.6.3.	Blade Out Study 3 – vertical support beam, airplane, FEA stress plot.	88
Figure 6.6.4.	Blade Out Study 4 – vertical support beam, airplane, FEA stress plot.	89
Figure 6.6.5.	Blade Out Study 5 – adjusting L-bracket, airplane, stress plot.	90
Figure 6.6.6.	Blade Out Study 6 – adjusting L-bracket, airplane, stress plot.	91
Figure 6.6.7.	Blade Out Study 7 – adjusting L-bracket, helicopter, stress plot.	92
Figure 6.6.8.	Blade Out Study 8 – adjusting L-bracket, helicopter, stress plot.	93

LIST OF TABLES

Table 1.	Material properties of 17-4PH H900 stainless steel.	2
Table 2.	Material properties of AISI 4130 heat treated to 180 ksi	2
Table 3.	Material properties of 13-8PH H950 stainless steel.	2
Table 4.	Material properties of 15-5PH H1150 stainless steel.	3
Table 5.	Maximum loads for safety of flight.	5
Table 6.	Safety factor summary.	7
Table 7.	Flat, no rotation of rotors, helicopter mode.	34
Table 8.	Rotors rotated 45 degrees forward.....	35
Table 9.	Rotors rotated 90 degrees forward, airplane mode.	37
Table 10.	Rotors rotated 90 degrees forward, airplane mode.	39
Table 11.	Force through linear actuator – Calculation 4	71

DEFINITIONS AND ACRONYMS

MTB	Multicopter Test Bed
FEA	Finite Element Analysis
eVTOL	Electric Vertical Take-Off and Landing
SF	Safety Factor
rpm	Revolutions Per Minute
ksi	1000 pounds per square inch

NOMENCLATURE FOR BOLT ANALYSIS

n	Number of Bolts
v	Shear Force (lb)
m	Moment (in-lb)
T	Tensile Force
r	Resultant (in)
d	Bolt Diameter (in)
b	Threads per Inch
L	Length of Engagement
σ_{UTS}	Ultimate Tensile Strength (psi)
SB	Breaking Strength
A_t	Tensile Area (in ²)
A_s	Shear Area (in ²)
F'	Direct Load (lbs/bolt)
F''	Moment Load (lb/bolt)
F	Total Shear Load (lb)
τ	Shear Stress (psi)
σ	Tensile Stress (psi)
σ_{vm}	Von Mises Stress (psi)

FORMULAS FOR BOLT CALCULATIONS:

$$A_t = \frac{\pi}{4} \left(d - \frac{0.9743}{b} \right)^2$$

$$A_s = \frac{\pi}{2} \left(d - \frac{0.64952}{b} \right) * L$$

$$F' = \frac{v}{n}$$

$$F'' = \frac{m}{nr}$$

$$F \text{ (worst case)} = F' + F''$$

$$\tau = \frac{4 F}{3 A_s}$$

$$\sigma = \frac{T}{n A_t}$$

$$\sigma_{vm} = \sqrt{\sigma^2 + 3\tau^2}$$

$$SF = \frac{\sigma_{UTS}}{\sigma_{vm}}$$

1. PROJECT SCOPE

The Multirotor Test Bed (MTB) is a new capability for testing a wide array of advanced vertical take-off and landing (VTOL) rotor configurations, with a primary focus on testing in the U.S. Army 7- by 10-Foot Subsonic Wind Tunnel at NASA Ames Research Center. The MTB was designed to allow adjustment of the vertical, lateral, and longitudinal placement of up to six rotors, as well as allow tilt adjustment of each rotor and pitch adjustment of the whole assembly. The six-axis load cells under each rotor give the MTB the capability of measuring the rotor performance in a wide array of configurations. The overall goal of the MTB project is to help gain a better understanding of the performance, control, interactional aerodynamics, and acoustics of multirotor and tilting-rotor systems.

The MTB project was initiated to build upon the knowledge and capabilities developed during the multirotor unmanned aerial systems (MUAS) tests in 2015 and 2017. By measuring individual rotor loads and allowing for adjustments to individual rotor position and attitude, the MTB provides a wealth of data on the aeroperformance of arbitrary multirotor configurations. The flexibility in positioning up to six rotors allows the multirotor design space to be parametrically explored and potentially optimized. The MTB is also at a larger scale than the small unmanned aerial systems (UAS) tested before, which allows for testing at rotor tip Reynolds numbers more relevant to full-scale piloted electric vertical take-off and landing (eVTOL) aircraft.

This document contains the complete documentation of the design, loads, and stress analysis of the MTB.

2. REQUIREMENTS

Per the National Full-Scale Aerodynamics Complex Operations Manual Test Planning Guide, a minimum safety factor is required for all components. The safety factor required over yield strength is 3 and over ultimate strength is 4. In addition, a safety factor greater than 1 is required for blade-out conditions.

3. MATERIALS

Besides the off-the-shelf parts, all manufactured parts will be one of four materials: 17-4PH H900, AISI 4130, 13-8PH H950, 15-5PH H1150. The specifications of the materials are described below:

17-4PH H900, ultimate strength 200 ksi (1000 pounds per square inch), yield strength 185 ksi.

AISI 4130 steel heat treated, ultimate strength 180 ksi, yield strength 160 ksi.

13-8PH H950, ultimate strength 220 ksi, yield strength 205 ksi.

15-5PH H1150, ultimate strength 135 ksi, yield strength 105 ksi.

Originally, the 4130 parts were to be annealed at 865 degrees Celsius and have a yield strength of 66.72 ksi. This is the yield strength used in the original load and stress analysis, but since the

materials have changed, the analysis has been updated with the correct material properties. Tables 1 through 4 show the material properties for all the materials used in the analyses.

Table 1. Material properties of 17-4PH H900 stainless steel.

17-4 PH H900	Value	Units
Elastic Modulus	2.85E+10	psi
Poisson's Ratio	0.272	N/A
Shear Modulus	11000000	psi
Mass Density	0.282	lb/in ³
Tensile Strength	200000	psi
Yield Strength	185000	psi
Thermal Expansion (-100 to 70°C)	5.80E-06	in/in/°F

Source: AK Steel

Table 2. Material properties of AISI 4130 heat treated to 180 ksi

AISI 4130 Steel Heat Treated	Value	Units
Elastic Modulus	2.97E+07	psi
Poisson's Ratio	0.285	N/A
Shear Modulus	11603019.01	psi
Mass Density	0.283599162	lb/in ³
Tensile Strength	180000	psi
Yield Strength	160000	psi
Thermal Expansion (-100 to 70°C)	7.00E-06	in/in/°F

Source: Manufacturer/Vendor

Table 3. Material properties of 13-8PH H950 stainless steel.

13-8PH H950	Value	Units
Elastic Modulus	3.21E+07	psi
Poisson's Ratio	0.272	N/A
Shear Modulus	11100000	psi
Mass Density	0.282	lb/in ³
Tensile Strength	220000	psi
Yield Strength	205000	psi
Thermal Expansion (-100 to 70°C)	5.90E-06	in/in/°F

Source: SAE International

Table 4. Material properties of 15-5PH H1150 stainless steel.

15-5PH H1150	Value	Units
Elastic Modulus	1.00E+07	psi
Poisson's Ratio	0.272	N/A
Shear Modulus	11100000	psi
Mass Density	0.284	lb/in ³
Tensile Strength	135000	psi
Yield Strength	105000	psi
Thermal Expansion (-100 to 70°C)	6.10E-06	in/in/°F

Source: AK Steel

*Note that sometimes after testing the materials, the yield strength was slightly different. Refer to the Load and Stress Analyses section for the correct yield strength.

4. SUMMARY OF RESULTS

The load and stress analysis showed the MTB would be able to withstand all testing conditions as well as be able to take accurate measurements. The following summarizes the results from the analysis.

The strongback was analyzed in several testing configurations as well as non-operational cases. The worst case was a non-operational case, where one rotor was in helicopter mode and all the other rotors were off. Although this is not a planned testing configuration, this could happen if there was an operational error.

The various components of the strut assembly were subjected to several FEA cases. In order to perform the FEA for each part, the forces on each part were calculated. Calculation 1 derived the force on the pitching mechanism in all configurations. The overall maximum operational load case was for a rotor rotation of 45 degrees forward, in its short configuration, when the strongback was rotated 20 degrees forward. The overall maximum operational load was 666 pounds. The overall maximum theoretical load case was for a rotor rotation of 90 degrees forward, in its tall configuration, when the strongback was rotated 30 degrees forward. The overall maximum theoretical load was 1,453 pounds. These forces were used in the FEA of the designed lug (Strut Assembly Study 4), the bottom clevis (Strut Assembly Study 5), and the top clevis (Strut Assembly Study 6).

Calculation 2 derived the force on the upstream hard stop in the worst-case scenario, when all the rotors were in the tall position, rotated 90 degrees forward and with 30 pounds of thrust. It should be noted that this is a theoretical configuration. The load was found to be 2,254.6 pounds and was used in the FEA of the upstream hard stop. The SF of the upstream hard stop was 9.2 (Strut Assembly Study 2).

Calculation 3 derived the force on the downstream hard stop in the worst-case scenario, when all the rotors were in the tall position, rotated 14.25 degrees backward with 30 pounds of thrust. It should be noted that this is an operational configuration. The load was found to be 2,816.6 pounds and was used in the FEA of the downstream hard stop. The SF of the downstream hard stop was 6.25 (Strut Assembly Study 3).

After performing FEA on the strut assembly components, several hand calculations were done. Some of the McMaster-Carr Supply Company bearings had a SF less than 5. It was assumed that a SF was included in the maximum load provided by McMaster, so the actual SF would be greater. The maximum load was also a dynamic load for the bearings, which implies the bearing will be able to take more force at lower speeds. The operational rpm is expected to be very slow. The bearings will also be press fit into the clevises, so the clevises will help to take some of the load as well. The top and bottom clevises showed a SF of 12.43 and 12.49, respectively, after performing a shear tear-out calculation.

The components of beam assembly were subjected to various FEA in all operational and theoretical loading conditions. Of all the manufactured components, the lowest SF was 5.1 for the vertical adjusting beam (Study 6 of beam assembly).

The rotor assembly components were subjected to FEA and hand calculations. The force going through the linear actuator was calculated for all the different configurations of the MTB (Calculation 4). The maximum force was found to be less than 145 pounds. This force was used for the FEA of the clevis interface and the bottom clevis as well as for hand calculations of the bearings and the linear actuator.

Finally, a blade-out analysis was performed. This analysis showed that the MTB would be able to withstand blade-out conditions (i.e., had a SF greater than 1). Blade out would occur if one of the blades came off of the rotor, and the rotor kept spinning, causing an imbalance and a rotating load on the assembly.

It was expected that the rotors will produce in-plane loads less than ± 34 pounds. For the analysis that included the in-plane load, a 34-pound load was applied in the four directions, in the plane of the rotor. Since the in-plane load is actually a vibratory load, assuming the in-plane load to be a single point load gives a more conservative safety factor (conservative study). Because of this, an oscillatory load analysis was not necessary. Although mitigating fatigue was considered in the design, a fatigue analysis has not been performed on the components of the MTB.

In order to obtain accurate measurements, and therefore accurate data, the maximum allowable angle of deflection was set to be 0.1 degrees. Many of the parts were over designed in terms of stress, because they need to be stiff enough to satisfy the deflection requirement.

When performing FEA on assemblies, the assembly files were saved as part files. This was done to decrease run time and to simplify the FEA. Each part could still be selected to have the correct material properties, but saving the assembly as a part file meant that the parts were bonded together. It was assumed that using the part file of the assembly for FEA would not affect the resulting SFs by a significant amount.

When performing all of the different FEA studies, if the resulting safety factor was less than 1.2, the mesh of the part was refined in high stress areas to obtain more accurate results. In some cases, the areas of high stress were stress singularities. Stress singularities could be found in sharp corners or places where a constraint or boundary was applied. When decreasing the mesh size, the stress singularity will keep increasing, whereas the stress from a stress concentration will eventually plateau. Sometimes multiple studies had to be done to determine if an area of high stress was a stress concentration or a stress singularity.

Table 5 shows the loads that were used in the analysis and the load limits that were incorporated into the Safety of Flight (SOF). The SOF display is used during testing to monitor the load and allows the test team to see when load limits are being approached.

Table 5. Maximum loads for safety of flight.

	Fx [lb]	Fy [lb]	Fz [lb]	Mx [in-lb]	My [in-lb]	Mz [in-lb]
Load Limit	± 34	± 34	30	± 86.6	± 86.7	60

Table 6 shows a summary of the safety factors of all the components in the MTB. Where the SF is noted “conservative,” this is because the SFs were calculated using McMaster specified maximum loads/stresses. It is expected that McMaster included a SF in these numbers as well. An asterisk, “ * ”, notes that this SF was obtained from the maximum theoretical load, and that the MTB is not planned to operate in that configuration. It should be noted that a SF of 4 on ultimate strength and a SF of 3 on yield is required for testing in the wind tunnel.

Table 6. Safety factor summary.

PART	MATERIAL	MAX STRESS /LOAD	SF YIELD	SF ULTIMATE	PART #	Page
Strongback Assembly	17-4	5.08 ksi	36.4		3	25
Strongback Support Interface	17-4	2.33 ksi	79.4		12	47
Upstream Stopper	17-4	20.20 ksi	9.2		13	48
Downstream Stopper	17-4	29.62 ksi	6.25		14	49
Strut Assembly - Designed Lug	17-4	5.2 ksi	35.5		18	50
Bottom Strut Clevis	4130	1453 lbs	12.43		16	58
Top Strut Clevis	4130	1453 lbs	12.49		15	58
Large Hinge	17-4	0.66 ksi	280		11	53
Strut Assembly - Flanged Sleeve Bearing	954 Al-Brz	726.5 lbs		*1.45 (conservative)	McM	55
Strut Assembly - Dowel Pin	416 SS	1453 lbs		7.57 (conservative)	McM	55
Strut Assembly - Screw (for lug)	Alloy Steel	726.5 lbs		13.8 (conservative)	McM	56
Strut Washer	932 Brz	210 lbs	97.75		38	54
Main Strut Shaft	17-4	420 lbs	23.84		40	57
Threaded Rod	17-4	1453 lbs	18.3		17	57
Adjusting L-Bracket	17-4	24.12 ksi	7.67		23/24	63
Vertical Support Beam	13-8	40.23 ksi	5.1		25	65
Lateral Support Beam	13-8	5.94 ksi	34.5		22	69
Clevis Interface - Rotor Assembly	17-4	10.19 ksi	18.16		27	72
Custom Linear Actuator Mount (Right and Left)	17-4	6.87 ksi	22.55		41/42	74
Ultra Motion Linear Actuator		145 lbs	5.86		A1	77
Linear Actuator Top Clevis	17-4	150 lbs	28.7		44	75
Bottom Actuator Interface	17-4	150 lbs	83.5		43	76
Flanged Sleeve Bearing - Bottom of Linear Actuator	841 Brz	75 lbs		3.33 (conservative)	McM	77
Flanged Sleeve Bearing – Rotor	863 Brz	12.75 lbs	32		McM	78
Shoulder Screw - Rotor Top	Alloy Steel	150 lbs		6.3 (conservative)	McM	79
Sleeve Bearing - Top of Linear Actuator	Alloy Steel	150 lbs		3.67 (conservative)	McM	79
Screw – Custom Mount to Bottom Actuator Interface	Alloy Steel	37.5 lbs		107.7	McM	80
Gearbox-Pillow Block Interface	17-4	50 lbs	74.5		47	82
Pillow Block	Steel (A36)	162.4 psi	222		31	83
Screw - Gearbox to Pillow Block	Alloy Steel	851 psi	200		McM	84

5. DESIGN

OVERVIEW OF THE MTB

The Multirotor Test Bed (MTB) consists of six individual rotor systems, each with its own lateral, vertical, and rotational adjustment systems. Each rotor has a 24-inch diameter and can pitch forward 90 degrees and backwards 5 degrees in its standard configuration. The center of the design features the strongback, which acts as a structural backbone for the assembly. Lateral support beams are held in the strongback and connect to the lateral and vertical adjusting beams. The rotor assemblies are connected to the vertical support beams. The rotation system for the rotors uses a linear actuator that is to be controlled remotely during testing. The rotational adjustment for the strongback is controlled by a stepper motor interfacing with a jackscrew within the single heavy strut. The whole assembly can pitch 30 degrees forward (nose down) and 10 degrees backward (nose up). There are load cells under each rotor to capture loads and vibrations.

The total weight of the assembly is slightly less than 240 pounds, not including the strut. The maximum dimensions are 80.625-inches long by 62.45-inches wide by 33.625-inches tall (not including the strut). The MTB is planned to be tested in the 7- by 10-Foot Subsonic Wind Tunnel at NASA Ames Research Center. The maximum thrust load from the rotors is 30 pounds, with an expected ± 20 pounds in-plane vibratory load (load limits set to ± 34 pounds). The MTB was designed to be able to withstand testing conditions (with considerable margin) in the wind tunnel, as well as be able to take accurate measurements.

UPDATE: Note that the linear actuator was replaced and there is some new hardware. This is not reflected in all the photos such as the one below.

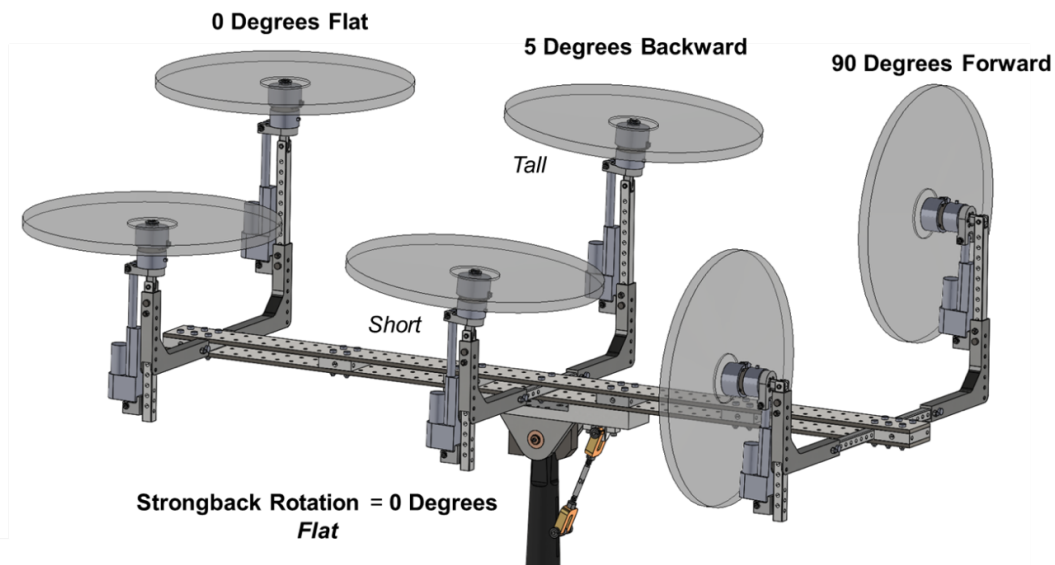


Figure 5.1. MTB assembly side view.

5.1 Strongback Assembly

The strongback assembly was designed for optimal strength and adjustability. The strongback is comprised of top and bottom plates, center support blocks, and shoulder bolts (see Fig. 5.1.1). The lateral supports can slide along the top and bottom plates and can be fixed in place by fitting shoulder bolts through the holes. The center support blocks hold the top and bottom plates together, stiffening the strongback assembly and holding the assembly together. Locknuts can be screwed onto the shoulder bolts, ensuring that they stay in place. Stainless steel grade 17-4PH H900 was chosen as the material due to the need for stiffness. As shown in the loads and analysis section, the safety factors are quite high. The concern is that the measurements taken are accurate. Thus, a stiff material is needed to maintain small deflections of the system under testing conditions.

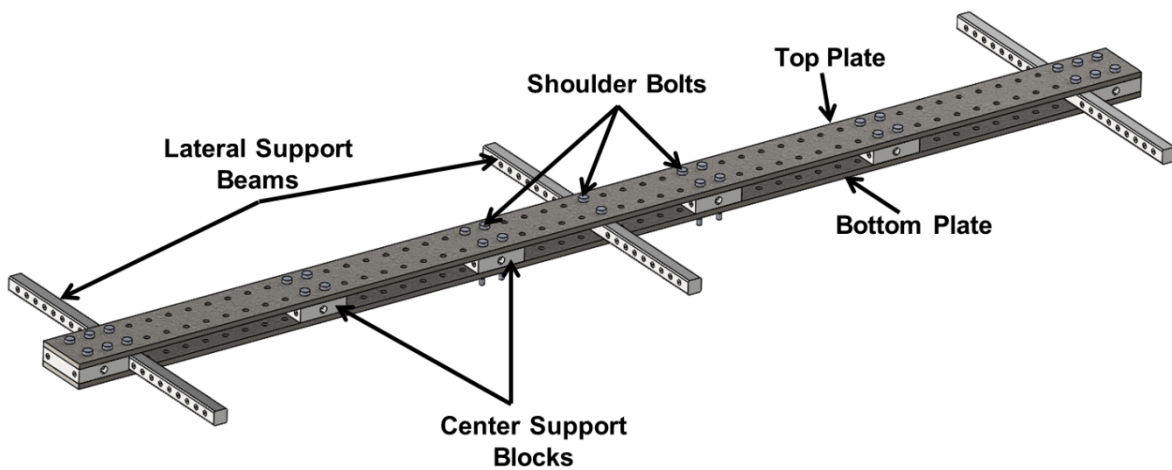


Figure 5.1.1. Isometric view of strongback.

The strongback top and bottom plates were originally designed to be two-inches wide, with only one row of holes. It was modified to be four-inches wide, with two rows of holes to ensure that the lateral support beams would not rotate, and also to add more support to the lateral support beams. The thickness of the top and bottom plates was increased from 1/4 inch to 3/8 inch. The length of the supporting interface (not shown in Fig. 5.1.1) was increased as well. It should be noted that if the strongback starts to resonate during testing (i.e., if testing is done at a resonant frequency of the assembly) additional support blocks can be added or removed from the strongback to change the natural frequency of the assembly.

5.2 Strut Assembly

From top to bottom, the strut assembly consists of: the strongback support interface, large hinges, shaft, strut washers, strut washer interfaces, hard stops, single heavy strut, designed lug, screws, dowel pins, top clevis, locknuts, threaded rod, bottom clevis, shaft collars, and lug (ear).

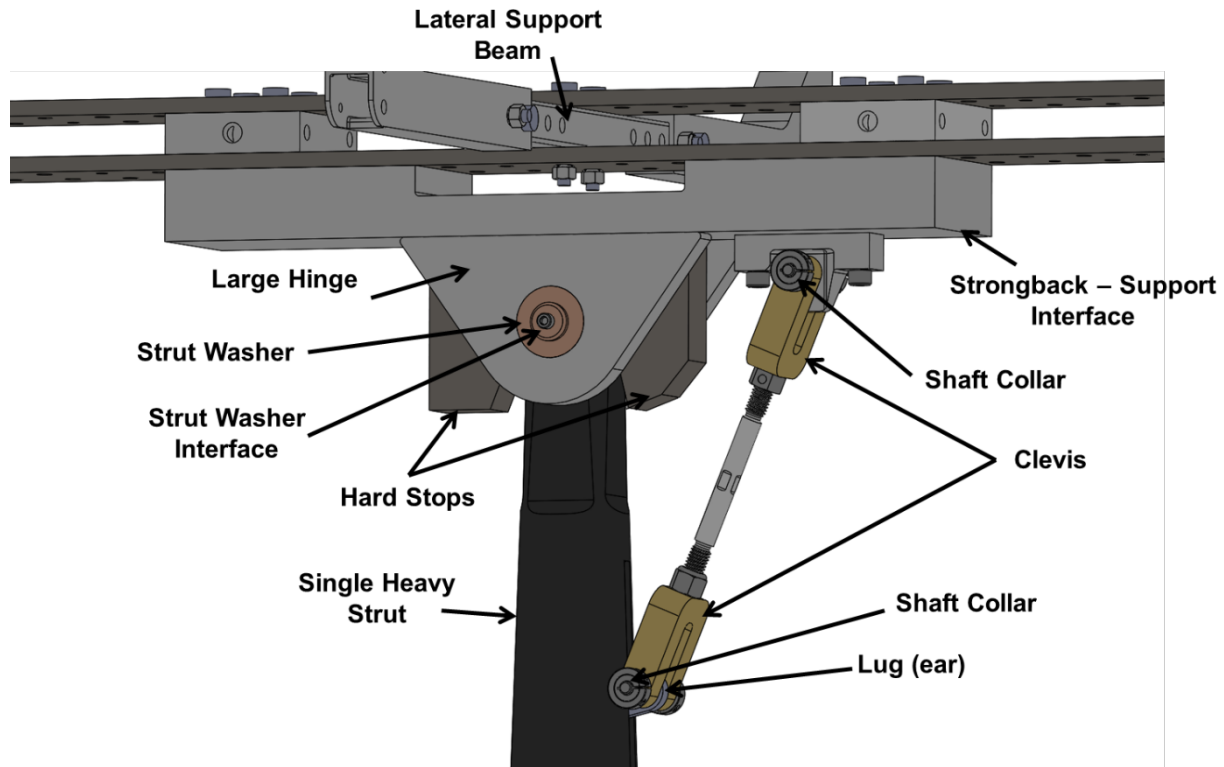


Figure 5.2.1. View of strut assembly.

The single heavy strut has a built-in jackscrew that moves the lug (ear) up and down. The single heavy strut is already built and has been used in past experiments in the 7- by 10-Foot Wind Tunnel. The single heavy strut will be secured to the base of the wind tunnel, where there is a scale that can measure the loads from the entire assembly.

The strongback support interface supports the strongback assembly. Shoulder bolts pass through the strongback assembly, through support blocks, and tap into the strongback support interface. There are four columns of holes on each side of the strongback support interface for the shoulder bolts to tap into. Only two columns of holes are needed for the support blocks. This purpose of the extra columns allows the positioning of the support blocks and shoulder bolts to be placed in three different configurations. This was done in case a different configuration was desired in which the beam assemblies were moved closer to the center of the strongback.

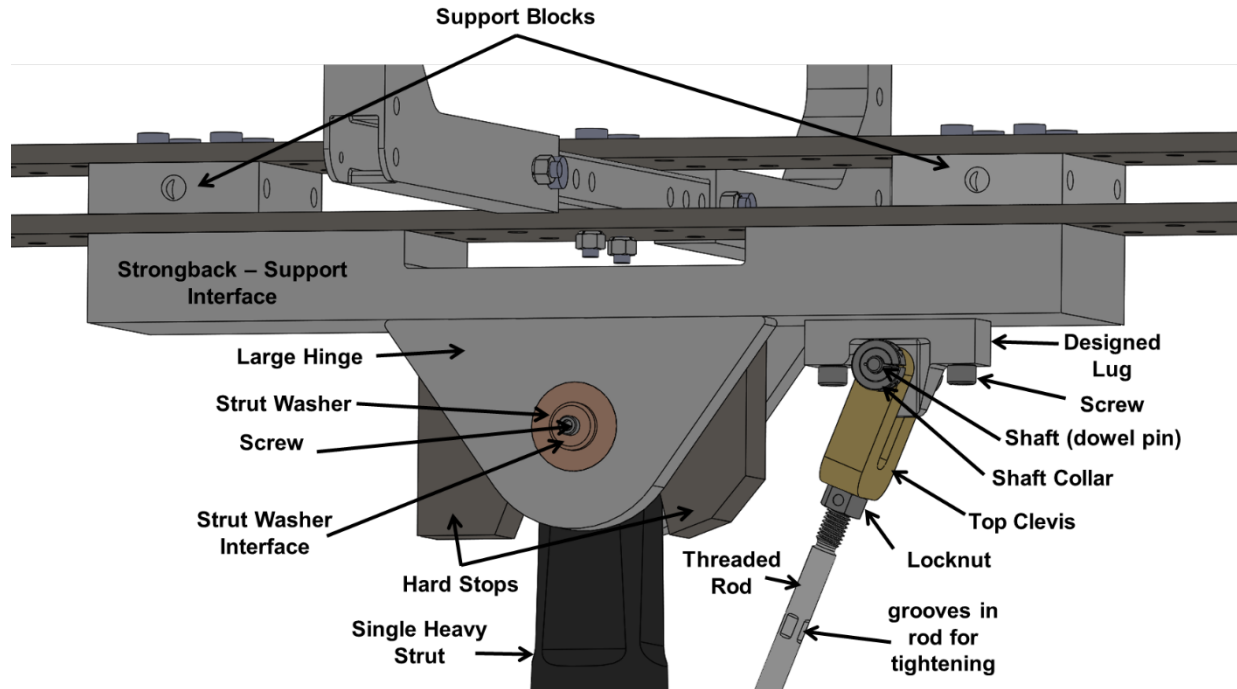


Figure 5.2.2. Close up view of top of strut assembly.

The large hinges and strut washers allow the entire assembly to rotate on the shaft that passes through the top of the single heavy strut. The strut washers act as bearings and are press fit into the large hinges and the shaft has a slip fit with the strut washers. The shaft is tapped on each end and is secured in place by the strut washer interfaces and screws on either side. The intent of this design is to reduce friction along the shaft as well as any slop between the strut and the hinge. Originally the strut assembly was manufactured with high-load ball bearings and there was a smaller contact surface between the strut and the hinge. As a result, the strongback could be moved fairly easily at the ends. To reduce the sideways movement, the strut washers were created to have more surface contact between the strut and the hinge, as well as take away any additional slop or movement that was given by the ball bearings. Countersunk shoulder bolts secure the large hinges to the strongback support interface (i.e., shoulder bolts fit through the interface and tap into the hinges) and a dowel pin is press fit into the hinge and used for location on the strongback support interface.

Similar to the large hinges, the hard stops are secured to the strongback support interface by shoulder bolts, which are countersunk into the interface and tap into the hard stops. There is an upstream (left) and downstream (right) hard stop. The purpose of the hard stops is to prevent the MTB from damaging the wind tunnel in the event of a mechanical failure of the threaded rod or adjacent parts. If the rotating mechanism fails or becomes disconnected, the MTB will rotate forward or backward depending on the configuration of the rotors. The hard stops will prevent the MTB from rotating before it hits the walls (floor or ceiling) of the wind tunnel. It should be noted that when the back two rotors are in their tallest configuration, and the MTB is pitched 22 degrees forward and the rotors are tilted between 13 and 67 degrees forward, the rotors will hit the ceiling

of the 7- by 10-Foot Wind Tunnel. When operating in the wind tunnel, care should be taken to make sure the back two rotors are not in their tallest or second tallest configuration. The tallest safe operating condition for the back two rotors is when they are in their third tallest position.

The designed lug screws into the bottom of the strongback support interface (see Fig. 5.2.2). A swivel joint (not shown) is press fit into the designed lug. Flanged bearings are press fit into the top clevis, and the dowel pin has a slip fit with the flanged bearings and the swivel joint. Thus, the top clevis can rotate about the dowel pin that passes through the designed lug, and the dowel is held in place with shaft collars on either side. Originally a ball joint rod end was to be used as the point of rotation instead of the designed lug. However, the manufacturers could not give information about the maximum loads or stresses that the rod ends could handle, or the maximum loads were too small. So, a lug was designed in its place.

The top clevis is connected to the bottom clevis by a custom-threaded rod. All parts described up to now that are not off-the-shelf parts will be made from 17-4 except for the clevises, which will be made from AISI 4130. The rod is threaded on both ends in different directions (right- hand and left-hand threads). When it is turned one way it will screw into both the top and bottom clevis, and when it turns the other way, it will screw out of the clevises. This was done for ease of assembly. The threaded rod has grooves in the center so a wrench can easily be used to rotate the threaded rod.

The clevises are tapped and there are locknuts that secure the position of the threaded rod with respect to the points of rotation, and to prevent backout. The distance between the points of rotation was optimized to get the maximum amount of rotation for the assembly. The placement of the designed lug was part of this optimization. The operational range of motion of the MTB is currently 20 degrees forward and 10 degrees backward, but the maximum range of motion could be extended to 32.5 degrees forward and 13.6 degrees backward.

Flanged bearings are also press fit into the bottom clevis. A dowel pin has a slip fit into these bearings and also through the lug (which is part of the single heavy strut) and is held in place by shaft collars. Additional thrust bearings are placed between the clevis and the lug so the clevis can rotate freely along the dowel pin.

5.3 Beam System

The beam system consists of the lateral support beam, vertical support beam, adjusting L-bracket, shoulder bolts, and locknuts. The lateral support beam is fixed to the middle of the strongback between the top and bottom strongback plates, by two shoulder bolts (see Fig. 5.3.1). There are two adjusting L-brackets on either side of the lateral support beams. The adjusting L-brackets have two through holes on the horizontal side and on the vertical side and slide along the fixed lateral support beam and the vertical support beam, respectively.

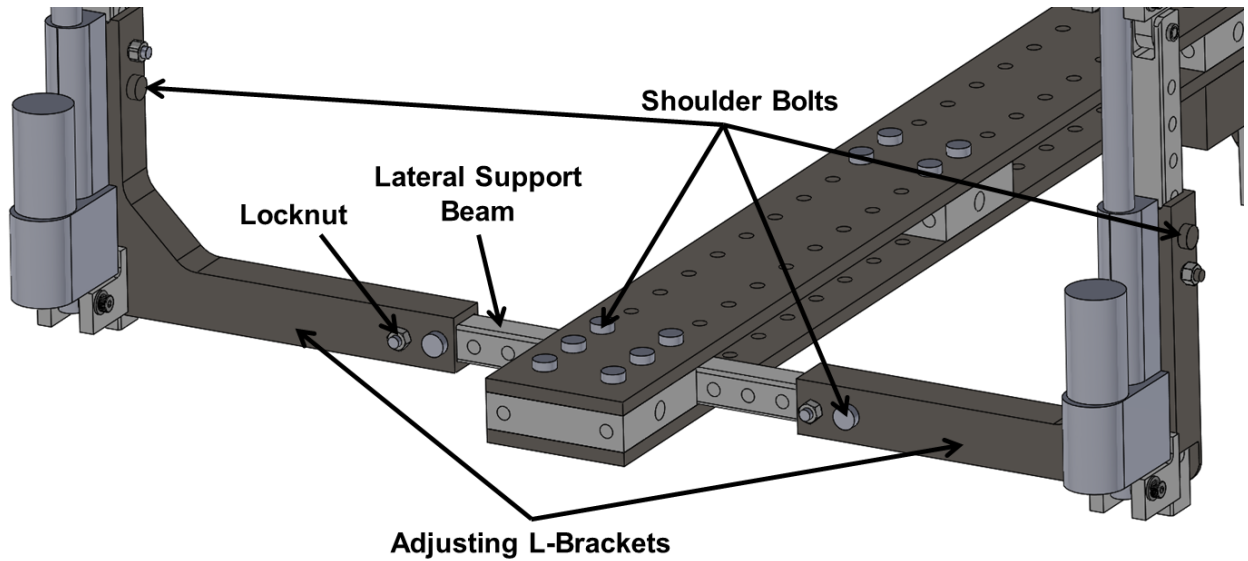


Figure 5.3.1. Isometric view of lateral beam system. (Older model)

To change the lateral position of the rotor, the shoulder bolts and locknuts are removed. The adjusting L-bracket is manually moved to the desired location and secured to that location by shoulder bolts and locknuts. The gap between the propellers is smallest when the adjusting L-brackets are fixed closest to the strongback (see Fig. 5.3.2), and the gap is the largest when the adjusting L-brackets are fixed to the farthest holes on the lateral support beam (see Fig. 5.3.3).

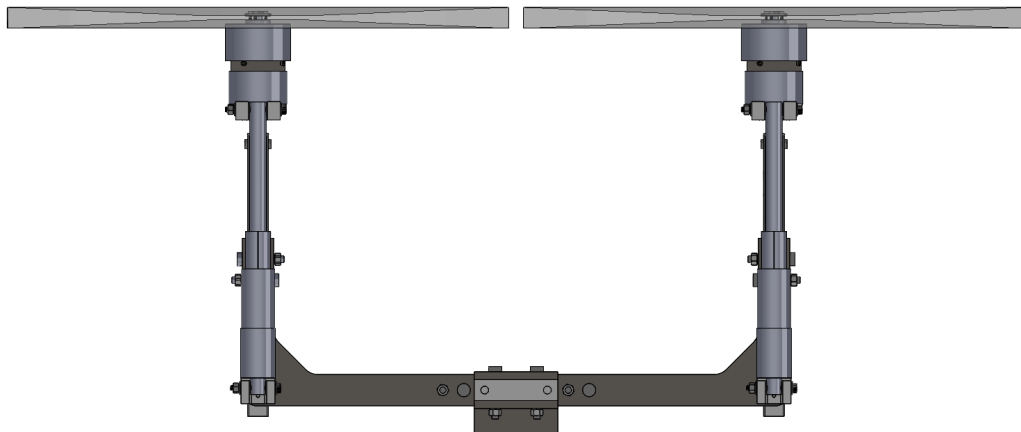


Figure 5.3.2. Front view of small gap with 24-inch diameter propellers. (Older model)

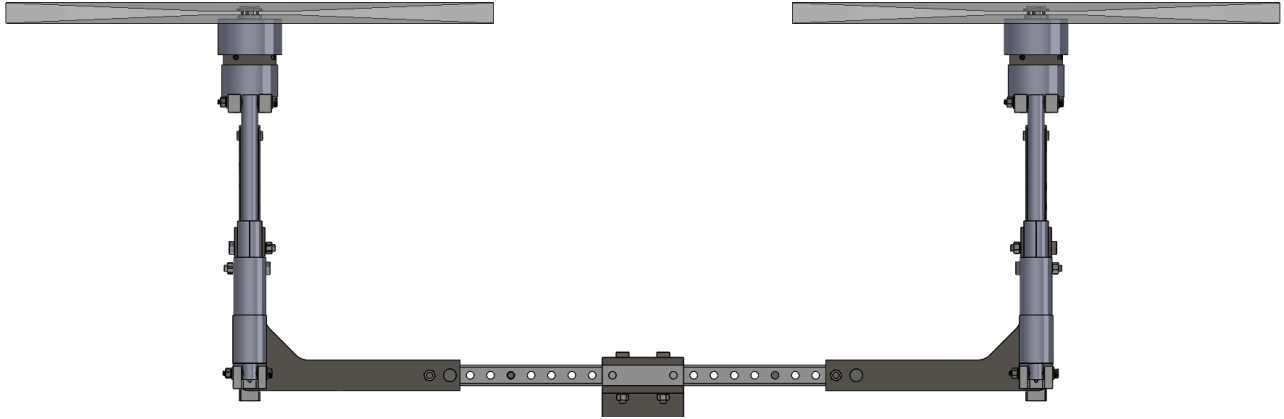


Figure 5.3.3. Front view of large gap with 24-inch diameter propellers. (Older model)

The length of both the lateral support beam and the adjusting L-brackets were optimized to ensure the smallest small-gap and the largest large-gap. It was determined that it was more important to have a small small-gap than to have a large large-gap. The most up-to-date model has 24.5-inch diameter propellers, which gives a small gap of 0.2 inches (Fig. 5.3.2) and a large gap of 14.2 inches (Fig. 5.3.3).

When the adjusting L-bracket is in its shortest position, closest to the strongback, there is a 0.35-inch gap between the lateral support beam and the vertical support beam (see Fig. 5.3.4).

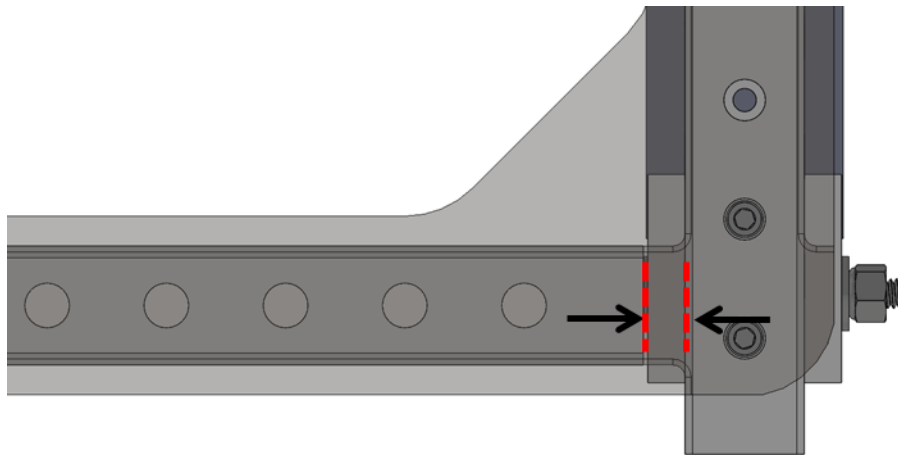


Figure 5.3.4. View of gap between lateral support beam and vertical support beam.

After analysis, it was determined that the adjusting L-brackets would be made out of 17-4PH H900 stainless steel and the support beams would be made out of 13-8PH H950 stainless steel. The adjusting L-brackets and the support beams were chosen to be different materials to prevent galling. It is essential this assembly be very stiff to obtain accurate measurements.

There is a slip fit between the adjusting L-brackets and the support beams. The tolerance on the slip fit is very small because the slip fit must be retained at temperatures ranging from 35 to 105 degrees Fahrenheit. In order to create this fit, the cut outs in the adjusting L-brackets needed to be EDM (electrical discharge machined).

The original goal was to have the small gap equal to zero and the large gap equal to 24 inches, when the 24-inch diameter propellers were in the assembly. With the current design, this is not possible. However, it would be possible if there were different sized lateral beams that could be exchanged. There are plans for other lateral support beams to be designed in the future (same design, just modifying the length). If there were multiple lateral support beams, the larger gap could be extended and the MTB would be capable of being tested in even more configurations.

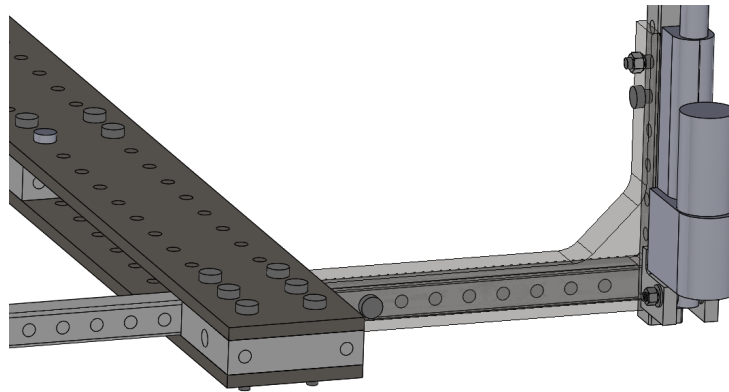


Figure 5.3.5. View of transparent adjusting L-bracket in shortest position. (Older model)

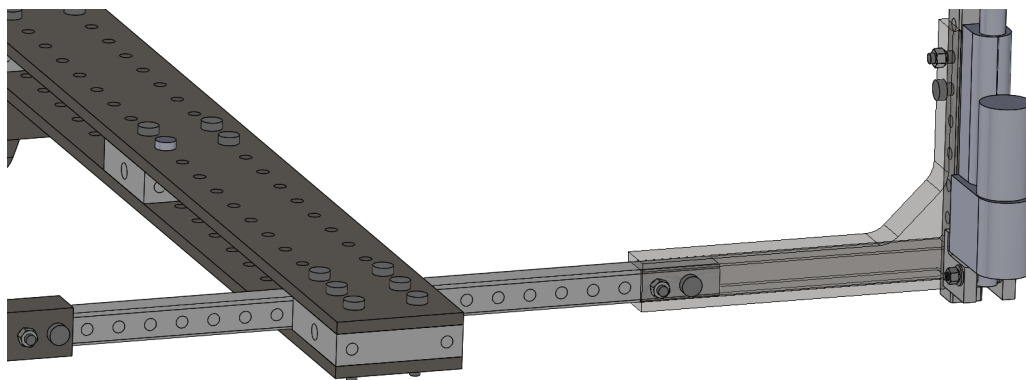


Figure 5.3.6. View of transparent adjusting L-bracket, fully extended. (Older model)

The thickness of the lateral adjusting beams was increased along the vertical side to increase stiffness.

To adjust the height of the rotor, the vertical support beam moves up and down inside the adjusting L-bracket. The shoulder bolts and locknuts are removed, the vertical support is manually moved to the desired location, and the shoulder bolts are placed in the holes and secured to that location by locknuts.

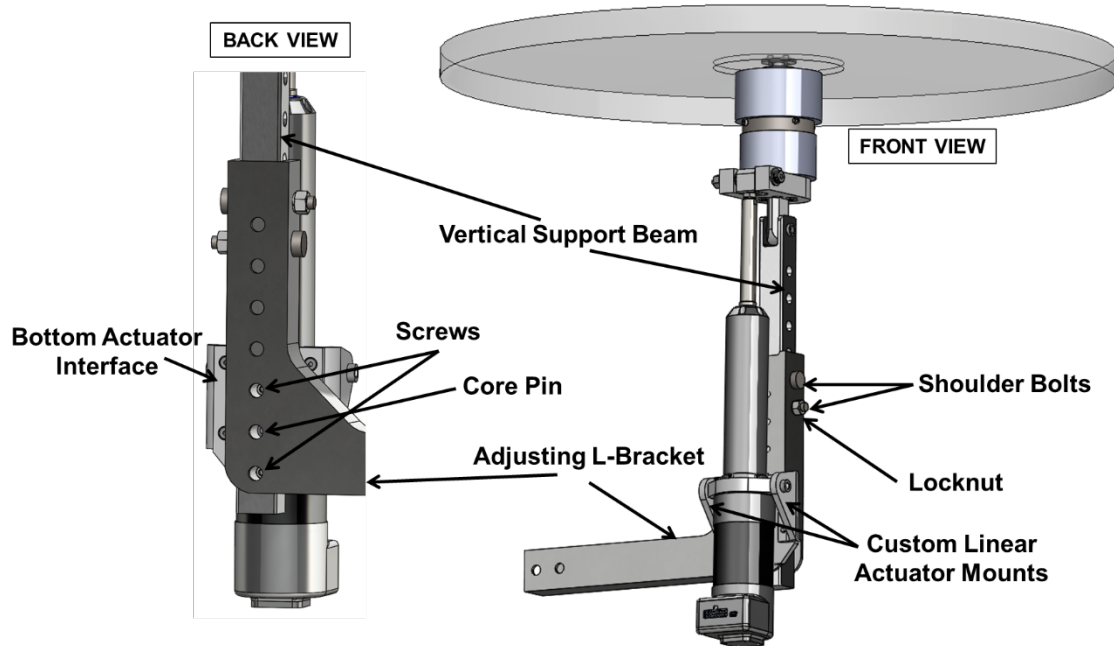


Figure 5.3.7. Front (right) and back (left) view of vertical beam system in medium height configuration. (Updated image)

Along the back of the vertical beams, there are screw access holes. This allows the screws that secure the bottom actuator interface (that holds up the custom linear actuator mounts) to the vertical support beam for ease of installation. When moving the vertical support beam up and down, these two screws will have to be removed and put back in. There is also a core pin in between the two screws that will be able to take the shear load. The core pin is press fit into the bottom actuator interface.

The range of motion of the new linear actuator (the stroke length) is 3.75 inches (same as the old linear actuator). The kinematics and geometry of the system were optimized to allow for maximum range of motion while still maintaining enough clearance between the linear actuator and the support beams. At 90 degrees forward the actuator is at 0.0206 inches. At -5 degrees the actuator is at 3.734 inches. Since the range of motion is from zero to 3.75 inches, this leaves a little wiggle room on each end to make sure the full range can be obtained.

The minimum and maximum height of the vertical beam assembly above the strongback is 12 inches (see Fig. 5.3.8) and 21 inches (see Fig. 5.3.9) with a range of 9 inches. If a different minimum or maximum height is desired, a new vertical support beam can be designed with a

different length. It should be noted that the safety mechanisms (the stoppers) used to prevent the rotors from hitting the walls (including ceiling and floor) of the wind tunnel were designed using the current dimensions of the beam assembly. If these dimensions are modified, the stoppers may need to be redesigned.

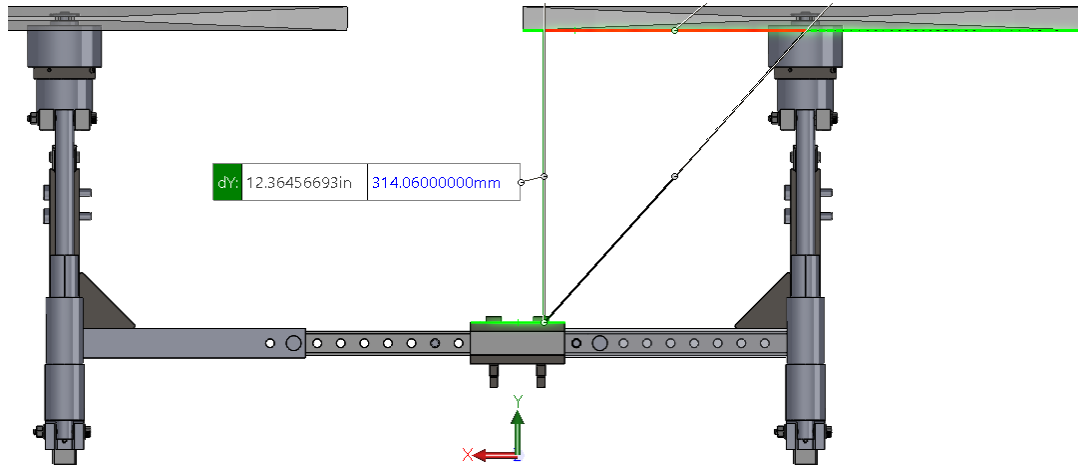


Figure 5.3.8. Front view of front right rotor assembly at minimum height of 12.36 inches (dimensions correct, model outdated).

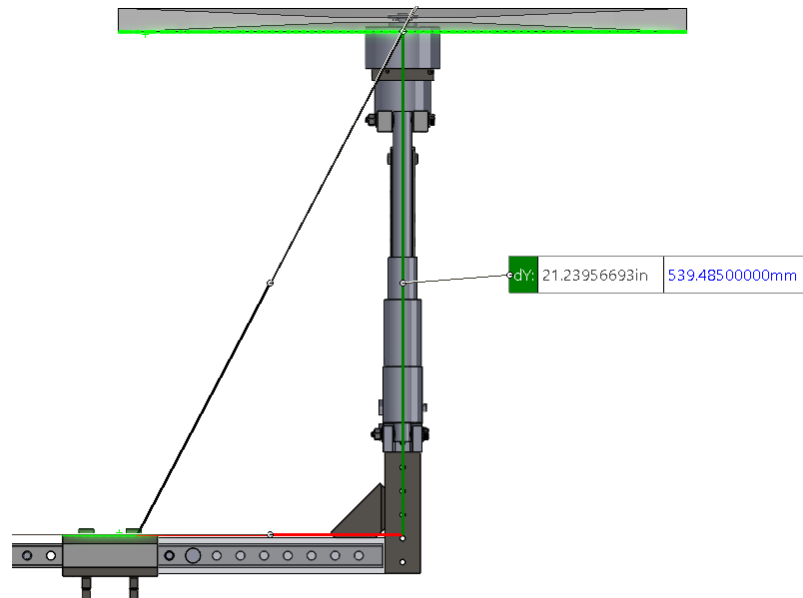


Figure 5.3.9. Front view of front right rotor assembly at maximum height of 21.24 inches (dimensions correct, model outdated).

5.4 Rotor Assembly

From top to bottom, the rotor assembly consists of: rotor cover, rotor, rotor motor, motor-load cell interface, load cell, clevis interface, hinge, flanged bearings, dowel pin, shoulder bolts, thrust bearings, linear actuator top clevis, linear actuator, custom linear actuator mounts, off-the-shelf linear actuator mounts, locknuts, and screws (see Figures 5.4.1 and 5.4.2). The dowel pin is press fit into the flanged bearings and the hinge, making sure the bearings take all the rotation. If the dowel pin is not press fit into the bearings, the shaft may wear down. The dowel pin may have to be purchased oversized and then machined down for the proper fit. The outside of the flanged bearings is press fit into the vertical support beam. The dowel pin is the point of rotation for the rotor.

UPDATE: The linear actuator has been replaced with a new linear actuator from Ultra Motion LLC (Model A1). This new linear actuator has an off-the-shelf linear actuator mount as well as custom linear actuator mounts made in house. The linear actuator was replaced because the old one had some play. This new linear actuator has tighter tolerances and can handle higher loads. The pictures prior to this section did not discuss the hardware for the linear actuator so the pictures have the old design with the old linear actuator. The analysis in sections below have been updated for the new hardware and increased loads (increased in-plane load from 20 to 34 pounds).

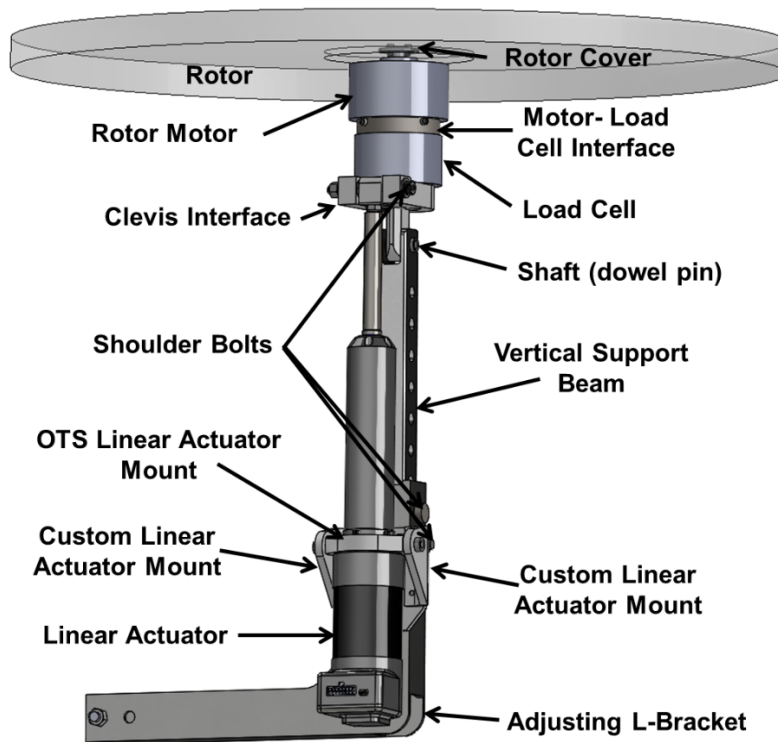


Figure 5.4.1. View of rotor assembly.

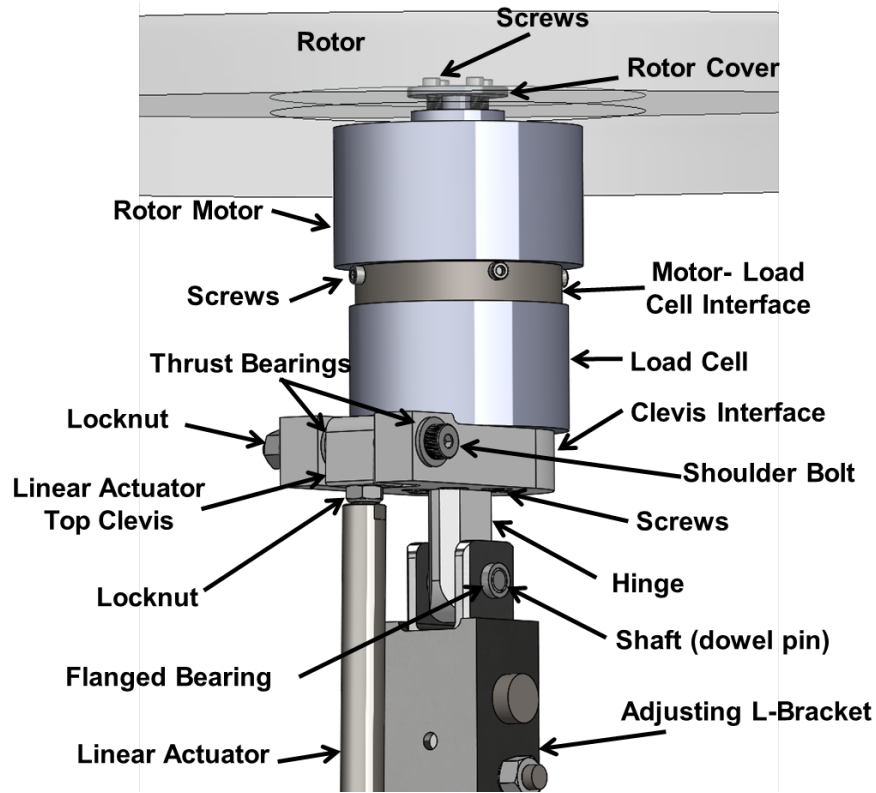


Figure 5.4.2. Close up view of the top of the rotor assembly.

The clevis interface is connected to the load cell via screws coming in from the bottom. A shoulder bolt passes through the clevis interface and through the linear actuator top clevis. It is then secured by a locknut on the other side. This shoulder bolt is the point of rotation for the top part of the linear actuator. There are thrust bearings between each of the parts to provide a smooth surface against which the parts can rotate. There is also a bearing inside of the linear actuator top clevis that rotates on the shoulder bolt. A set screw is threaded into the linear actuator top clevis (secured with a locknut) and into the top of the actuator. As the actuator moves up and down, it moves the clevis interface, causing the rotor assembly to rotate about the dowel pin.

The custom linear actuator mount holds the bottom of the actuator to the vertical support beam (see Figures 5.4.1 and 5.4.3). It is connected to the vertical support beam, not the vertical adjusting beam. This is because the point of rotation (dowel pin) is about the top of the vertical support beam. It is essential that this placement be maintained. The position of the actuator has been optimized to ensure maximum range of motion. The custom linear actuator mount is secured to the bottom actuator interface (two counterbored screws coming in from the back), which is secured to the vertical support beam by two screws and a core pin to take the shear load. The actuator is secured to an off-the-shelf linear actuator mount with pins that rotate on flanged bearings that are press fit into the custom linear actuator mount.

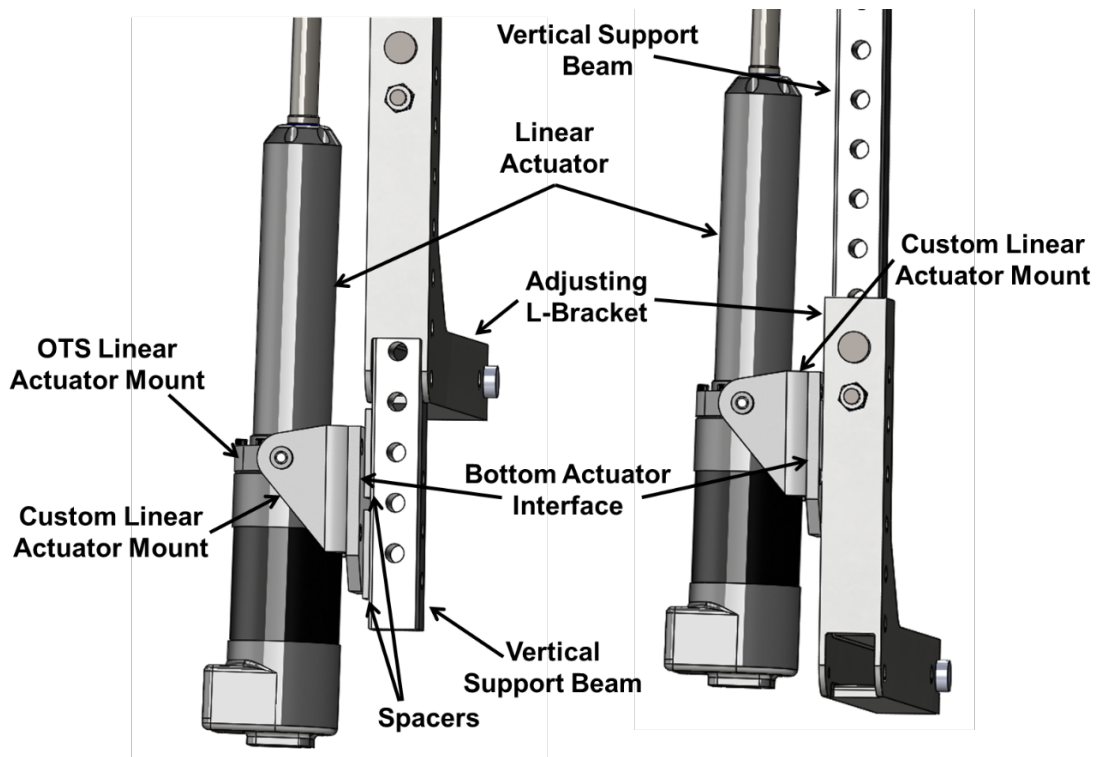


Figure 5.4.3. Close up side view of bottom of rotor assembly in short (left) and tall (right) configurations.

The linear actuator mounts move with the beam to maintain the same vertical distance for the actuator to work properly. It is also important for the horizontal distance to be maintained in order to maintain the kinematics of the pitching mechanism at all vertical rotor positions. In the taller configurations, the bottom actuator interface rests against the vertical adjusting beam, but in the shorter configurations there is a 0.125-inch gap. This gap is filled with two custom spacers shown in Figure 5.4.3. These spacers maintain the actuator in the proper position as well as provide enough surface contact for a strong connection.

Looking back to the top of the rotor assembly, the hinge is connected to the clevis interface. The top of the clevis interface has countersunk holes that line up with holes on the top of the hinge. There are holes that go through the clevis interface as well, which line up with holes on the bottom of the load cell (see Fig. 5.4.2).

The manufacturer of the load cell refers to the “tool side” as the top side, and the “mounting side” as the bottom side (mounting to the hinge). The motor-load cell interface is connected to the load cell and the propeller motor. There are two interfaces used to do this. The top interface slides into the bottom interface, and they are connected together by screws through the holes on the outside (screws are not shown in Fig. 5.4.4). The holes on the inside of the interface align with holes on the propeller motor and the load cell. These holes are countersunk so the parts lie flat. For the

physical part (not the Solidworks model), the countersinks should be slightly lower than the face so the screws rest slightly below the face. This ensures there is no interference from the screws. The cutout in each piece is for the rpm sensor. The top piece has two tapped holes that secure the bent piece of sheet metal holding the sensor.

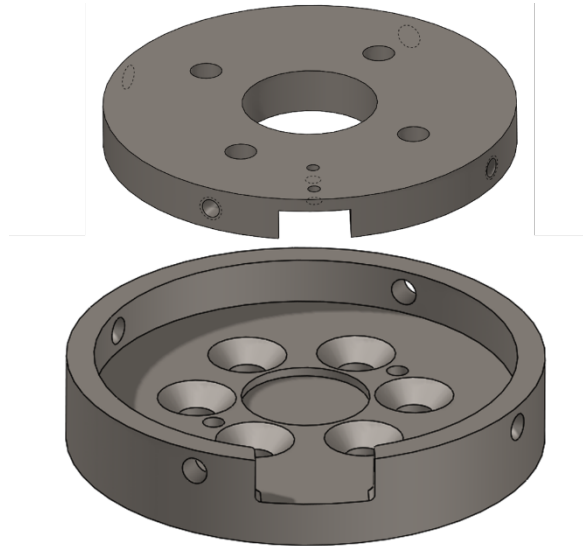


Figure 5.4.4. Motor-load cell interface.

The rotor itself has holes corresponding to the holes in the rotor cover and the rotor motor (note that the actual rotor cover has different geometry). Screws are used to secure the rotor to the motor. The rotor can be removed and replaced with a different rotor as long as the corresponding holes have the same dimensions. If a new rotor requires a different motor, a new motor-load cell interface may be required. Each motor will be individually controlled by a servo controller and LabVIEW feedback control system.

All manufactured parts of this assembly will be constructed of 17-4 except for the inside motor-load cell interface, which will be made from 15-5PH H1150 so no galling occurs. Originally aluminum was considered, but because of the stiffness requirement, the analysis showed that steel would be the better option. Also, since the interface between the rotor motor and the load cell will be made from steel, the heat cannot travel as easily from the motor to the load cell. If this interface were made from aluminum (which is more thermally conductive), the load cell would be more likely to be affected by thermal drift (i.e., the change in load cell measurements that occurs as the temperature changes). The purchased load cell is designed to have very low thermal drift, so this should not be an issue.

5.5 Installation Assembly

The installation assembly consists of the MTB strut assembly (everything mounted on top of the strut), large screws, mounting block (a.k.a pillow block), gearbox-pillow block interface, gearbox, stepper-gearbox bushing, motor-gearbox interface, and stepper motor.

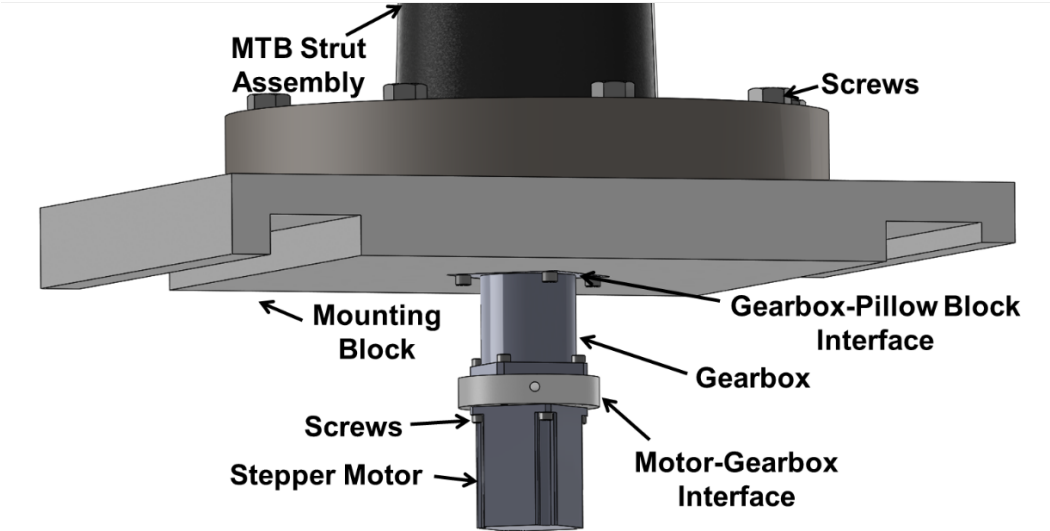


Figure 5.5.1. Installation assembly.

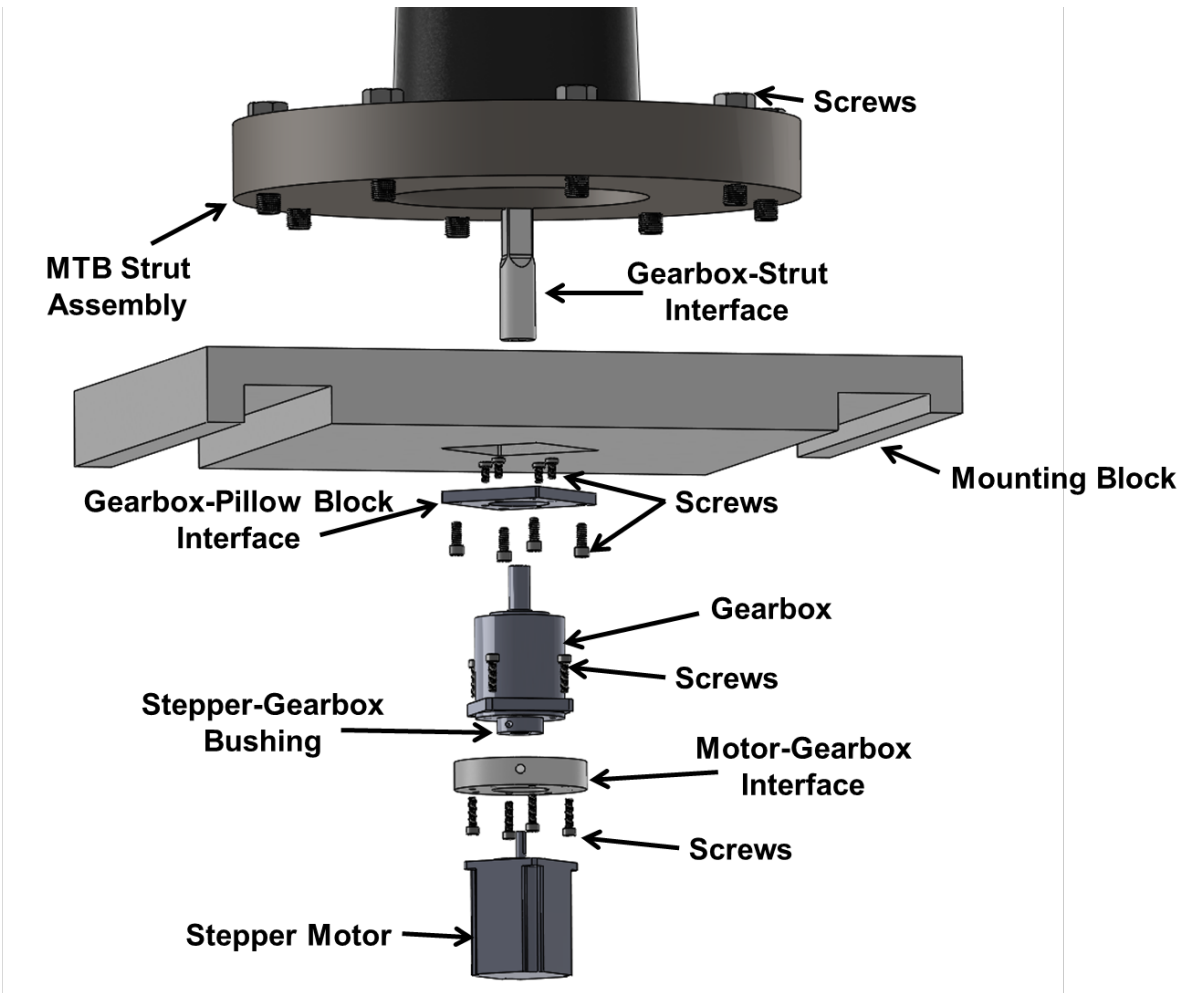


Figure 5.5.2. Exploded view of installation assembly.

To assemble, the mounting block (pillow block) is secured to the bottom of the turn table in the test section. Next the strut is lowered onto the mounting block and secured with large screws. The gearbox-motor assembly is assembled separately and then secured to the bottom of the mounting block with the four screws upside down as seen in Figure 5.5.2. The four small screws at the top pass through the gearbox-pillow block interface and into the gearbox, holding the assembly together.

6. LOAD AND STRESS ANALYSIS

This section discusses in detail the complete load and stress analysis of the MTB. Analysis was performed on each component in the strut assembly, beam assembly, and the rotor assembly. A blade out analysis was also performed on essential parts. Finite Element Analysis (FEA) was performed using SolidWorks. Several hand calculations were done to determine the loads that various components of the system would experience. The propellers were capable of producing a maximum 30-pound thrust load with an estimated maximum in-plane load of ± 20 pounds. For the analysis however, the maximum in plane load was eventually set to ± 34 pounds. This was the largest in-plane load that the components could handle with still maintaining safety factors greater than 5. This ± 34 -pound load was used in the safety of flight loads monitoring. The off-the-shelf components were also analyzed.

The positions of the rotors are often referred to as being in helicopter mode or airplane mode. Helicopter mode is when the rotors are straight up and have zero degrees rotation, similar to a helicopter taking off from the ground. Airplane mode is when the rotors are tilted the full 90 degrees forward and produce a forward thrust, similar to an airplane.

The maximum loads that were used in the analysis are shown in Table 5: Maximum loads for the safety of flight.

6.1 Strongback Assembly Analysis

FEA was done in SolidWorks on the strongback assembly to determine the maximum stress and the maximum deflection in various configurations. The maximum allowable angular deflection was set to be 0.1 degrees in order to obtain accurate data. For this reason, many of the parts have very high safety factors and are over designed. Taking the length of the strongback, 80.625 inches, and dividing by 2 and multiplying by the sine of 0.1 degrees would give the maximum vertical deflection allowed, 0.07036 inches. For all of the FEA studies in this section, the strongback assembly was saved as a part file in order to minimize the run time of the study. This could make the study less accurate. The weight of the strongback assembly, including the lateral support beams was about 102 pounds. The weight of each rotor assembly was 14 pounds. Note that the material of the lateral support beams has changed from 17-4PH H900 to 13-8PH H950 and the material of the strongback plates and support blocks has changed from AISI 4130 (with lower yield strength of 66.7 ksi) to 17-4PH H900. Since these materials were changed to stronger/stiffer materials, the FEA was not redone. It should be noted that the actual SF will be higher than what is given.

STRONGBACK STUDY 1: Dead weight on strongback

MATERIALS: Lateral support beams – 17-4PH H900 – Yield Strength of 185 ksi.
Strongback plates and support blocks – AISI 4130 steel annealed at 865 °C – Yield Strength of 66.7 ksi.

APPLIED LOADS: Weight of entire strongback assembly and support beams (gravitational load).
Weight of each rotor assembly 14 pounds, applied at each end of the lateral support beams (six total).

FIXTURES: Underside of bottom strongback plate fixed at location of strongback – support interface.

NOTES: Mesh was refined to obtain more accurate results.

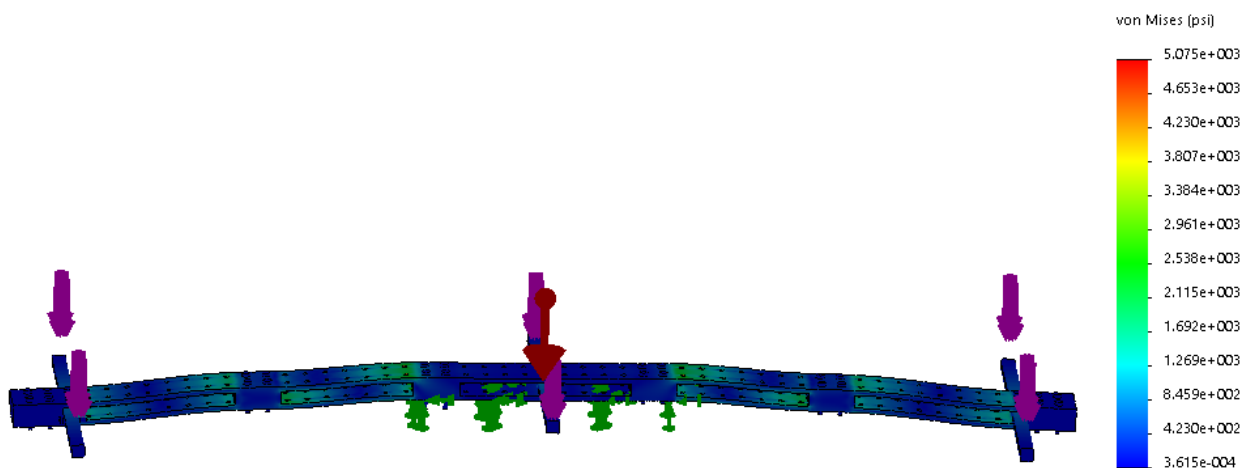


Figure 6.1.1. Strongback Study 1 – FEA stress plot.

STRESS SAFETY FACTOR: 13.15 (updated with new materials: 36.4)

MAXIMUM DEFLECTION [inches]: 0.023

STRONGBACK STUDY 2: Helicopter mode

- MATERIALS:** Lateral support beams – 17-4PH H900 – Yield Strength of 185 ksi.
Strongback plates and support blocks – AISI 4130 steel annealed at 865 °C – Yield Strength of 66.7 ksi.
- APPLIED LOADS:** Weight of entire strongback assembly and support beams (gravitational load).
Weight of each rotor assembly 14 pounds, applied at each end of the lateral support beams (six total).
Upwards thrust of 30 pounds, applied at each end of the lateral support beams (six total).
- FIXTURES:** Underside of bottom strongback plate fixed at location of strongback – support interface.
- NOTES:** Net load applied at end of lateral support beams was 16 pounds upwards (six total). 30 pounds up – 14 pounds down = 16 pounds up.

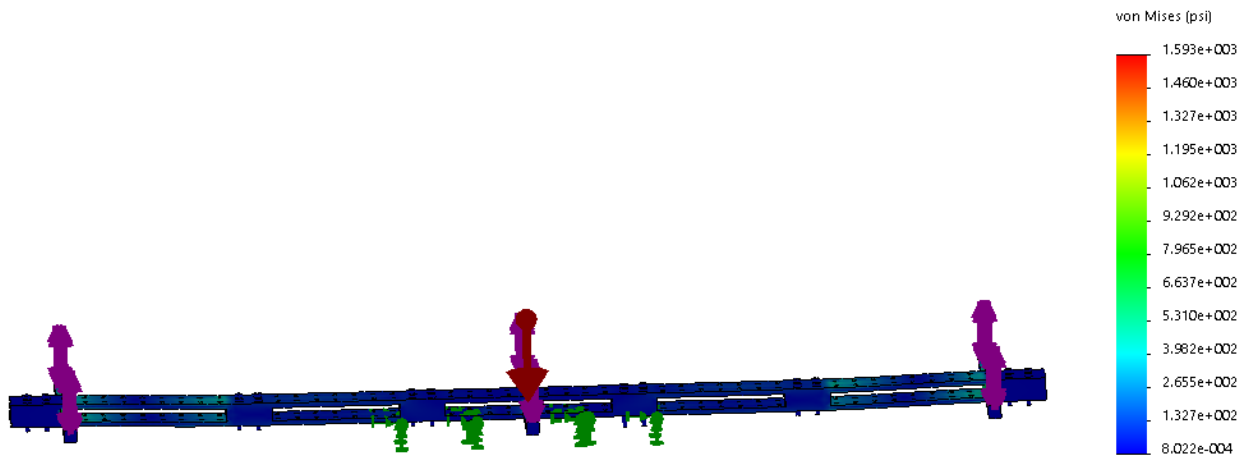


Figure 6.1.2. Strongback Study 2 – FEA stress plot.

STRESS SAFETY FACTOR: 41.87 (updated with new materials: 116)

MAXIMUM DEFLECTION [inches]: 0.0038

OBSERVATIONS: The SF for this study is less than that of Study 1 because the six 16-pound upward loads help to counteract the weight of the strongback.

STRONGBACK STUDY 3: Airplane mode

MATERIALS: Lateral support beams – 17-4PH H900 – Yield Strength of 185 ksi.
Strongback plates and support blocks – AISI 4130 steel annealed at 865 °C – Yield Strength of 66.7 ksi.

APPLIED LOADS: Weight of entire strongback assembly and support beams.
Weight of each rotor assembly 14 pounds, applied at each end of the lateral support beams (six total).
Forward thrust of 30 pounds (airplane mode), applied at each end of the lateral support beams (six total).

FIXTURES: Underside of bottom strongback plate fixed at location of strongback – support interface.

NOTES: Mesh was refined to obtain more accurate results.

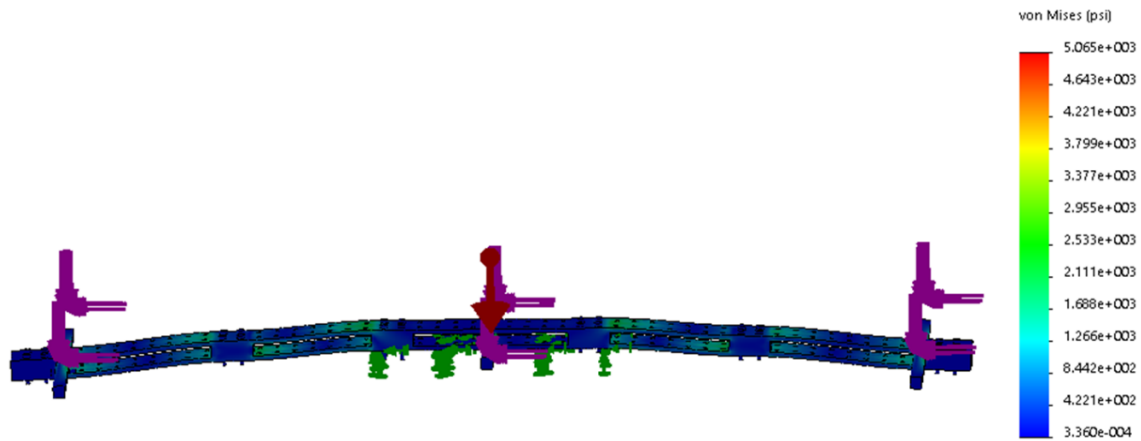


Figure 6.1.3. Strongback Study 3 – FEA stress plot.

STRESS SAFETY FACTOR: 13.18 (updated with new materials: 36.53)

MAXIMUM DEFLECTION [inches]: 0.023

STRONGBACK STUDY 4: Non-operational case – full side load

MATERIALS: Lateral support beams – 17-4PH H900 – Yield Strength of 185 ksi.
Strongback plates and support Blocks – AISI 4130 steel annealed at 865 °C – Yield Strength of 66.7 ksi.

APPLIED LOADS: Weight of entire strongback assembly and support beams (gravitational load).
Weight of each rotor assembly 14 pounds, applied at each end of the lateral support beams (six total).
Upward thrust of 30 pounds, applied at the three far ends of the lateral support beams (three total).

FIXTURES: Underside of bottom strongback plate fixed at location of strongback – support interface.

NOTES: This case is a hypothetical situation when all of the rotors on one side of the strongback are running and the rotors on the other side (close side) are off.

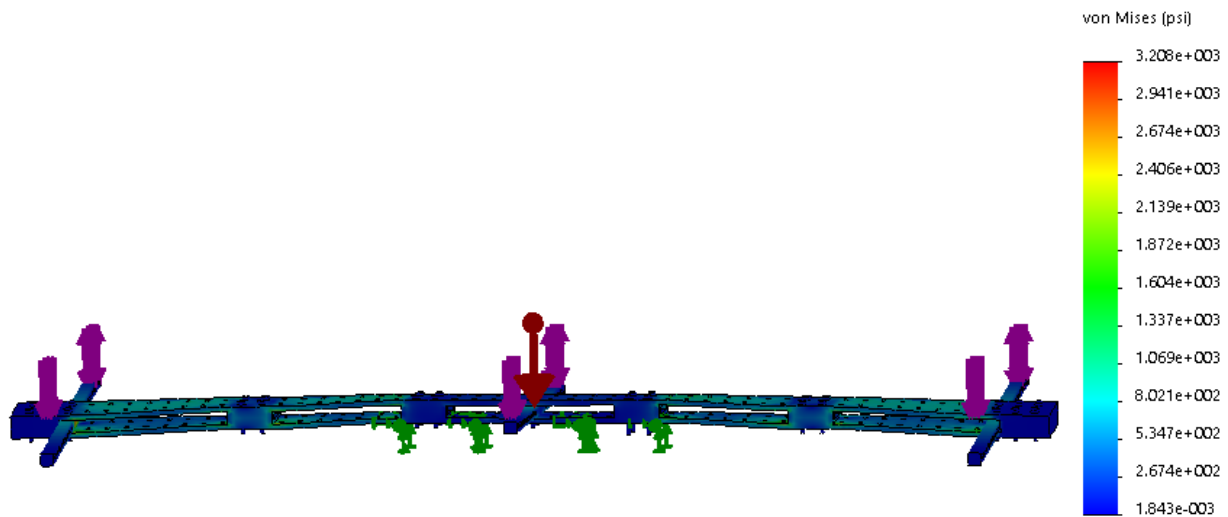


Figure 6.1.4. Strongback Study 4 – FEA stress plot.

STRESS SAFETY FACTOR: 20.79 (updated with new materials: 57.67)

MAXIMUM DEFLECTION [inches]: 0.026

STRONGBACK STUDY 5: Non-operational case –single rotor load

- MATERIALS:** Lateral support beams – 17-4PH H900 – Yield Strength of 185 ksi.
Strongback plates and support blocks – AISI 4130 steel annealed at 865 °C – Yield Strength of 66.7 ksi.
- APPLIED LOADS:** Weight of entire strongback assembly and support beams (gravitational load).
Weight of each rotor assembly 14 pounds, applied at each end of the lateral support beams (six total).
Upward thrust of 30 pounds, applied at the far-left rotor.
- FIXTURES:** Underside of bottom strongback plate fixed at location of strongback – support interface.
- NOTES:** Mesh was refined to obtain more accurate results. This case is a hypothetical situation in which all of the rotors are off except for one (at the far side on the left).

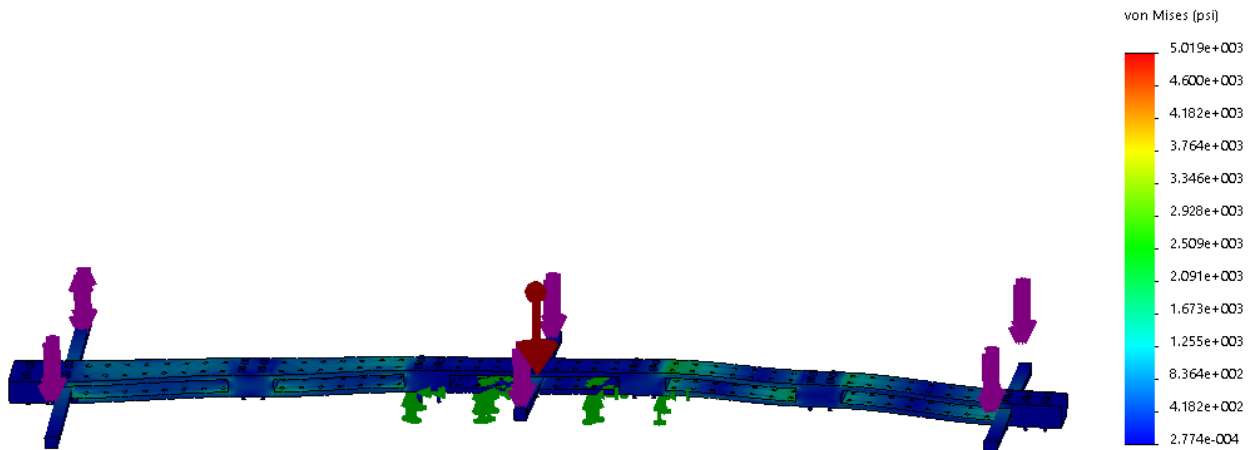


Figure 6.1.5. Strongback Study 5 – FEA stress plot.

STRESS SAFETY FACTOR: 13.29 (updated with new materials: 36.86)

MAXIMUM DEFLECTION [inches]: 0.026

Strongback analysis conclusion:

WORST CASE: Study 1

LOWEST SAFETY FACTOR: 36.4

6.2 Strut Assembly Analysis

The main areas for concern for the Strut Assembly were the forces on the pitching mechanism (threaded rod, lug, clevises, and bearings) and the forces on the upstream and downstream stopper. These three forces were derived and calculated in their respective worst-case scenarios. These forces were then used in stress analyses and FEA for the different parts of the strut assembly. Calculation 1 derives the force on the pitching mechanism. Calculation 2 derives the maximum force on the upstream stopper. Calculation 3 derives the maximum force on the downstream stopper.

CALCULATION 1: Force through the Pitching Mechanism

To simplify the problem, the force on the pitching mechanism F_{a_s} was solved for, without including the thrust from the propellers. It should be noted that the photos of the strut assembly in this section are outdated, but the kinematics are still the same. For pictures of the most recent design, see Figure 5.2.1.

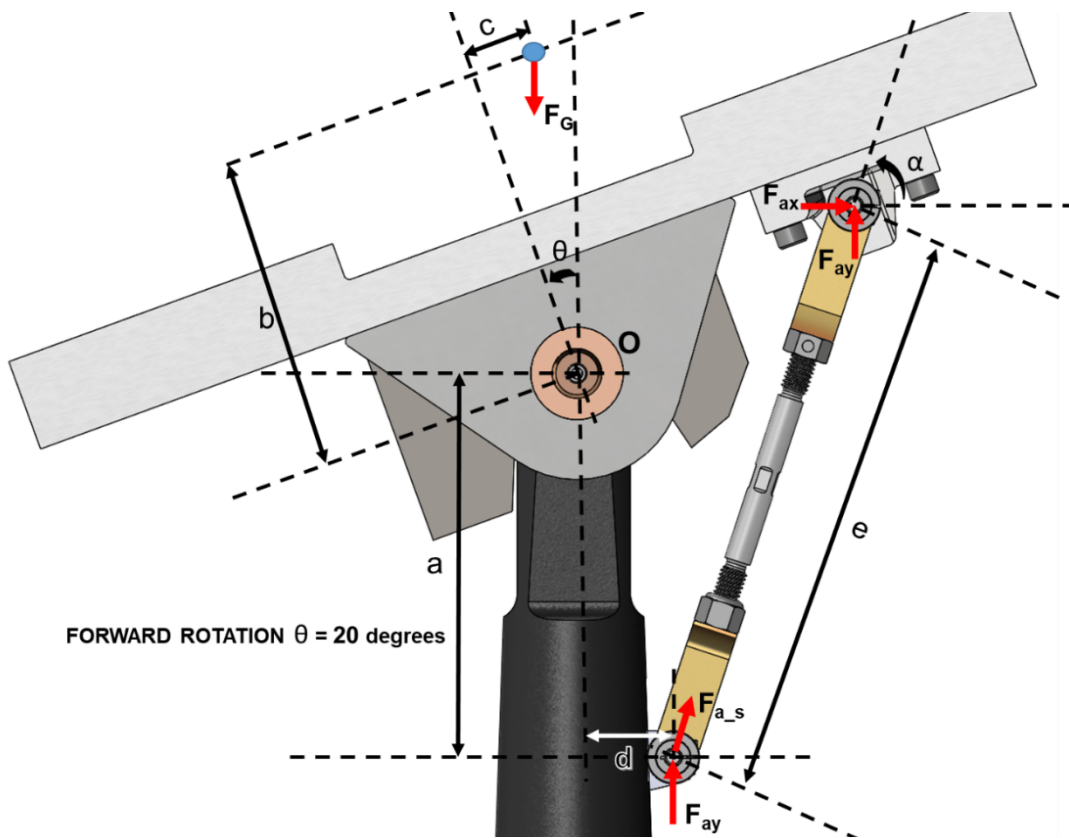


Figure 6.2.1. Strut assembly in pitched configuration when strongback rotation is 20 degrees forward without propeller load.

The strut assembly shown in Figure 6.2.1 shows the axial force on the pitching mechanism F_{a_s} , the weight of the assembly F_G , the vertical force required to move the lug F_{ay} , and the various dimensions. The angle α represents the angle of the axial force on the pitching mechanism with respect to the horizontal axis. The angle θ represents the rotation of the strongback with respect to the vertical axis. The location of the center of mass of weight was found using the model in SolidWorks. The sum of the moments was taken about point O and set to zero.

$$\sum M_O = F_G * (b * \sin \theta - c * \cos \theta) + F_{ay} * (d + e * \cos \alpha) - F_{ax} * (e * \sin \alpha - a) = 0 \quad (7.1)$$

where $F_{ax} = \frac{F_{ay}}{\tan \alpha}$ (7.2)

$$F_{ay} = \frac{F_G * (b * \sin \theta - c * \cos \theta)}{\frac{(e * \sin \alpha - a)}{\tan \alpha} - (d + e * \cos \alpha)} \quad (7.3)$$

and $F_{a_s} = \frac{F_{ay}}{\sin \alpha}$ (7.4)

Next, the force F_P from the rotors was added, as shown in Figure 6.2.2. Beta is the angle when the rotors are rotated relative to their respective vertical axes.

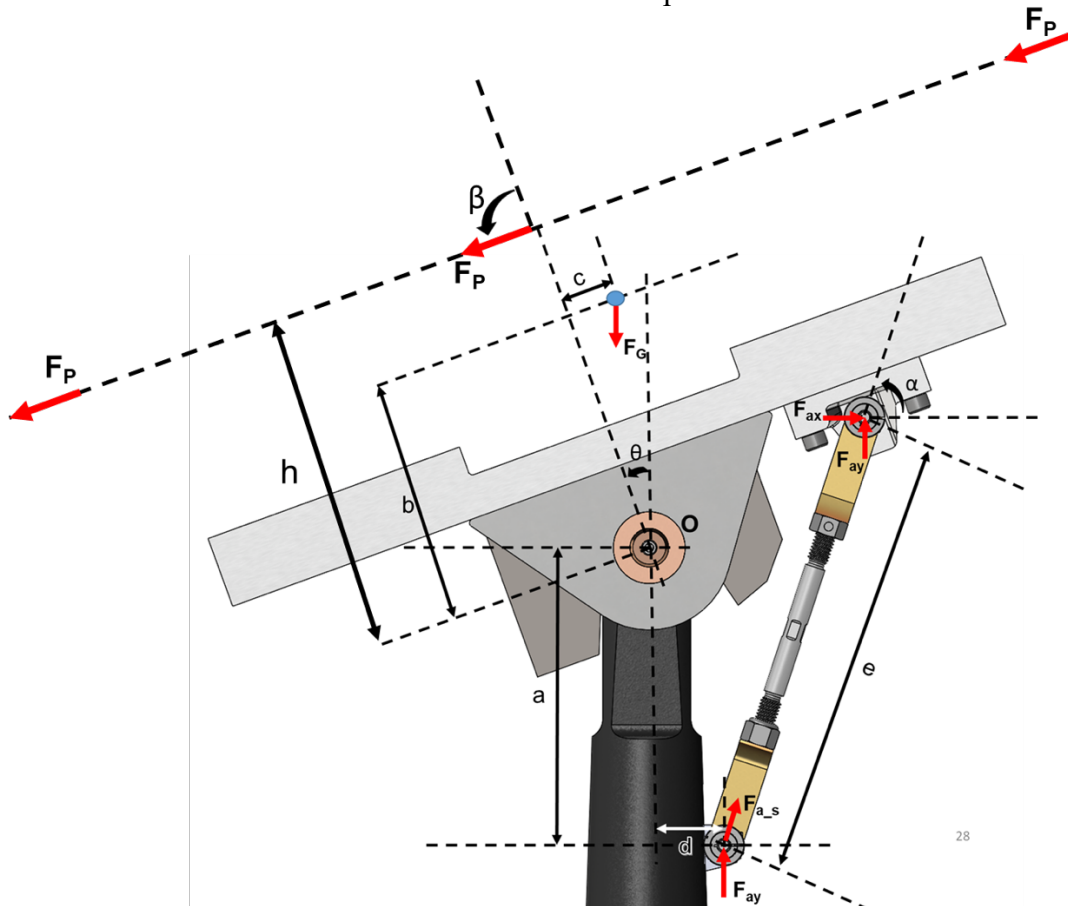


Figure 6.2.2. Schematic of strut assembly in pitched configuration when strongback rotation is 20 degrees forward with propeller load.

The sum of the moments about point O was set to zero and solved again, this time including the force from the rotors.

$$\sum M_O = 3 * F_P * h * \sin \beta + F_G * (b * \sin \theta - c * \cos \theta) + F_{ay} * (d + e * \cos \alpha) - F_{ax} * (e * \sin \alpha - a) = 0 \quad (7.5)$$

where $F_{ax} = \frac{F_{ay}}{\tan \alpha}$ (7.6)

$$F_{ay} = \frac{6 * F_P * h * \sin \beta + F_G * (b * \sin \theta - c * \cos \theta)}{\frac{(e * \sin \alpha - a)}{\tan \alpha} - (d + e * \cos \alpha)} \quad (7.7)$$

and $F_{as} = \frac{F_{ay}}{\sin \alpha}$ (7.8)

The final equation solving for the axial force on the pitching mechanism was:

$$F_{as} = \frac{6 * F_P * h * \sin \beta + F_G * (b * \sin \theta - c * \cos \theta)}{-a * \cos \alpha - d * \sin \alpha} \quad (7.9)$$

Equation 7.9 was used to solve for the axial force in various configurations. For the purposes of this analysis the range of the rotor angle is between 90 degrees forward and 10 degrees backward. The bottom clevis of the rotor assembly is secured to the two bottom holes in the vertical support beam. (See Sections 6.3 and 6.4 for details.)

There are several configurations for the MTB when the blades come closer than five inches to the walls. There are also configurations in which we have to ability to operate at a 30-pound thrust load, but are not planning to do so. For example, the rotors are planned to have only 10 pounds of thrust in airplane mode. Although the MTB is not planning to operate in these problematic configurations, the load for these configurations will be calculated. This load will be referred to as a theoretical load and will be shown highlighted in yellow so they can be easily differentiated from the operational loads. The maximum theoretical load will be color coded in orange. The maximum operational load will be shown in red. The maximum operational loads and maximum theoretical loads were found for different rotations of the rotors and rotations of the strongback. The following tables show the calculations of the axial force in these different configurations.

It should be noted that the value of the thrust from the rotors/propellers, F_p , can range between zero and 30 pounds. The values shown for the various studies were the worst cases and the operational cases. Some pictures of the worst cases, in terms of loads or proximity to the wind tunnel walls, are shown. Note that although pictures for every configuration are not presented, all of the different configurations were tested. The value of a, alpha, and theta was determined from the rotation of the strongback.

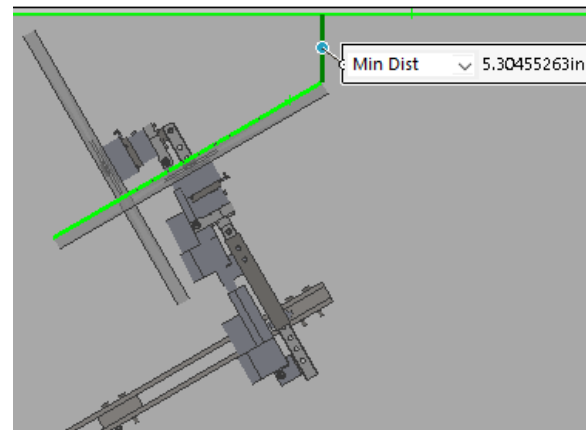
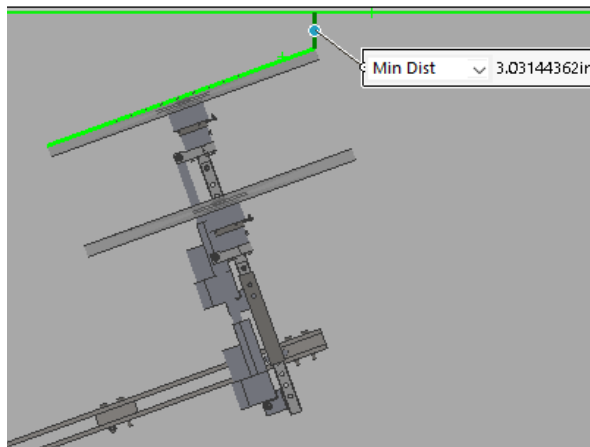
Max Operational Load = max load expecting to test in, used for analyses of tilting mech, etc
Max Theoretical Load = max load that can theoretically be obtained
Theoretical configuration = blades too close to wall, or operating at higher than planned loads.

Table 7. Flat, no rotation of rotors, helicopter mode.

0 DEGREES TALL	Rotation of Strongback			
	Flat	10 back	20 forward	30 forward
a (in)	8.140	9.968	6.797	6.577
b (in)	8.133	8.133	8.133	8.133
c (in)	-0.147	-0.147	-0.147	-0.147
d (in)	1.875	1.875	1.875	1.875
e (in)	9.638	9.638	9.638	9.638
alpha (radians)	1.154	1.173	1.235	1.318
theta (rad)	0.000	2.966	0.349	0.523
MTB Weight (lbs)	236.880	236.880	236.880	236.880
Propeller Thrust (lbs)	30.000	30.000	30.000	30.000
beta (rad)	0.000	0.000	0.000	0.000
h (in)	27.588	27.588	27.588	27.588
Fya (lbs)	6.362	49.941	162.697	278.077
Fax (lbs)	2.818	21.010	56.835	71.715
Fa (lbs)	6.958	54.180	172.338	287.176

0 DEGREES SHORT	Rotation of Strongback			
	Flat	10 back	20 forward	30 forward
a (in)	8.140	9.968	6.797	6.577
b (in)	5.763	5.763	5.763	5.763
c (in)	-0.148	-0.148	-0.148	-0.148
d (in)	1.875	1.875	1.875	1.875
e (in)	9.638	9.638	9.638	9.638
alpha (radians)	1.154	1.173	1.235	1.318
theta (rad)	0.000	2.966	0.349	0.523
MTB Weight (lbs)	236.880	236.880	236.880	236.880
Propeller Thrust (lbs)	30.000	30.000	30.000	30.000
beta (rad)	0.000	0.000	0.000	0.000
h (in)	18.588	18.588	18.588	18.588
Fya (lbs)	6.376	33.729	117.556	199.538
Fax (lbs)	2.825	14.189	41.066	51.460
Fa (lbs)	6.974	36.592	124.523	206.066

The left side of Table 7 shows the forces for the various rotations of the strongback when the rotor is tall and is not rotated. The right side of the table shows the forces for the various rotations of the strongback (flat or 0 degrees rotation, 10 degrees back, 20 degrees forward, and 30 degrees forward) when the rotor was short and was not rotated. For this set of configurations, the maximum operational load was 206 pounds and the maximum theoretical load was 287 pounds.



Figures 6.2.3 and 6.2.4. Distance from the wind tunnel ceiling for zero-degrees rotor rotation. Left - strongback rotation 20 degrees forward. Right - strongback rotation 30 degrees forward.

It was assumed that the rotor could produce accurate measurements if it maintained at least a five inch clearance from the wall. As the rotor gets closer to the wall, the airflow would be affected and it would start to interfere with the loads and acoustics measurements. As shown in Figure

6.2.3, the rotor is too close to the wall. Thus, when the rotor was tall and had 0 degrees rotor rotation, a rotation of the strongback of 20 degrees or more would be a theoretical configuration. Figure 6.2.4 shows that the rotor in its short and zero degrees rotor rotation configuration would not interfere with the ceiling of the wind tunnel.

Table 8. Rotors rotated 45 degrees forward.

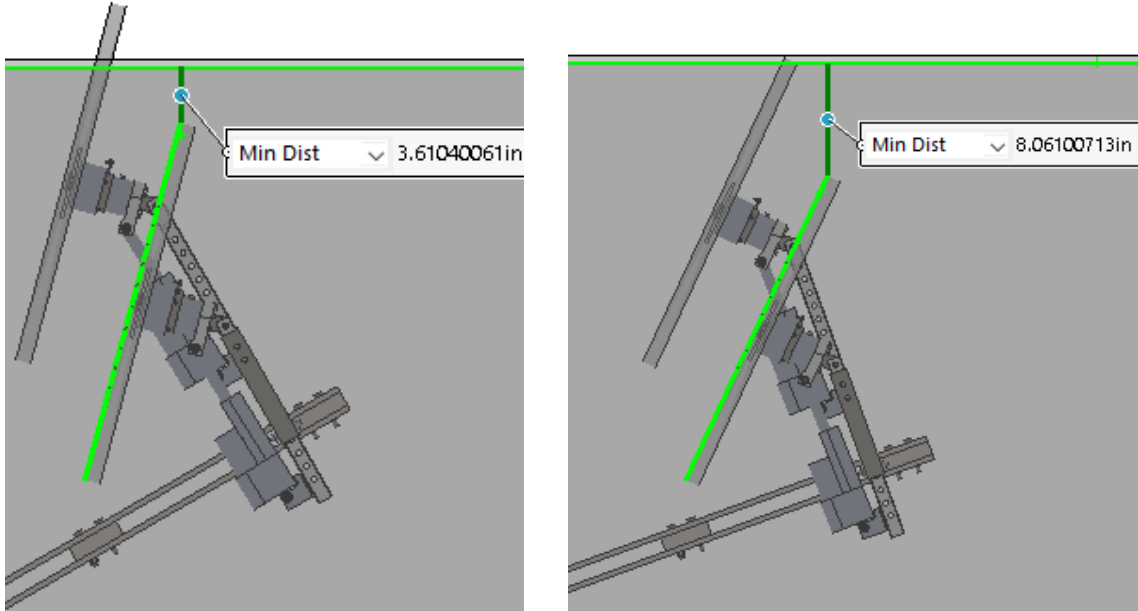
45 DEGREES TALL	Rotation of Strongback			
	Flat	10 back	20 forward	30 forward
a (in)	8.140	9.968	6.797	6.577
b (in)	7.998	7.998	7.998	7.998
c (in)	-0.384	-0.384	-0.384	-0.384
d (in)	1.875	1.875	1.875	1.875
e (in)	9.638	9.638	9.638	9.638
alpha (radians)	1.154	1.173	1.235	1.318
theta (rad)	0.000	2.966	0.349	0.523
MTB Weight (lbs)	236.880	236.880	236.880	236.880
Propeller Thrust (lbs)	15.000	15.000	15.000	15.000
beta (rad)	0.785	0.785	0.785	0.785
h (in)	25.753	25.753	25.753	25.753
Fya (lbs)	315.478	309.892	558.040	745.949
Fax (lbs)	139.758	130.369	194.941	192.378
Fa (lbs)	345.048	336.198	591.110	770.357

45 DEGREES SHORT	Rotation of Strongback			
	Flat	10 back	20 forward	30 forward
a (in)	8.140	9.968	6.797	6.577
b (in)	5.632	5.632	5.632	5.632
c (in)	-0.384	-0.384	-0.384	-0.384
d (in)	1.875	1.875	1.875	1.875
e (in)	9.638	9.638	9.638	9.638
alpha (radians)	1.154	1.173	1.235	1.318
theta (rad)	0.000	2.966	0.349	0.523
MTB Weight (lbs)	236.880	236.880	236.880	236.880
Propeller Thrust (lbs)	15.000	15.000	15.000	15.000
beta (rad)	0.785	0.785	0.785	0.785
h (in)	16.753	16.753	16.753	16.753
Fya (lbs)	211.020	199.374	378.220	507.187
Fax (lbs)	93.483	83.875	132.124	130.802
Fa (lbs)	230.800	216.298	400.633	523.782

	Flat	10 back	20 forward	30 forward
Propeller Thrust (lbs)	30.000	30.000	30.000	30.000
Fya	614.372	579.855	943.567	1204.709
Fax	272.169	243.940	329.617	310.691
Fa	671.960	629.078	999.483	1244.127

	Flat	10 back	20 forward	30 forward
Propeller Thrust (lbs)	30.000	30.000	30.000	30.000
Fya	405.459	374.992	629.015	805.622
Fax	179.620	157.756	219.734	207.768
Fa	443.464	406.824	666.291	831.982

It is unclear as to what thrust the MTB will operate when the rotors are rotated 45 degrees forward. This was why Table 8 results were shown for both 15- and 30-pounds of rotor thrust. For this set of configurations, the maximum operational load was 666 pounds and the maximum theoretical load was 1,244 pounds.



Figures 6.2.5 and 6.2.6. Distance from the wind tunnel ceiling for 45-degree rotor rotation.
Left - strongback rotation 30 degrees forward.
Right - strongback rotation 20 degrees forward.

Figure 6.2.5 shows that when the strongback was pitched 30 degrees forward and the rotor was tilted 45 degrees forward, the rotor was too close to the ceiling even when in its shortest configuration. Figure 6.2.6 shows that when the strongback was pitched only 20 degrees forward and the rotor was tilted 45 degrees forward, the rotor was too close in its tall configuration, but was at an acceptable distance from the ceiling in its short configuration.

Table 9. Rotors rotated 90 degrees forward, airplane mode.

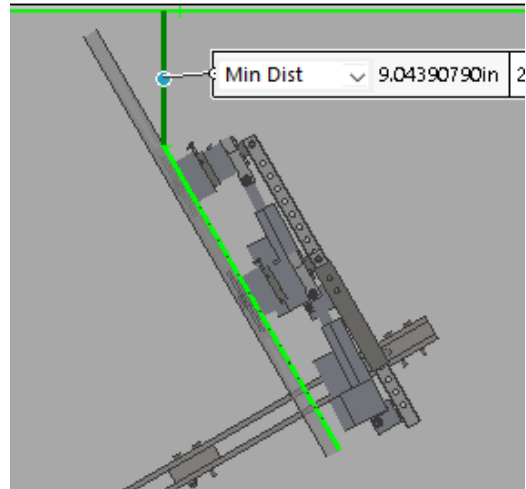
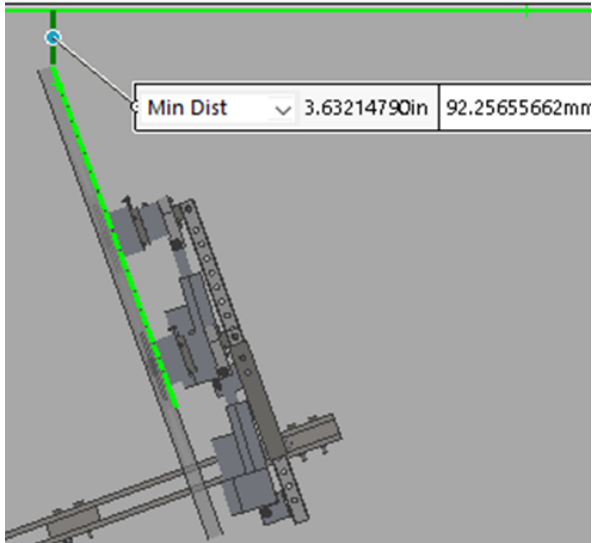
90 DEGREES TALL Strongback Tilt	Rotation of Strongback			
	Flat	10 back	20 forward	30 forward
a (in)	8.140	9.968	6.797	6.577
b (in)	7.756	7.756	7.756	7.756
c (in)	-0.452	-0.452	-0.452	-0.452
d (in)	1.875	1.875	1.875	1.875
e (in)	9.638	9.638	9.638	9.638
alpha (radians)	1.154	1.173	1.235	1.318
theta (rad)	0.000	2.966	0.349	0.523
MTB Weight (lbs)	236.880	236.880	236.880	236.880
Propeller Thrust (lbs)	10.000	10.000	10.000	10.000
beta (rad)	1.570	1.570	1.570	1.570
h (in)	21.625	21.625	21.625	21.625
Fya (lbs)	256.272	249.448	476.829	646.439
Fax (lbs)	113.530	104.940	166.571	166.715
Fa (lbs)	280.293	270.623	505.086	667.591

90 DEGREES SHORT	Rotation of Strongback			
	Flat	10 back	20 forward	30 forward
a (in)	8.140	9.968	6.797	6.577
b (in)	5.386	7.756	7.756	5.386
c (in)	-0.450	-0.450	-0.450	-0.450
d (in)	1.875	1.875	1.875	1.875
e (in)	9.638	9.638	9.638	9.638
alpha (radians)	1.154	1.173	1.235	1.318
theta (rad)	0.000	2.966	0.349	0.523
MTB Weight (lbs)	236.880	236.880	236.880	236.880
Propeller Thrust (lbs)	10.000	10.000	10.000	10.000
beta (rad)	1.570	1.570	1.570	1.570
h (in)	12.625	12.625	12.625	12.625
Fya (lbs)	157.647	160.555	349.626	416.524
Fax (lbs)	69.838	67.544	122.135	107.420
Fa (lbs)	172.424	174.184	370.345	430.153

	Flat	10 back	20 forward	30 forward
Propeller Thrust (lbs)	30.000	30.000	30.000	30.000
Fya	729.721	677.069	1087.503	1373.114
Fax	323.269	284.837	379.898	354.122
Fa	798.120	734.544	1151.948	1418.042

	Flat	10 back	20 forward	30 forward
Propeller Thrust (lbs)	30.000	30.000	30.000	30.000
Fya	434.054	410.207	706.147	840.767
Fax	192.288	172.571	246.679	216.832
Fa	474.739	445.028	747.993	868.277

Next the rotors were put in airplane mode, a full 90 degrees forward rotation. When the rotors are in airplane mode, the thrust load for the rotors is not planning to exceed 10 pounds. That is why all configurations with the 30-pound thrust load are theoretical (highlighted in yellow). For this set of configurations, the maximum operational load was 430 pounds and the maximum theoretical load was 1,418 pounds. Note this value is updated to 1,453 because of the increased weight of the test stand.



Figures 6.2.7 and 6.2.8. Distance from the wind tunnel ceiling for 90-degree rotor rotation.
 Left - strongback rotation 20 degrees forward.
 Right - strongback rotation 30 degrees forward.

Figure 6.2.7 shows the distance from the ceiling to the rotor in its tall 90 degree forward rotation configuration, when the strongback is pitched 20 degrees forward. The rotor is too close to the wall for this configuration. Figure 6.2.8 shows that the rotor in its tall 90 degree forward rotation configuration, when the strongback is pitched 20 degrees forward, is also too close to the ceiling. However, in the short configuration, the rotor is at an acceptable distance of about nine inches from the ceiling.

Table 10. Rotors rotated 90 degrees forward, airplane mode.

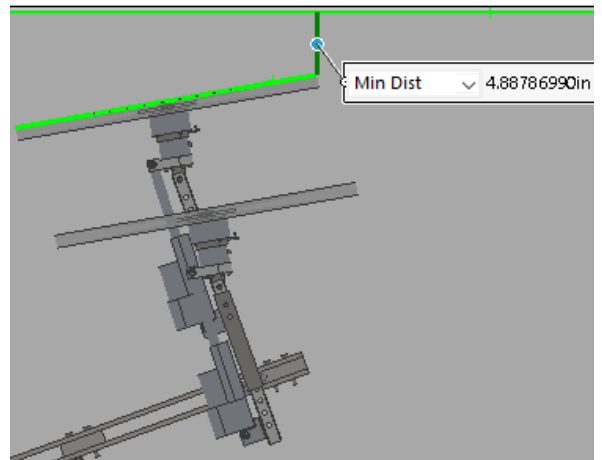
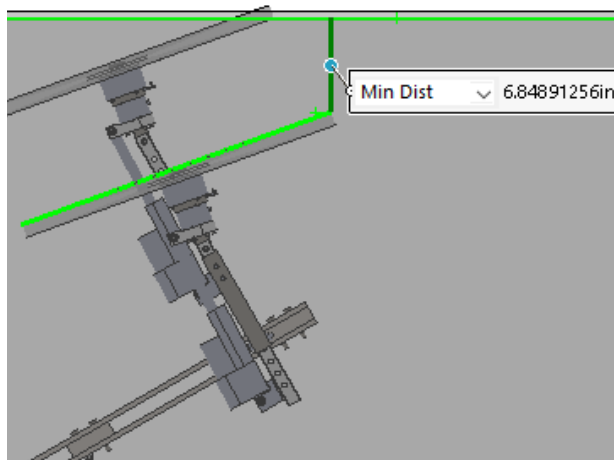
-10 DEGREES TALL	Rotation of Strongback			
	Flat	10 back	20 forward	30 forward
a (in)	8.140	9.968	6.797	6.577
b (in)	8.117	8.117	8.117	8.117
c (in)	-0.085	-0.085	-0.085	-0.085
d (in)	1.875	1.875	1.875	1.875
e (in)	9.638	9.638	9.638	9.638
alpha (radians)	1.154	1.173	1.235	1.318
theta (rad)	0.000	2.966	0.349	0.523
MTB Weight (lbs)	236.880	236.880	236.880	236.880
Propeller Thrust (lbs)	30.000	30.000	30.000	30.000
beta (rad)	-0.174	-0.174	-0.174	-0.174
h (in)	27.374	27.374	27.374	27.374
Fya (lbs)	-152.346	-88.709	-42.111	34.498
Fax (lbs)	-67.490	-37.319	-14.711	8.897
Fa (lbs)	-166.626	-96.240	-44.607	35.627

-10 DEGREES SHORT	Rotation of Strongback			
	Flat	10 back	20 forward	30 forward
a (in)	8.140	9.968	6.797	6.577
b (in)	5.748	5.748	5.748	5.748
c (in)	-0.086	-0.086	-0.086	-0.086
d (in)	1.875	1.875	1.875	1.875
e (in)	9.638	9.638	9.638	9.638
alpha (radians)	1.154	1.173	1.235	1.318
theta (rad)	0.000	2.966	0.349	0.523
MTB Weight (lbs)	236.880	236.880	236.880	236.880
Propeller Thrust (lbs)	30.000	30.000	30.000	30.000
beta (rad)	-0.174	-0.174	-0.174	-0.174
h (in)	18.374	18.374	18.374	18.374
Fya (lbs)	-101.035	-58.586	-21.074	34.715
Fax (lbs)	-44.759	-24.647	-7.362	8.953
Fa (lbs)	-110.505	-63.559	-22.323	35.850

	Flat	10 back	20 forward	30 forward
Propeller Thrust (lbs)	0.000	0.000	0.000	0.000
Fya	3.680	52.215	159.138	273.976
Fax	1.630	21.966	55.592	70.658
Fa	4.025	56.647	168.569	282.940

	Flat	10 back	20 forward	30 forward
Propeller Thrust (lbs)	0.000	0.000	0.000	0.000
Fya	3.695	36.007	114.011	195.460
Fax	1.637	15.148	39.828	50.409
Fa	4.041	39.063	120.768	201.855

The last configuration for the rotors was at 10-degrees backward rotation. For this set of configurations, the maximum operational load was 202 pounds and the maximum theoretical load was 283 pounds.



Figures 6.2.9 and 6.2.10. Distance from the wind tunnel ceiling for -10-degrees rotor rotation.
 Left - strongback rotation 30 degrees forward.
 Right - strongback rotation 20 degrees forward.

Figure 6.2.9 shows that the rotor in its short, or 10 degrees, backward configuration is at an acceptable distance from the ceiling when the strongback is rotated 30 degrees forward. However, the rotor in its tall configuration is too close to the ceiling. Figure 6.2.10 shows that the rotor in its

tall, or 10 degrees backward configuration, is also too close to the ceiling when the strongback is rotated 20 degrees forward.

Using Equation 7.9 for all the different configurations of the MTB, the worst-case axial load on the pitching mechanism was determined. The overall maximum operational load case was for a rotor rotation of 45 degrees forward, in its short configuration, when the strongback was rotated 20 degrees forward. The overall maximum operational load was 666 pounds.

The overall maximum theoretical load case was for a rotor rotation of 90 degrees forward, in its tall configuration, when the strongback was rotated 30 degrees forward. The overall maximum theoretical load was 1,418 pounds.

UPDATE: The weight of the assembly was increased from 236.88 to 265.5 pounds (estimate including electronic hardware). The new overall maximum theoretical load was 1,453 pounds ($F_{ya} = 1,407$ pounds and $F_{ax} = 363$ pounds).

CALCULATION 2: Force on the Upstream Hard Stop

In this section, the maximum force on the upstream hard stop was calculated. The purpose of the upstream hard stop was to stop the MTB from rotating forward in the event that the pitching mechanism (the threaded rod, clevises, etc.) failed. The hard stop was positioned to hit the single heavy strut when the MTB was 22 degrees forward. The worst-case scenario that would result in the maximum load on the hard stop was when all the rotors were in the tall position, rotated 90 degrees forward, with 30 pounds of thrust. During testing, when the rotors are rotated 90 degrees forward, the thrust for each rotor was planned to be less than 10 pounds. Therefore, this worst loading case is a theoretical loading case.

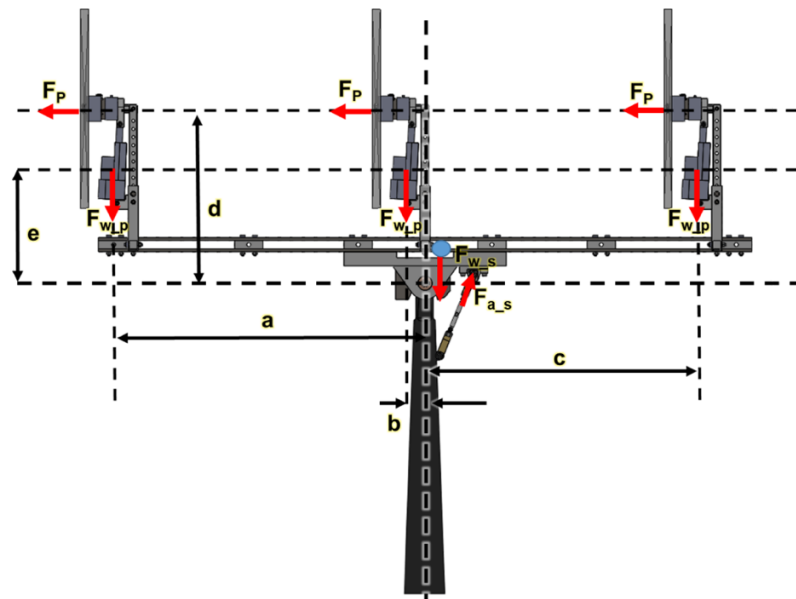


Figure 6.2.11. Schematic of MTB with zero-degrees strongback rotation and 90-degree rotor rotation.

The MTB was first modeled with zero degrees strongback rotation in Figure 6.2.11. F_{w_p} was the weight of two of the propeller assemblies and one lateral support beam. F_p was the thrust from the propeller. F_{w_s} was the weight of the strongback assembly and the top of the strut assembly (hinges and supporting interfaces). The location of the center of mass of the different weights were found using the model in SolidWorks. Note that the picture of the MTB in this figure is outdated, but the kinematics are still the same. For an updated picture of the MTB, see the Design Section.

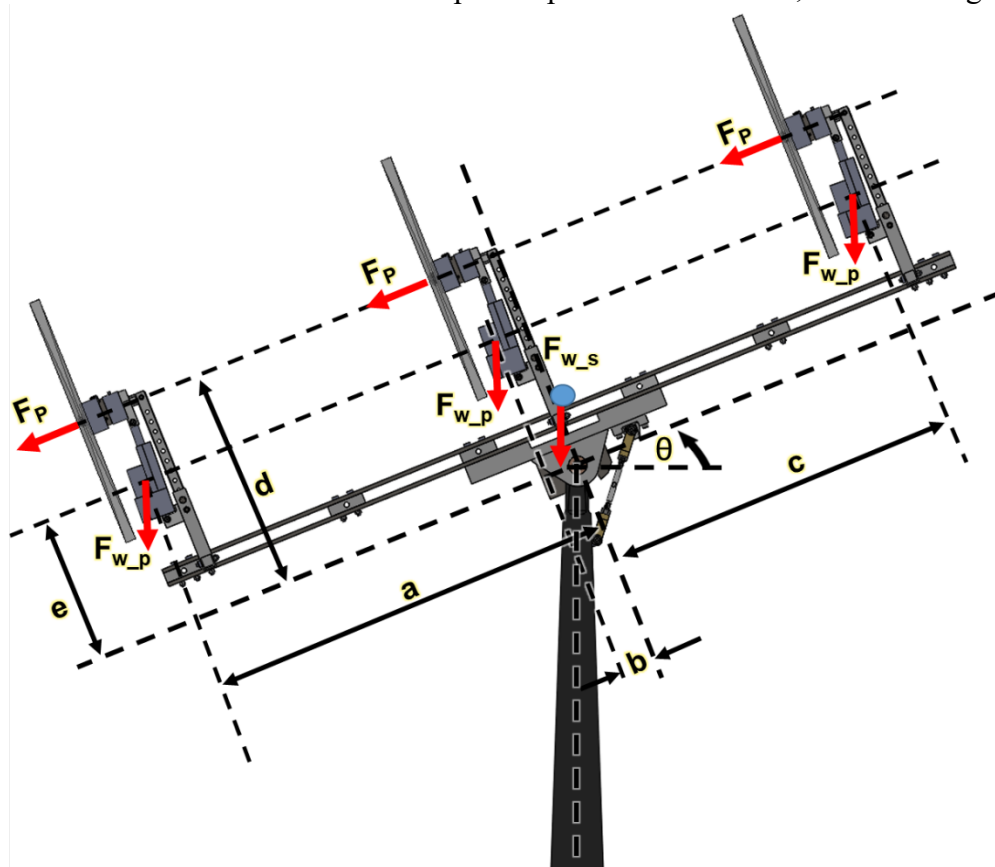


Figure 6.2.12. Schematic of MTB with 22-degrees strongback rotation and 90-degrees rotor rotation – Calculation 2.

The MTB was then rotated forward 22 degrees, as shown in Figure 6.2.12. Note that some similar variables were used in Calculation 1, but they may have different values in Calculation 2. Figure 6.1.13 shows a close up view of the schematics about the center of rotation. This figure shows that the force F_{a_Uhs} is the force on the upstream hard stop. Using these schematics, this force was derived and calculated.

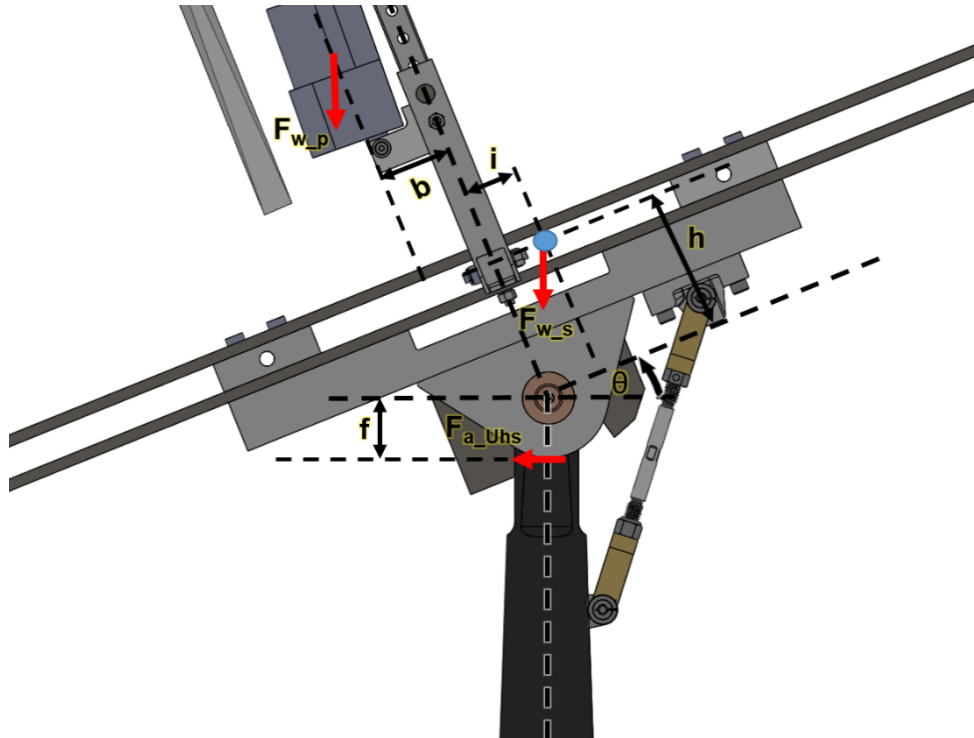


Figure 6.2.13. Close up schematic of MTB with 22-degrees strongback rotation and 90- degrees rotor rotation – Calculation 2.

The sum of the moments about the center shaft (point of rotation) was set to zero.

$$\sum M_O = F_{wp} * (a * \cos \theta + e * \sin \theta) + F_{wp} * (b * \cos \theta + e * \sin \theta) - F_{wp} * (c * \cos \theta - e * \sin \theta) + 6 * F_p * d + F_{ws} * (-i * \cos \theta + h * \sin \theta) - F_{a_{ahs}} * f = 0 \quad (7.10)$$

$$F_{a_{ahs}} = (F_{wp} * (\cos \theta * (a + b - c) + 3 * e * \sin \theta) + 6 * F_p * d + F_{ws} * (-i * \cos \theta + h * \sin \theta)) * \frac{1}{f} \quad (7.11)$$

Where:

$$a = 37.1 \text{ inches} \quad b = 1.1 \text{ inches} \quad c = 34.9 \text{ inches} \quad d = 20.74 \text{ inches}$$

$$e = 12.596 \text{ inches} \quad f = 2.0317 \text{ inches} \quad \theta = 22^\circ \quad h = 3.885 \text{ inches}$$

$$i = 0.0469 \text{ inches} \quad F_{wp} = 37.3 \text{ pounds} \quad F_p = 30 \text{ pounds} \quad F_{ws} = 145.4 \text{ pounds}$$

The force on the upstream hard stop, $F_{a_{ahs}}$ was calculated to be 2,254.6 pounds. This force was used in the FEA of the upstream hard stop.

CALCULATION 3: Force on the Downstream Hard Stop

In this section, the maximum force on the downstream hard stop was calculated. The purpose of the downstream hard stop was to stop the MTB from rotating backward in the event that the pitching mechanism (threaded rod, clevises, etc.) failed. The hard stop was positioned to hit the single heavy strut when the MTB was 14.25 degrees backward. The worst-case scenario that would result in the maximum load on the hard stop was when all the rotors were in the tall position, rotated 10 degrees backward, with 30 pounds of thrust. This worst loading case is an operational loading case.

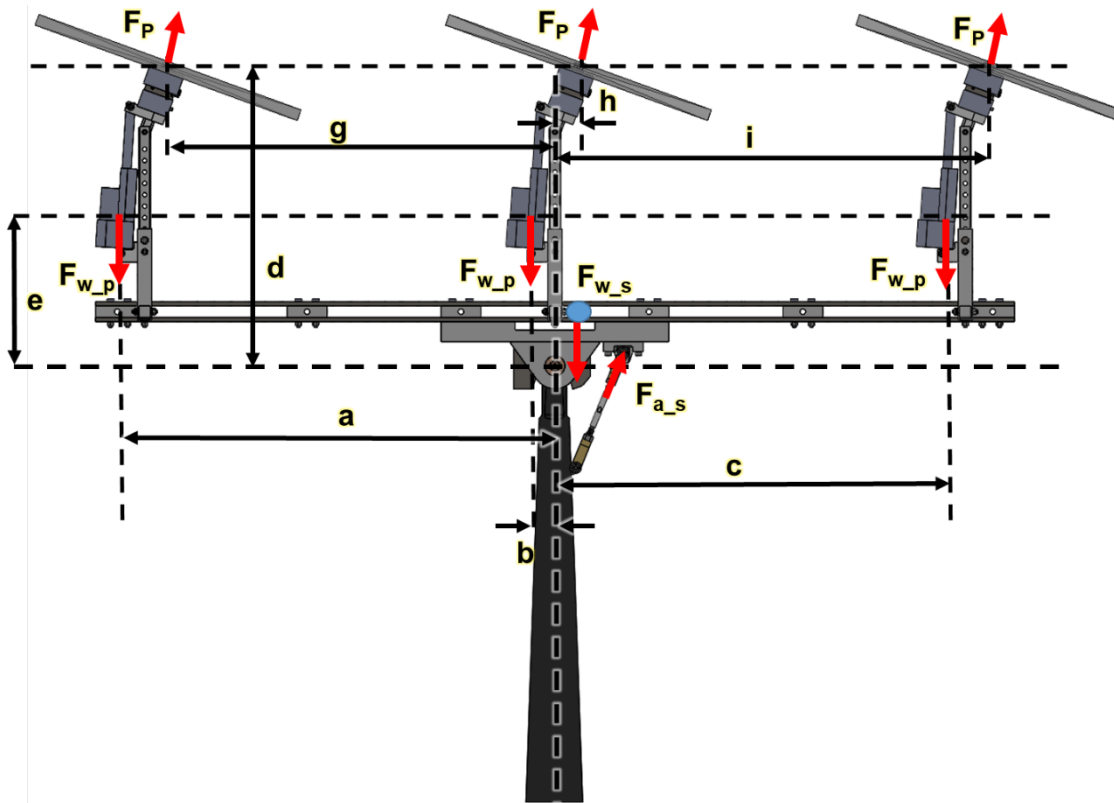


Figure 6.2.14. Schematic of MTB with zero-degrees strongback rotation and -10-degrees rotor rotation – Calculation 3.

The MTB was first modeled with zero-degrees strongback rotation in Figure 6.2.14. Similar to Calculation 2, F_{w_p} was the weight of two of the propeller assemblies and one lateral support beam. F_p was the thrust from the propeller. F_{w_s} was the weight of the strongback assembly and the top of the strut assembly (hinges and supporting interfaces). The location of the center of mass of the different weights were found using the SolidWorks model. Note that the picture of the MTB in this figure is outdated, but the kinematics are still the same. For an updated picture of the MTB, see Figure 5.1.

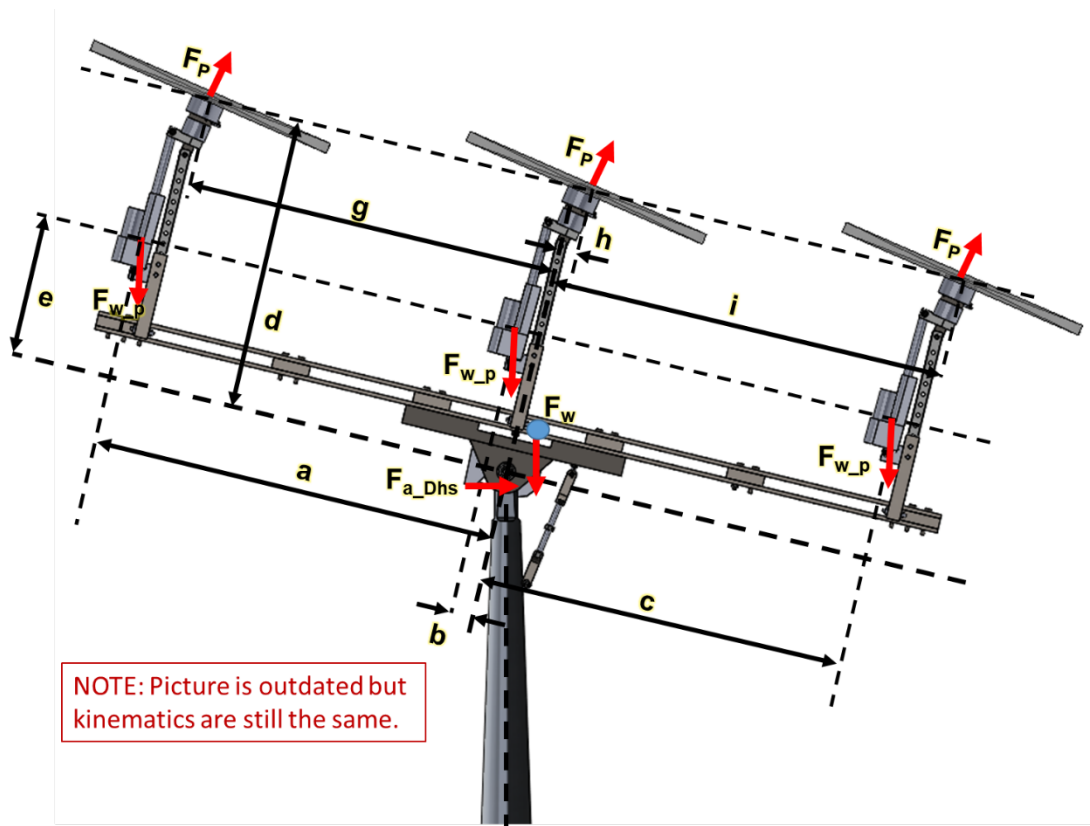
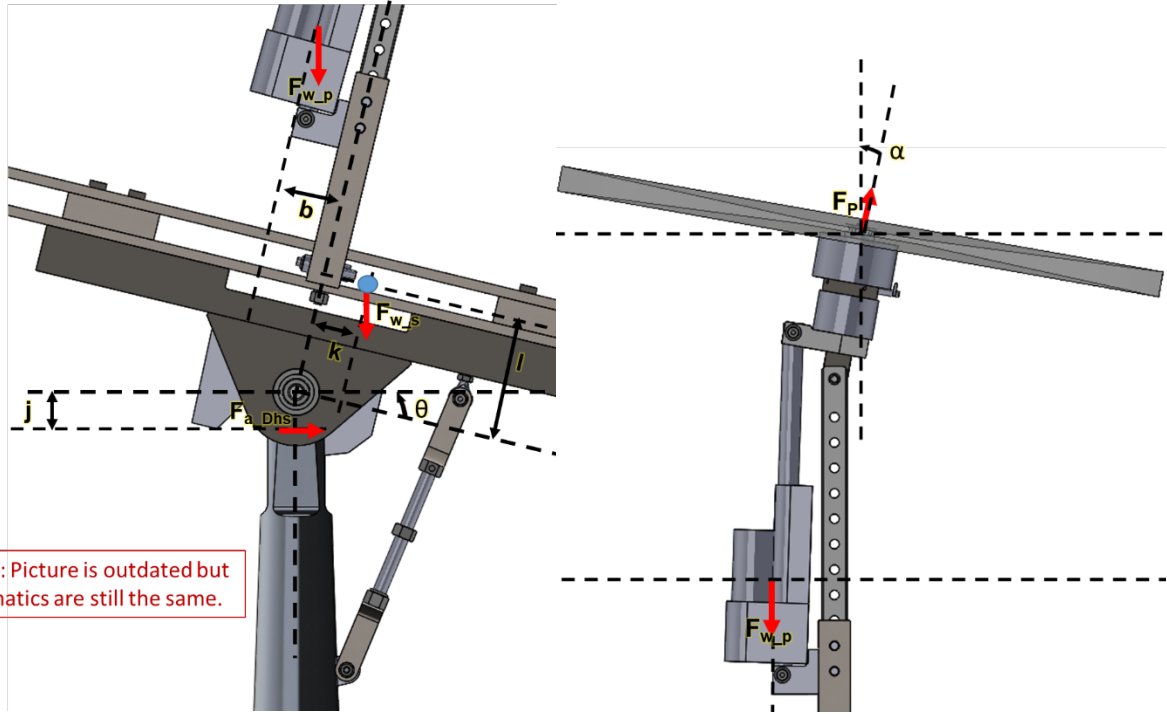


Figure 6.2.15. Schematic of MTB with -13.6-degrees strongback rotation and -10-degrees rotor rotation – Calculation 3.

The MTB was then rotated backward 13.6 degrees as shown in Figure 6.2.15. Note that some similar variables were used in Calculation 1 and 2, but they may have different values in Calculation 3. Figure 6.2.16 shows a focused view of the schematics about the center of rotation. This figure shows the force F_{a_Dhs} , which is the force on the upstream hard stop. Note that the angle θ , which represented the rotation of the strongback, was negative. θ was taken to be zero about the horizontal axis. Figure 6.2.17 shows a magnified view of the schematics of the rotor. Here, the angle α was also negative, however, zero degrees was defined at the vertical axis. Using these schematics, the force F_{a_Dhs} was derived and calculated.



Figures 6.2.16 and 6.2.17. Close up schematics of MTB with -13.6-degrees strongback rotation and -10-degree rotor rotation. Left - view of pitching mechanism. Right - view of rotor.

The sum of the moments about the center shaft (point of rotation) was set to zero.

$$\sum M_O = F_{w_p} * (a * \cos \theta + e * \sin \theta) + F_{w_p} * (b * \cos \theta + e * \sin \theta) - F_{w_p} * (c * \cos \theta - e * \sin \theta) + 6 * F_p * \sin \alpha * d + 2 * F_p * \cos \alpha * (-g + i + h) + F_{a_{Dhs}} * j + F_{w_s} * (-k * \cos \theta + l * \sin \theta) = 0 \quad (7.12)$$

$$F_{a_{Dhs}} = \left(-F_{w_p} * (\cos \theta * (a + b - c) + 3 * e * \sin \theta) - 6 * F_p * \sin \alpha * d - 2 * F_p * \cos \alpha * (-g + i + h) - F_{w_s} * (-k * \cos \theta + l * \sin \theta) \right) * \frac{1}{j} \quad (7.13)$$

Where:

$$a = -36.26 \text{ inches} \quad b = 0.119 \text{ inches} \quad c = 35.88 \text{ inches} \quad d = 26.25 \text{ inches}$$

$$e = 15.596 \text{ inches} \quad g = 33.907 \text{ inches} \quad h = 2.09 \text{ inches} \quad i = 38.09 \text{ inches}$$

$$j = 1.549 \text{ inches} \quad k = 0.066 \text{ inches} \quad l = 4.07 \text{ inches}$$

$$\theta = -14.25 \text{ degrees} \quad \alpha = -20 \text{ degrees} \quad F_{w_p} = 37.3 \text{ pounds} \quad F_{w_s} = 145.5 \text{ pounds}$$

The force on the downstream hard stop, $F_{a_{Dhs}}$ was calculated to be 2,816.6 pounds. This force was used in the FEA of the downstream hard stop.

Strut Assembly FEA

In this section, FEA was performed on several parts of the strut assembly in SolidWorks. A common load used in this analysis was 420 pounds. This load was derived from adding the weight of the entire assembly (not including the strut) 240 pounds and the six 30 pound loads of thrust from the rotors. This is an over estimate of the load that parts of the strut assembly would experience from the weight of the assembly and the thrust from the propellers. Since the propellers can only rotate to 90 degrees forward and the strongback can only go 30 degrees forward, the actual load on the strut assembly will be less than 420 pounds. Thus, the studies with the 420 pound load are conservative.

STRUT ASSEMBLY STUDY 1: Strongback support interface

MATERIALS: AISI 4130 steel annealed at 865 °C – Yield Strength of 66.7 ksi.

APPLIED LOADS: Weight of entire assembly is 420 pounds, plus 30 pounds of thrust from each rotor. Applied on top right and left faces of interface (total adding up to 420 pounds).
Gravitational load.

FIXTURES: Slider/roller support on underside of bottom of strongback interface where the hinges would be.
Fixed at holes for hinges.

NOTES: After analysis, the material was changed to 17-4PH H900, which has a yield strength of 185 ksi, so the actual SF will be higher.

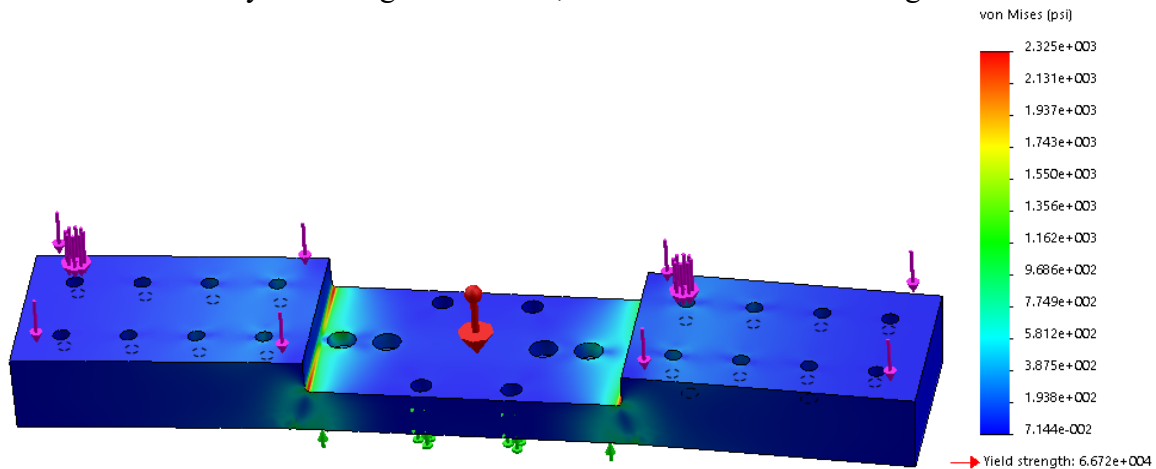


Figure 6.2.18. Strut Assembly Study 1 – strongback support interface, FEA stress plot.

STRESS SAFETY FACTOR: 79.4

MAXIMUM DEFLECTION [inches]: 0.00057

STRUT ASSEMBLY STUDY 2: Upstream stopper

MATERIALS: 17-4PH H900 – Yield Strength of 185 ksi.

APPLIED LOADS: 2,254.6 pounds applied to the face of the hard stop that would hit the single heavy strut.
Gravitational load.

FIXTURES: Slider/roller support top face.
Fixed at holes.

NOTES: Mesh was refined to obtain more accurate results.
The load came from Calculation 2, Equation 7.11.

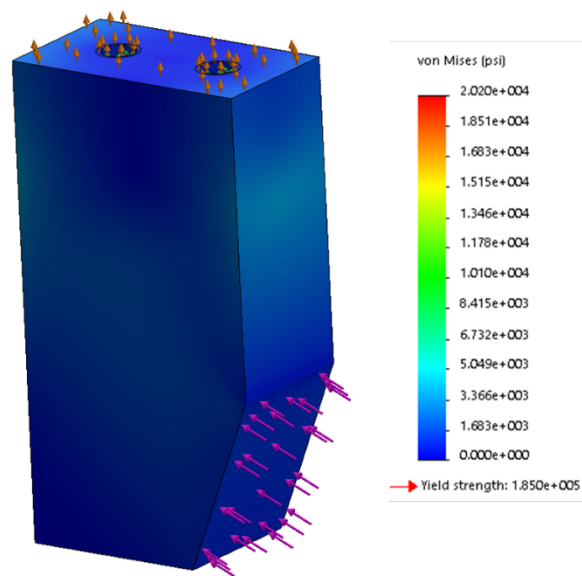


Figure 6.2.19. Strut Assembly Study 2 – upstream stopper, FEA stress plot.

STRESS SAFETY FACTOR: 9.2

MAXIMUM DEFLECTION [inches]: 8.23×10^{-7}

STRUT ASSEMBLY STUDY 3: Downstream stopper

MATERIALS: 17-4PH H900 – Yield Strength of 185 ksi.

APPLIED LOADS: 2,816.6 pounds applied to the face of the hard stop that would hit the single heavy strut.
Gravitational load.

FIXTURES: Slider/roller support top face.
Fixed at holes.

NOTES: The load came from Calculation 3, Equation 7.13.

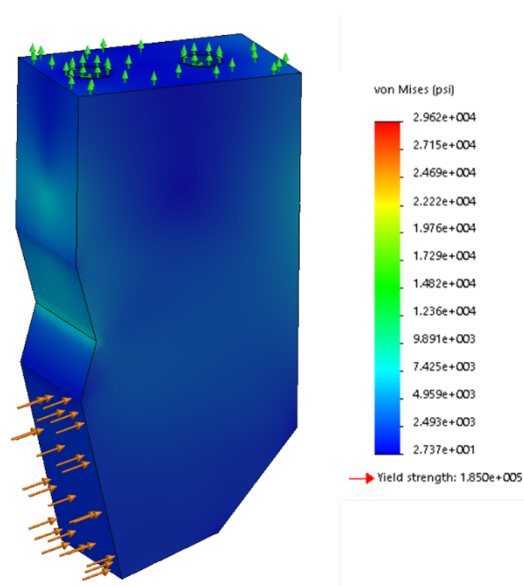


Figure 6.2.20. Strut Assembly Study 3 – downstream stopper, FEA stress plot.

STRESS SAFETY FACTOR: 6.25

MAXIMUM DEFLECTION [inches]: 1.47×10^{-6}

STRUT ASSEMBLY STUDY 4: Designed lug

MATERIALS: 17-4PH H900 – Yield Strength of 185 ksi.

APPLIED LOADS: 1,407 pounds applied downwards on center hole.
363 pounds applied left on center hole.

FIXTURES: Slider/roller support top face.
Fixed at holes for screws.

NOTES: The load came from Equation 7.9, Table 9. The propellers were rotated 90 degrees forward, in tall position, with the strongback rotated 30 degrees forward. This was the maximum theoretical load.
After analysis, the material was changed to 17-4PH H900, which has a yield strength of 185 ksi, so the actual SF will be higher.

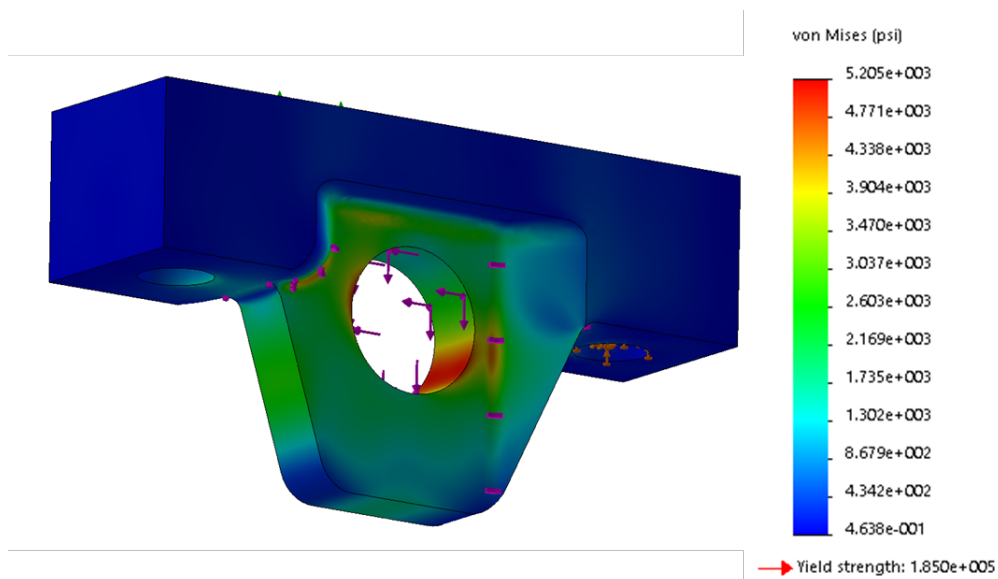


Figure 6.2.21. Strut Assembly Study 4 – designed lug, FEA stress plot.

STRESS SAFETY FACTOR: 35.5

MAXIMUM DEFLECTION [inches]: 1.28×10^{-7}

STRUT ASSEMBLY STUDY 5: Bottom strut clevis

MATERIALS: AISI 4130 steel heat treated to 180 ksi ultimate. Yield 160 ksi.

APPLIED LOADS: 1,453 pounds applied at the hole, along the axis of the hole in tension.

FIXTURES: Fixed at two holes for bearings.

NOTES: The load came from Calculation 1, Table 9. The propellers were rotated 90 degrees forward, in tall position, with the strongback rotated 30 degrees forward. This was the maximum theoretical load. Both the tension and compression cases yielded similar SF and deflection. Mesh was refined to obtain more accurate results.

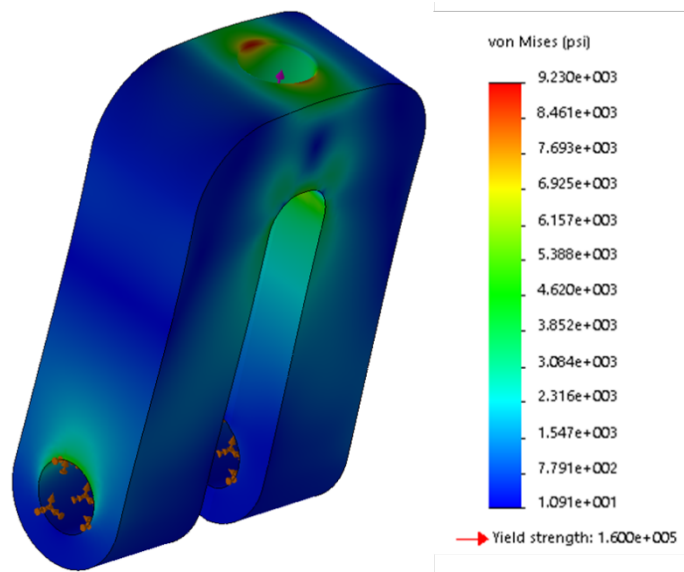


Figure 6.2.22. Strut Assembly Study 5 – bottom strut clevis, FEA stress plot.

STRESS SAFETY FACTOR: 17.33

MAXIMUM DEFLECTION [inches]: 1.80×10^{-4}

STRUT ASSEMBLY STUDY 6: Top strut clevis

MATERIALS: AISI 4130 steel heat treated to 180 ksi ultimate. Yield 160 ksi.

APPLIED LOADS: 1,453 pounds applied at the hole, along the axis of the hole in tension.

FIXTURES: Fixed at two holes for bearings

NOTES: The load came from Calculation 1, Table 9. The propellers were rotated 90 degrees forward, in tall position, with the strongback rotated 30 degrees forward. This was the maximum theoretical load. Both the tension and compression cases yielded similar SF and deflection. Mesh was refined to obtain more accurate results.

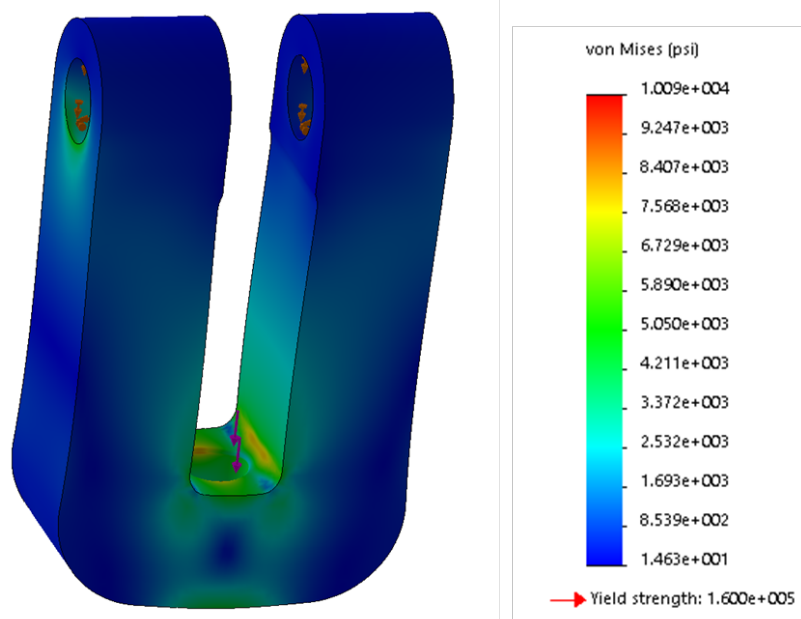


Figure 6.2.23. Strut Assembly Study 6 – top strut clevis, FEA stress plot.

STRESS SAFETY FACTOR: 16

MAXIMUM DEFLECTION [inches]: 1.9×10^{-4}

STRUT ASSEMBLY STUDY 7: Large hinge

MATERIALS: 17-4PH H900 – Yield Strength of 185 ksi.

APPLIED LOADS: Weight of entire assembly was 420 pounds, plus 30 pounds of thrust from each rotor. Applied on inside hole, going down.

FIXTURES: Slider/roller support on top face.
Fixed at holes for bolts.

NOTES: In the case that one hinge fails, the other hinge would take all the load. The actual load would be less than $420/2 = 210$ pounds. Recall that 420 pounds was greater than the expected load. Compression case yields similar results. After analysis, the material was changed to 17-4PH H900, which has a yield strength of 185 ksi, so the actual SF will be higher.

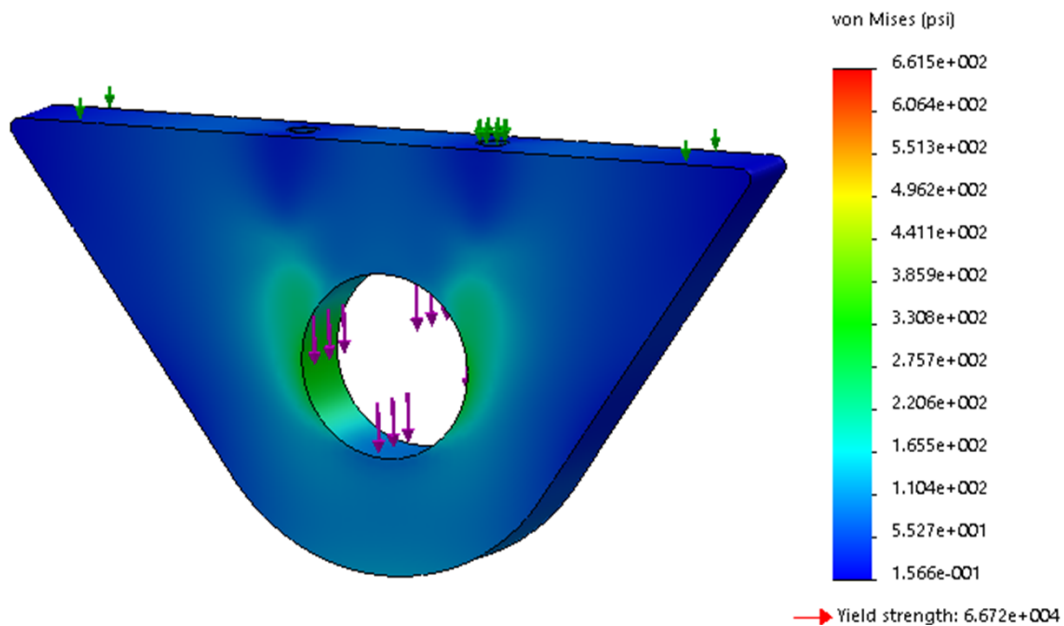


Figure 6.2.24. Strut Assembly Study 7 – large hinge, FEA stress plot.

STRESS SAFETY FACTOR: 280

MAXIMUM DEFLECTION [inches]: 1.9×10^{-5}

STRUT ASSEMBLY STUDY 8: Strut washer

MATERIALS: 932 bearing bronze – Yield Strength of 20 ksi.

APPLIED LOADS: Weight of entire assembly is 420 pounds divided by 2 for each side = 210-pound load. Applied on inside face, downward.

FIXTURES: Fixed on outside cylindrical surface (where it slides against the large hinge).

NOTES: Design modification, took out ball bearings and inserted strut washers.

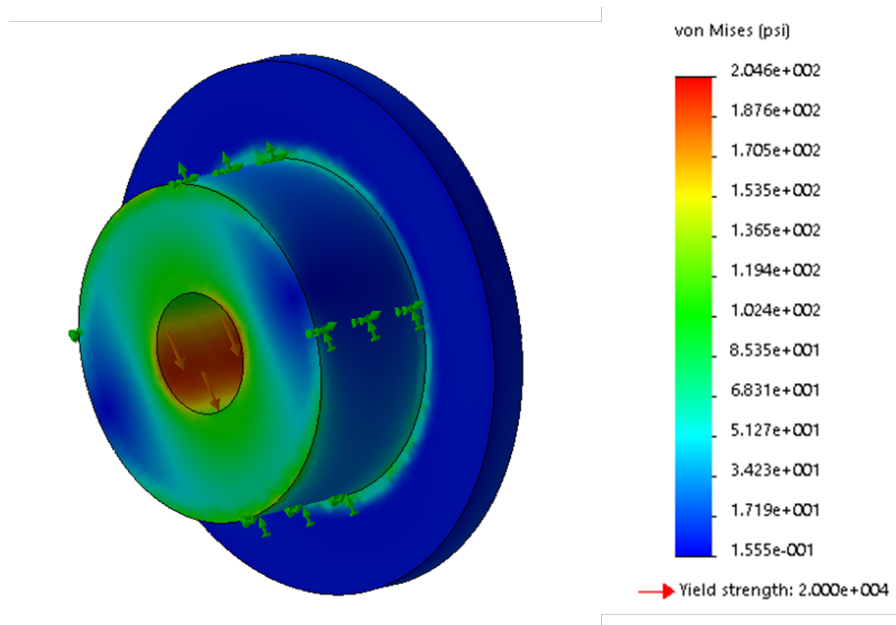


Figure 6.2.25. Strut Assembly Study 8 – strut washer, FEA stress plot.

STRESS SAFETY FACTOR: 97.75

MAXIMUM DEFLECTION [inches]: 5.504×10^{-6}

Strut Assembly Hand Calculations

In this section, the safety factors of off-the-shelf parts were found and additional analyses were performed on some of the manufactured components.

PART: Flanged sleeve bearing, McMaster # 2934T34

PLACEMENT WITHIN ASSEMBLY: Four will be used in conjunction with the top and bottom clevises.

RATED LOAD: 1,050 pounds at 120 rpm

SF CALCULATION: For 666-pounds operational load – $SF = 1050/(680/2) = 3.09$

For 1,453 pounds theoretical load – $SF = 1050/(1453/2) = 1.45$.

NOTES: The load rating given is for the dynamic radial load capacity, which means that the bearing can withstand a maximum load of 1,050 when going 120 rpm. Since for this application, the bearing will have an extremely small rpm, the maximum load will likely be higher. Also, the bearings will be press fit into the clevises, so the clevises will help to take some of the load as well.

PART: 5/16-inch dowel pin, 416 stainless steel, McMaster # 98380A593

PLACEMENT WITHIN ASSEMBLY: Two used to hold top and bottom clevis and bearings in pitching mechanism.

RATED LOAD: 11,000 pounds

SF CALCULATION: Operational $SF = 11000/680 = 16.18$

Theoretical $SF = 11000/1453 = 7.57$

NOTES: Dowel pin will be press fit into the bearings, lug, and swivel joint.

PART: Black-oxide alloy steel socket head screw, McMaster # 91251A430

PLACEMENT WITHIN ASSEMBLY: Two screws used to secure designed lug to the strongback support interface.

RATED TENSILE STRENGTH: 170,000 psi.

Ultimate Shear Strength = $0.55 * 170 \text{ ksi} = 93.5 \text{ ksi}$.

From Fastener Design Manual NASA Reference Publication 1228: 3/8 screw with 91 ksi ultimate shear strength can handle loads up to 10,050 pounds [1]

SF CALCULATION: $SF = 10050 / (1453/2) = 13.8$

PART: High load ball bearing, McMaster # 2782T83
[OLD DESIGN, NO LONGER USED]

PLACEMENT WITHIN ASSEMBLY: Two press fit into the two hinges that hold the strongback support interface.

RATED LOAD: 1,000 pounds for static, 2,559 for dynamic.

SF CALCULATION: Use static load. $1000 / (420/2) = 4.76$.

NOTES: Note the 420-pound load is larger than the expected loads. Reference the beginning of this section for derivation of the 420-pound load.

PART: 5/8" dowel pin, 416 stainless steel, McMaster # 98380A874
[OLD DESIGN, NO LONGER USED]

PLACEMENT WITHIN ASSEMBLY: Press fit into the two ball bearings and through the top hole in the strut.

RATED LOAD: 45,000 pounds

SF CALCULATION: $FS = 45000 / 420 = 107$

PART: Main strut shaft

PLACEMENT WITHIN ASSEMBLY: Passes through the strut washers and through the top hole in the strut, holding the whole assembly.

MATERIAL: 17-4PH H900 – Yield Strength of 185 ksi.

RATED TENSILE STRENGTH: 140 ksi

YIELD SHEAR STRENGTH: Estimated about 55 percent of yield strength = 101.75 ksi

[1] R. T. Barrett, "Fastener Design Manual," Mar. 1990.

SHEAR TEAROUT FROM BENDING CALCULATION:

$$\text{Max Bending Moment} = M_{max} = \frac{P}{2} \left(a + \frac{l}{4} \right) \quad (7.14)$$

Where P was the maximum load, a was half of the bearing thickness, and l was the distance between the bearings.

$$M_{max} = 210/2(0.94825/2+2/4)$$

$$M_{max} = 102.28 \text{ in} - \text{lbs}$$

The stress due to bending was then calculated using:

$$\sigma_B = \frac{Mc}{I} \quad \text{where } I = \frac{1}{64} \pi D^4 \quad (7.15)$$

$$\sigma_B = \frac{102.28 \text{ in} - \text{lbs} * 32}{\pi(0.625 \text{ in})^3}$$

$$\sigma_B = 4267.28 \text{ psi}$$

SF CALCULATION: SF = 101750/4267.28 = 23.84

PART: Threaded rod (designed part)

PLACEMENT WITHIN ASSEMBLY: Connects the two clevises in the pitching mechanism

MATERIAL: 17-4PH H900 – Yield Strength of 185 ksi.

THREAD PULLOUT CALCULATION: Yield Shear Strength = 0.55*185ksi = 101.75 ksi.

$$P = \frac{1}{3} \pi d_m F_s L \quad (7.16)$$

Where P is the pullout load, d_m is the mean diameter or pitch diameter of the threads, F_s is the material ultimate or yield stress, and L is the length of the thread engagement [1].

$$P = \frac{1}{3} * \pi * 0.4001 \text{ in} * 101750 \text{ psi} * 0.625 \text{ in}$$

$$P = 26,600 \text{ lbs}$$

SF CALCULATION: SF = 26,600lbs/1453lbs = 18.3

PART: Bottom clevis

PLACEMENT WITHIN ASSEMBLY: Connects to the threaded rod and the lug.

MATERIAL: AISI 4130 steel heat treated to ultimate strength of 180 ksi, Yield 160 ksi.

SHEAR TEAROUT CALCULATION:

AISC Allowable Shear Stress = $0.4 * 160 \text{ ksi} = 64 \text{ ksi}$

$$A_{shear} = A_s = 2t(e - \frac{d}{2}) \quad (7.17)$$

Where A_s is the shear area, t is the thickness of the clevis, e is the distance from the edge to the center of the hole, and d is the diameter of the hole.

$$A_s = 2 * 0.6875 * (0.425 - 0.4395/2) = 0.2822 \text{ in}^2$$

$$\sigma_s = \frac{F/2}{A_s} \quad (7.18)$$

$$\sigma_s = \frac{1453 \text{ lbs}/2}{0.2822 \text{ in}^2} = 5148.8 \text{ psi}$$

SF CALCULATION: $SF = 64000/5148.8 = 12.43$

PART: Top clevis

PLACEMENT WITHIN ASSEMBLY: Connects to the threaded rod and the designed lug that is secured to the strongback support interface.

MATERIAL: AISI 4130 steel heat treated to ultimate strength of 180 ksi, Yield 160 ksi.

SHEAR TEAROUT CALCULATION:

Using Equation 7.15 and 7.16:

$$A_s = 2 * 0.6875 * (0.425 - 0.4375/2) = 0.2836 \text{ in}^2$$

$$\sigma_s = \frac{F/2}{A_s} = \frac{1453 \text{ lbs}/2}{0.2836 \text{ in}^2} = 5123.4 \text{ psi}$$

SF CALCULATION: $SF = 64000/5123.4 = 12.49^*$

6.3 Beam System Analysis

FEA was done in SolidWorks on the different components of the beam system to determine the maximum stress and the maximum deflection in various configurations. The maximum allowable angular deflection was set to be 0.1 degrees, in order to obtain accurate data. For this reason, many of the parts have very high safety factors and are over designed. The maximum rotor loads are as follows: 34 pounds in plane, 30 pounds thrust, 60 in-lb moment. Some of the analyses used higher loads and have not been redone since they yield conservative values.

Beam Assembly FEA

The beam assembly consists of the left and right adjusting L-brackets, the vertical support beam, and the lateral support beam. These parts were subjected to various FEA for all the different possible configurations of the MTB. The worst cases are shown in this section. All the worst-case scenarios are for the beams in the tallest configuration.

BEAM ASSEMBLY STUDY 1: Adjusting L-bracket

MATERIALS: 17-4PH H900 – Yield Strength of 185 ksi.

APPLIED LOADS: Offset load applied at the four top holes – 30 pounds forward from thrust from the rotor (airplane mode), 40 pounds towards the left (in-plane load), 40 pounds down (in-plane load), and 120 in-lb moment in same direction as thrust (from the rotor).
Weight from rotor assembly, vertical support beam, and linear actuator applied at top four holes (10.57 pounds).
Gravitational load.

FIXTURES: Slider/roller fixtures were applied inside the L-bracket along the side where the L-bracket would interface with the lateral support beam. Does not account for vertical support beam that would also act as a slider fixture (thus a more conservative study).
Fixed at the two holes on the right side.

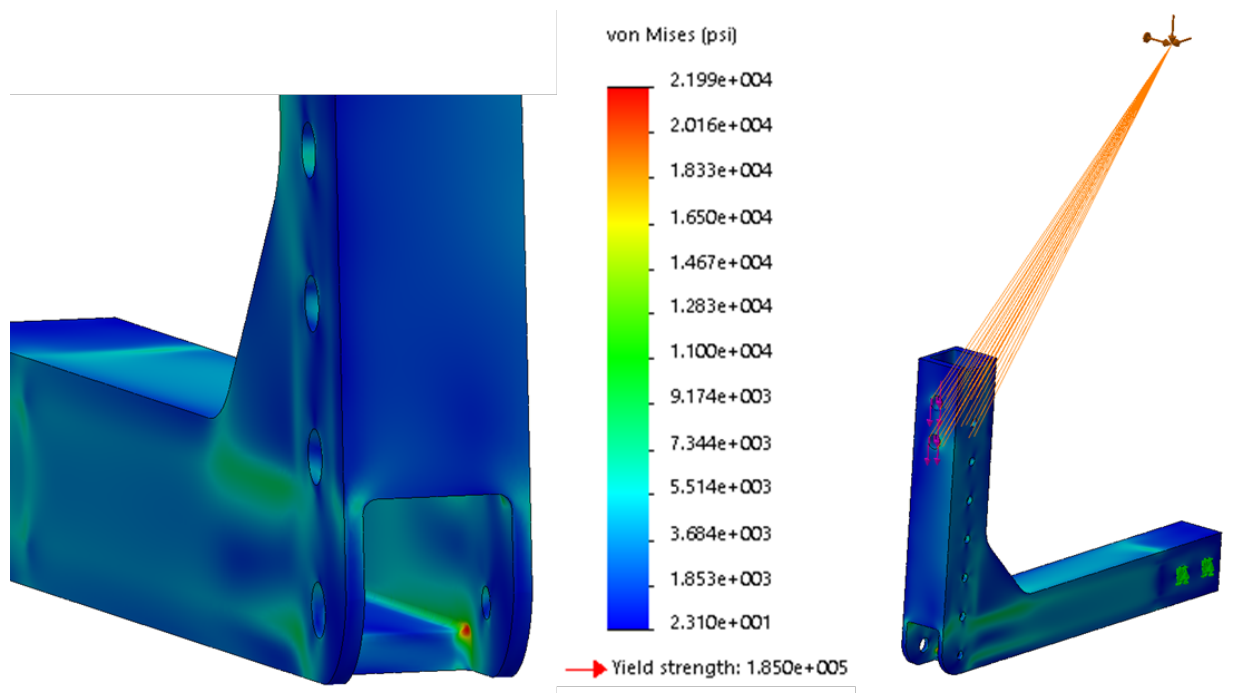


Figure 6.3.1. Beam Assembly Study 1 – adjusting L-bracket, FEA stress plot with close-up view of L-bracket on left.

STRESS SAFETY FACTOR: 8.4

MAXIMUM DEFLECTION [inches]: 0.00002

BEAM ASSEMBLY STUDY 2: Adjusting L-bracket

MATERIALS: 17-4PH H900 – Yield Strength of 185 ksi.

APPLIED LOADS: Offset load applied at the four top holes -- 30 pounds forward from thrust from the rotor (airplane mode), 40 pounds towards the right (in- plane load), 40 pounds down (in-plane load), and 120 in-lb moment in same direction as thrust (from the rotor).
Weight from rotor assembly, vertical support beam, and linear actuator applied at top four holes (10.57 pounds).

FIXTURES: Slider/roller fixtures were applied inside the L-bracket along the side where the L-bracket would interface with the lateral support beam. Does not account for vertical support beam which would also act as a slider fixture (thus a more conservative study).
Fixed at the two holes on the right side.

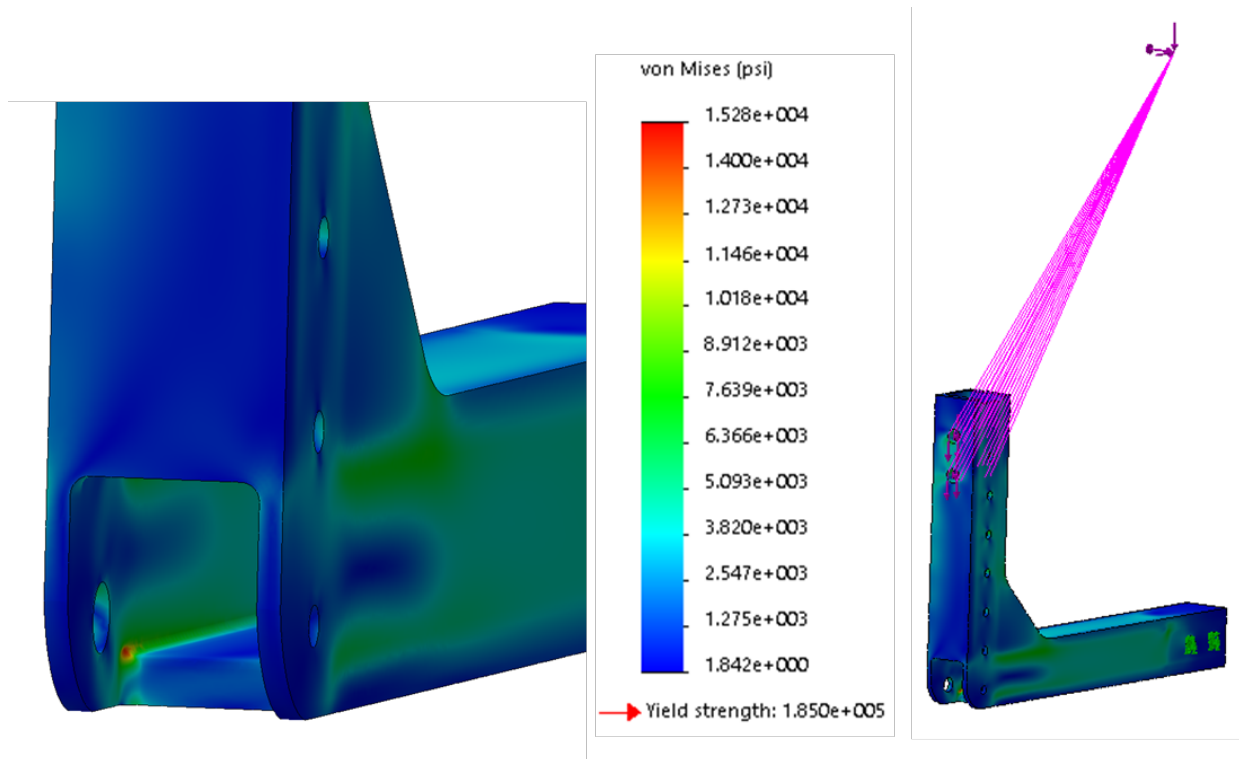


Figure 6.3.2. Beam Assembly Study 2 – adjusting L-bracket, FEA stress plot with close-up view of L-bracket on left.

STRESS SAFETY FACTOR: 12.1

MAXIMUM DEFLECTION [inches]: 2.08×10^{-5}

BEAM ASSEMBLY STUDY 3: Adjusting L-bracket

MATERIALS: 17-4PH H900 – Yield Strength of 185 ksi.

APPLIED LOADS: Offset load applied at the four top holes – 30 pounds upward from thrust from the propellers (helicopter mode), 40 pounds left (in-plane load), 40 pounds backward (in-plane load), and 120 in-lb moment from rotor. Weight from rotor assembly, vertical support beam, and linear actuator applied at top four holes (10.57pounds). Gravitational load.

FIXTURES: Slider/roller fixtures were applied inside the L-bracket along the side where the L-bracket would interface with the lateral support beam. This does not account for vertical support beam that would also act as a slider fixture (thus a more conservative study). Fixed at the two holes on the right side.

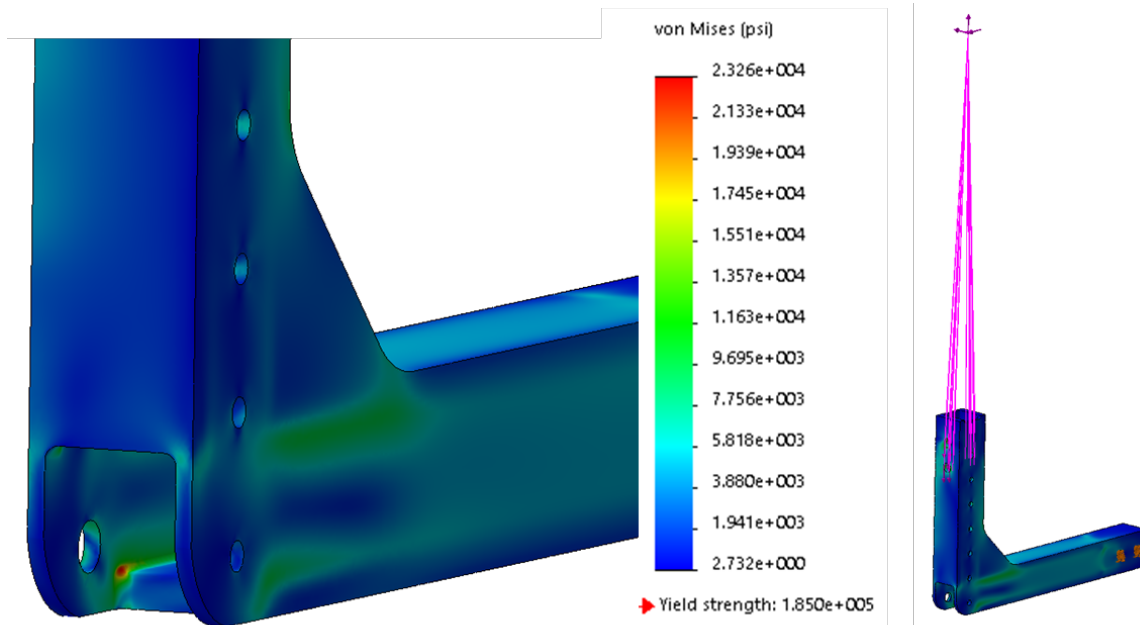


Figure 6.3.3. Beam Assembly Study 3 – adjusting L-bracket, FEA stress plot with close-up view of L-bracket on left.

STRESS SAFETY FACTOR: 7.95

MAXIMUM DEFLECTION [inches]: 2.33×10^{-5}

BEAM ASSEMBLY STUDY 4: Adjusting L-bracket

MATERIALS: 17-4PH H900 – Yield Strength of 185 ksi.

APPLIED LOADS: Offset load applied at the four top holes – 30 pounds upward from thrust from the propellers (helicopter mode), 40 pounds right (in-plane load), 40 pounds backward (in-plane load), and 120 in-lb moment from rotor. Weight from rotor assembly, vertical support beam, and linear actuator applied at top four holes (10.57pounds). Gravitational load.

FIXTURES: Slider/roller fixtures were applied inside the L-bracket along the side where the L-bracket would interface with the lateral support beam. This does not account for vertical support beam that would also act as a slider fixture (thus a more conservative study). Fixed at the two holes on the right side.

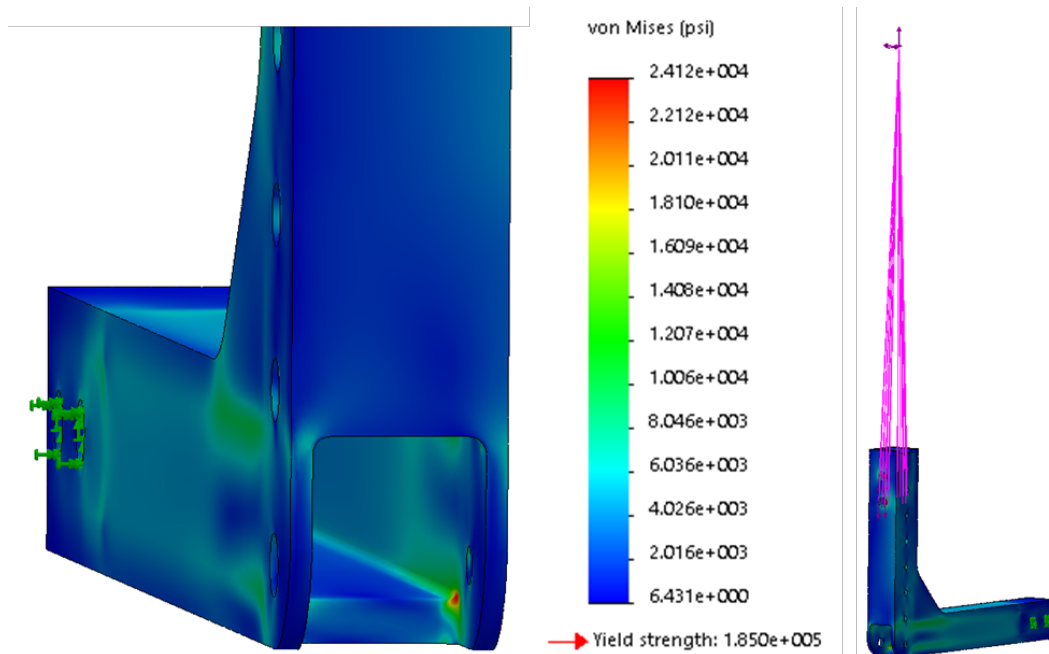


Figure 6.3.4. Beam Assembly Study 4 – adjusting L-bracket, FEA stress plot with close-up view of L-bracket on left.

STRESS SAFETY FACTOR: 7.67

MAXIMUM DEFLECTION [inches]: 2.4×10^{-5}

BEAM ASSEMBLY STUDY 5: Vertical support beam

MATERIALS: 13-8PH H950 – Yield Strength of 205 ksi (AMS5629).

APPLIED LOADS: Offset load applied at the two top holes – 30 pounds forward from thrust from the propellers (airplane mode), 34 pounds right and 34 pounds up (in-plane load), and 60 in-lb moment (thrust direction).
Weight from rotor assembly and linear actuator applied at top two holes and bottom two holes respectively.
Gravitational load.

FIXTURES: Slider/roller fixtures were applied along the faces of the beam towards the bottom, where the support beam would interface with the adjusting beam. Fixed at the bottom two holes.

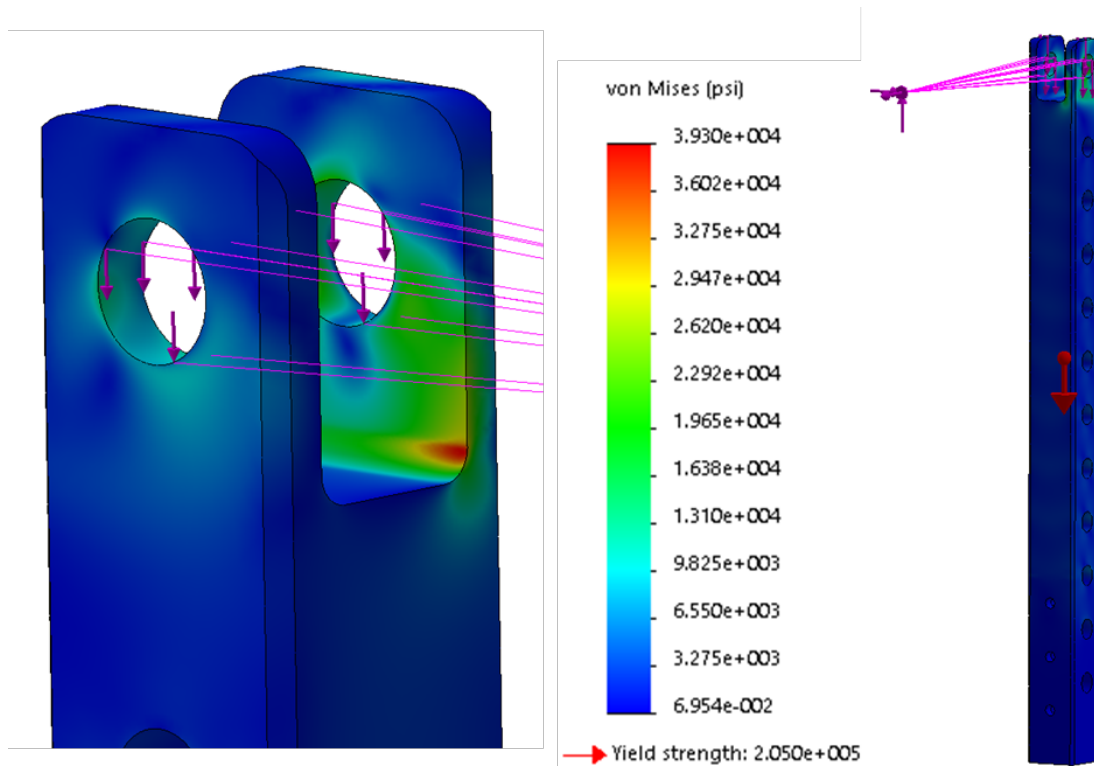


Figure 6.3.5. Beam Assembly Study 5 – vertical support beam, FEA stress plot with close-up view of beam on left.

STRESS SAFETY FACTOR: 5.2

MAXIMUM DEFLECTION [inches]: 1.86×10^{-5}

BEAM ASSEMBLY STUDY 6: Vertical support beam

MATERIALS: 13-8PH H950 – Yield Strength of 205 ksi (AMS5629).

APPLIED LOADS: Offset load applied at the two top holes – 30 pounds upward thrust from the propellers (helicopter mode), 34 pounds left and 34 pounds up (in-plane load), and 60 in-lb moment (in direction of thrust).
Weight from rotor assembly and linear actuator applied at top two holes and bottom two holes respectively.
Gravitational load.

FIXTURES: Slider/roller fixtures were applied along the faces of the beam towards the bottom, where the support beam would interface with the adjusting beam. Fixed at the bottom two holes.

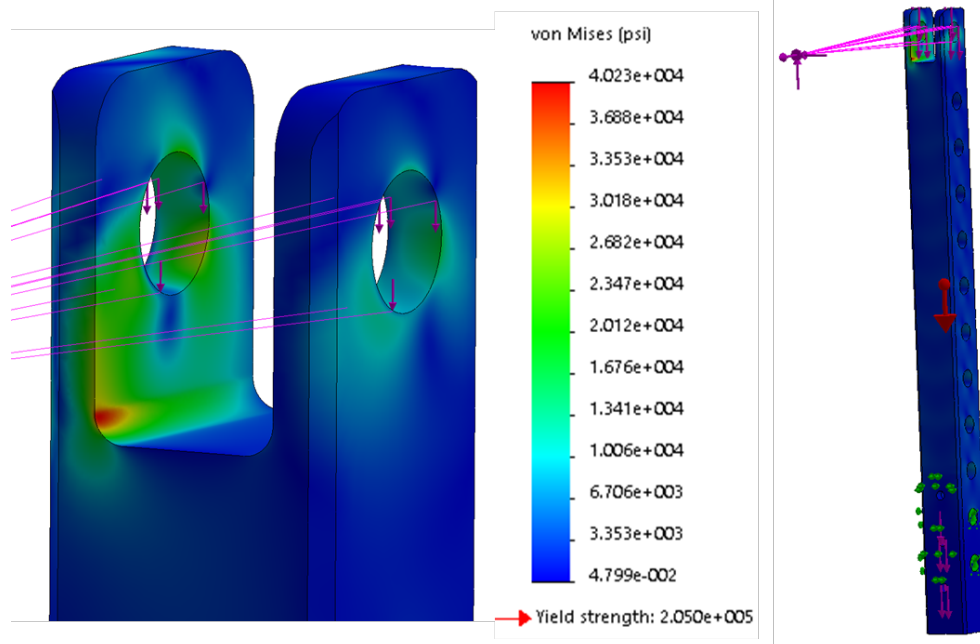


Figure 6.3.6. Beam Assembly Study 6 – vertical support beam, FEA stress plot with close-up view of beam on left.

STRESS SAFETY FACTOR: 5.1

MAXIMUM DEFLECTION [inches]: 3.39×10^{-5}

BEAM ASSEMBLY STUDY 7: Vertical Support Beam

MATERIALS: 13-8PH H950 – Yield Strength of 205 ksi (AMS5629).

APPLIED LOADS: Offset load applied at the two top holes – 30 pounds upward from thrust from the rotors (helicopter mode), and 34 pounds right and back (in-plane load), and 60 in-lb moment (in direction of thrust).
Weight from rotor assembly and linear actuator applied at top two holes and bottom two holes respectively.
Gravitational load.

FIXTURES: Slider/roller fixtures were applied along the faces of the beam towards the bottom, where the support beam would interface with the adjusting beam. Fixed at the bottom two holes.

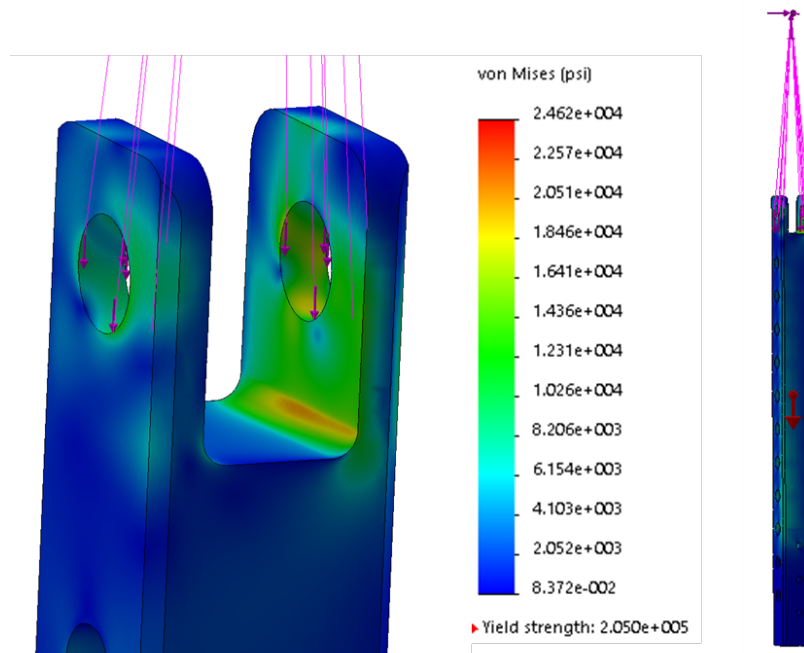


Figure 6.3.7. Beam Assembly Study 7 – vertical support beam, FEA stress plot with close-up view of beam on left.

STRESS SAFETY FACTOR: 8.3

MAXIMUM DEFLECTION [inches]: 1.535×10^{-3}

BEAM ASSEMBLY STUDY 8: Vertical support beam

MATERIALS: 13-8PH H950 – Yield Strength of 205 ksi (AMS5629).

APPLIED LOADS: Offset load applied at the two top holes – 30 pounds forward from thrust from the propellers (airplane mode), 34 pounds left and forward (in-plane load), and 60 in-lb moment (in direction of thrust).
Weight from rotor assembly and linear actuator applied at top two holes and bottom two holes respectively.
Gravitational load.

FIXTURES: Slider/roller fixtures were applied along the faces of the beam towards the bottom, where the support beam would interface with the adjusting beam. Fixed at the bottom two holes.

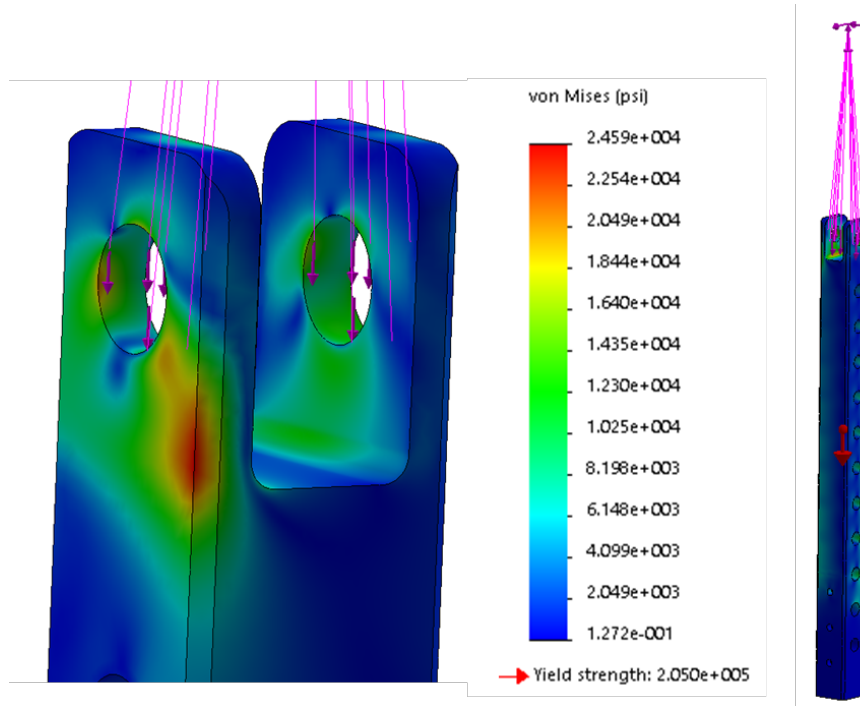


Figure 6.3.8. Beam Assembly Study 8 – vertical support beam, FEA stress plot with close-up view of beam on left.

STRESS SAFETY FACTOR: 8.3

MAXIMUM DEFLECTION [inches]: $1.581 \cdot 10^{-3}$

BEAM ASSEMBLY STUDY 9: Lateral Support Beam

MATERIALS: 13-8PH H950 – Yield Strength of 205 ksi (AMS5629).

APPLIED LOADS: 30-pound load upward (helicopter mode) applied at ends of support beam on the top face.
34-pound load forward and back, twisting counterclockwise (in-plane loads), applied at left and right ends of the top face of the support beam.
Gravitational load and weight of other components.

FIXTURES: Slider/roller fixtures were applied along the top and bottom faces of the beam where the beam is secured to the strongback.
Fixed at the center two holes.

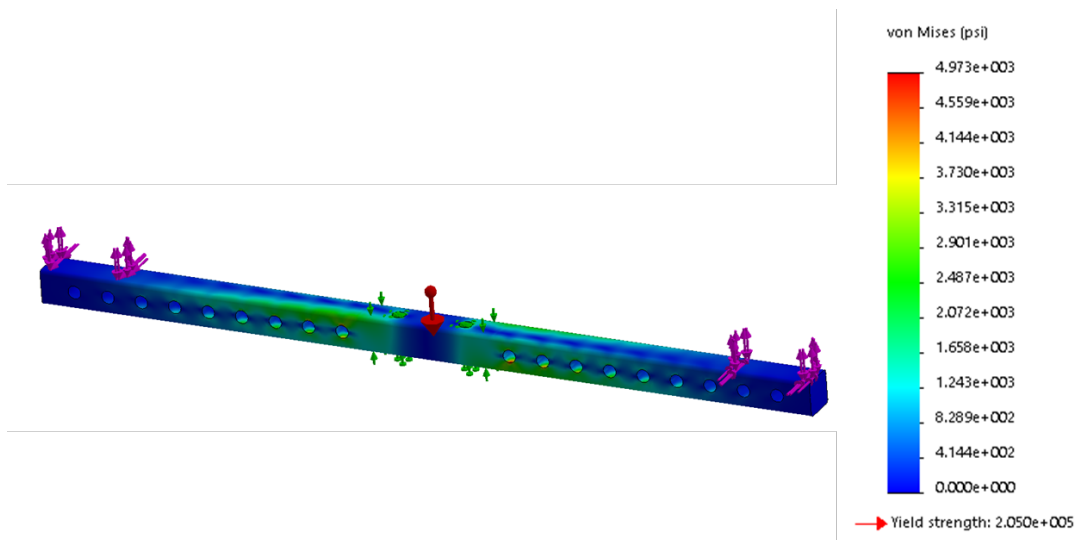


Figure 6.3.9. Beam Assembly Study 9 – lateral support beam, FEA stress plot.

STRESS SAFETY FACTOR: 41.2

MAXIMUM DEFLECTION [inches]: 1.658×10^{-3}

BEAM ASSEMBLY STUDY 10: Lateral support beam

MATERIALS: 13-8PH H950 – Yield Strength of 205 ksi (AMS5629).

APPLIED LOADS: 30-pound load forward (airplane mode) applied at ends of support beam on the top face.
34-pound load down (in-plane loads), applied at ends of the top face of the support beam.
Gravitational load.

FIXTURES: Slider/roller fixtures were applied along the top and bottom faces of the beam where the beam is secured to the strongback.
Fixed at the center two holes.

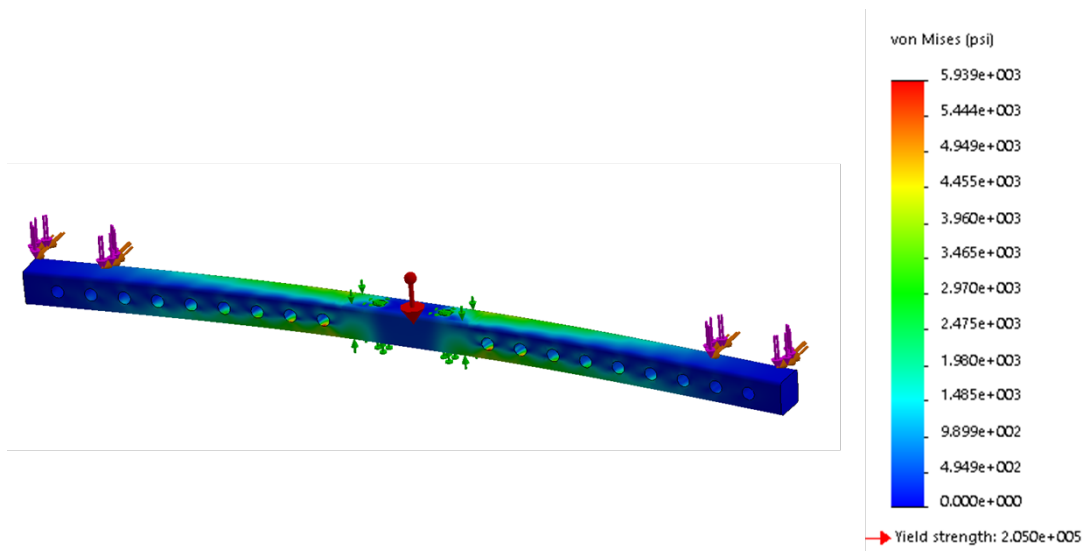


Figure 6.3.10. Beam Assembly Study 10 – lateral support beam, FEA stress plot.

STRESS SAFETY FACTOR: 34.5

MAXIMUM DEFLECTION [inches]: 7.21×10^{-3}

6.4 Rotor Assembly Analysis

One of the main areas of concern for the rotor assembly was the force on the linear actuator and clevises. This force was derived and calculated for the worst-case scenarios. This force was then used for stress analysis and FEA for the clevis interface and the bottom clevis in the rotor assembly.

CALCULATION 4: Force through the Linear Actuator

The schematic in Figure 6.4.1 shows the forces acting on the rotor. Note that the picture is out of date, but the kinematics remain the same. The angle θ represents the rotation of the rotor about point O with respect to the vertical axis. F_{w_p} is the weight of the rotor assembly above point O. Note that this weight is different than previous weights of the rotor assembly. F_{pp} is the in-plane load of the rotor. The thrust of the rotor is directly in line with the point of rotation, so it cancels out when solving for the moment. F_{a_L} is the axial force through the linear actuator. The angle α is the rotation of the axial force (or the linear actuator) about the horizontal axis.

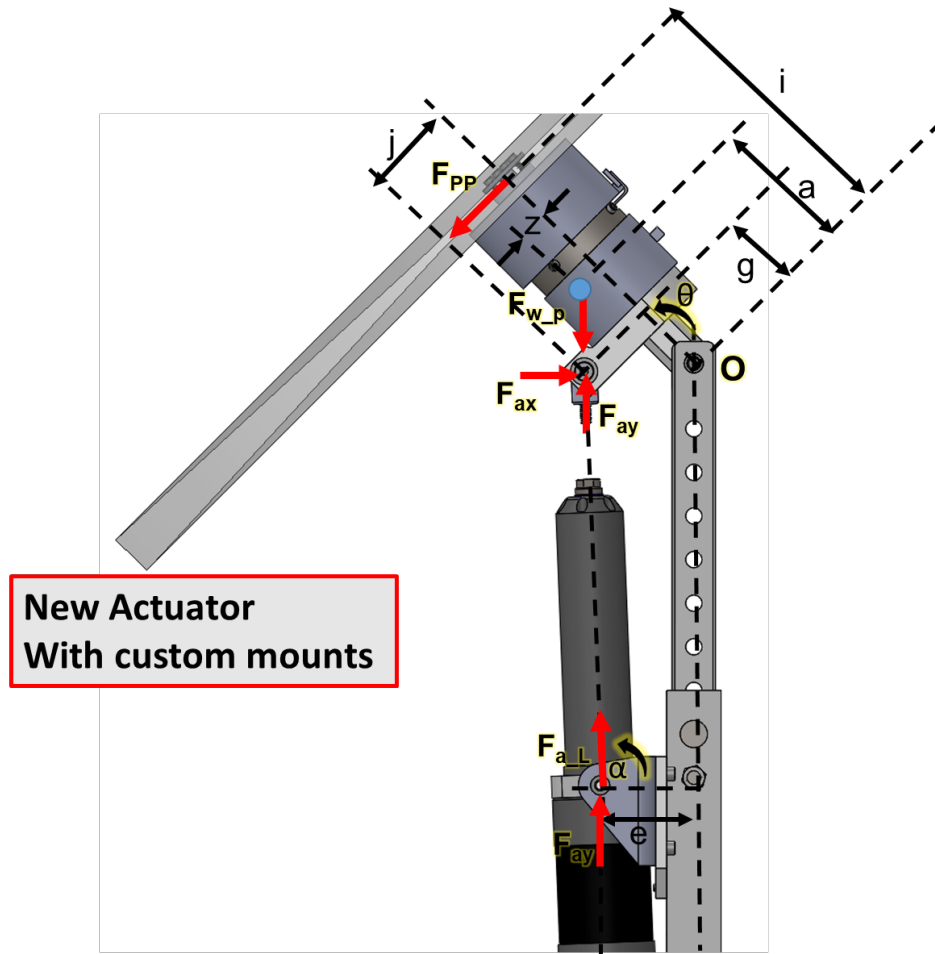


Figure 6.4.1. Schematic of rotor assembly – Calculation 4.

The sum of the moments about the point of rotation, O, was set to zero.

$$\sum M_O = (F_{wp} * a * \sin \theta) + (F_{pp} * i) - (F_{ay} * (j * \cos \theta + g * \sin \theta)) + \dots \quad (7.19)$$

$$\dots - (F_{ax} * (g * \cos \theta - j * \sin \theta)) = 0$$

Where $F_{ax} = F_{aL} * \cos \alpha$ and $F_{ay} = F_{aL} * \sin \alpha$. (7.20) (7.21)

$$F_{aL} = \frac{(F_{wp} * a * \sin \theta) + (F_{pp} * i)}{(\sin \alpha * (j * \cos \theta + g * \sin \theta)) + (\cos \alpha * (g * \cos \theta - j * \sin \theta))} \quad (7.22)$$

Table 11 shows the different values of the axial force for different configurations of rotor rotation. It should be noted that the rotation of the strongback was assumed to be zero. The maximum axial force on the linear actuator occurred at a rotor rotation of 90 degrees forwards. This value was 143.5 pounds (with the increased in-plane load of 34 pounds). For the purposes of the FEA, this value was rounded up to 145 pounds. Note only Table 11 is shown, but the analysis was done for both positive and negative in-plane loads.

Table 11. Force through linear actuator – Calculation 4

a	3.084	3.084	3.084	3.084
g	1.65	1.65	1.65	1.65
i	6.022044805	6.022044805	6.022044805	6.022044805
z	0.12780207	0.12780207	0.12780207	0.12780207
j	1.9125	1.9125	1.9125	1.9125
alpha degrees	86.31690771	92.22609399	88.79913901	88.0630993
alpha radians	1.50651424	1.609648996	1.549837349	1.536991032
theta degrees	90	45	0	-5
theta radians	1.570796327	0.785398163	0	-0.087266463
FG	4.513	4.513	4.513	4.513
Torsional Sprig M	0	0	0	0
Linear spring	0	0	0	0
In Plane load	34	34	34	34
Fa	143.5074264	85.16911924	105.4762115	112.050508

Rotor Assembly FEA

ROTOR ASSEMBLY STUDY 1: Clevis interface

MATERIALS: 17-4PH H900 – Yield Strength of 185 ksi.

APPLIED LOADS: 145-pound load applied at the two side holes (total), going down.
3.1 pounds applied on top face of clevis, weight of the rotor components above the clevis interface.

FIXTURES: Fixed at two center holes.

NOTES: After analysis, the material was changed to 17-4PH H900, which has a yield strength of 185 ksi, so the actual SF will be higher.

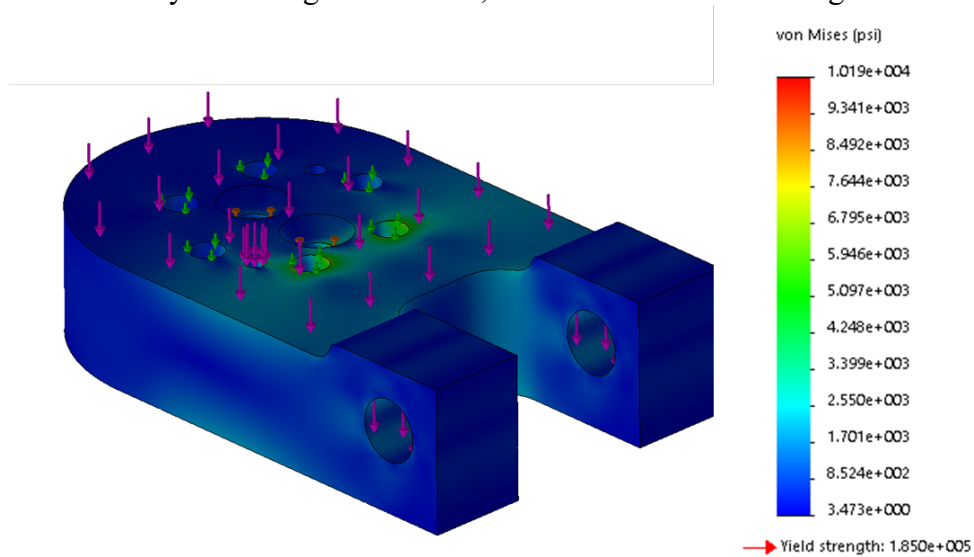


Figure 6.4.2. Rotor Assembly Study 1 – clevis interface, FEA stress plot.

STRESS SAFETY FACTOR: 18.16

MAXIMUM DEFLECTION [inches]: 5.408×10^{-7}

ROTOR ASSEMBLY STUDY 2: Bottom prop clevis

MATERIALS: AISI 4130 heat treated – Yield Strength of 160 ksi.

APPLIED LOADS: 75-pound load applied downward on two side holes.
7.05 pounds applied downward on two side holes (weight of rotor assembly and actuator).

FIXTURES: Fixed at two back holes.

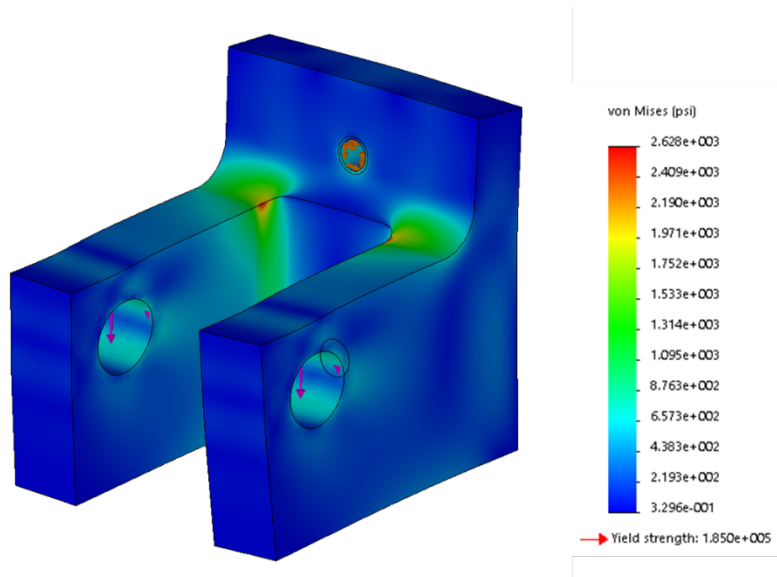


Figure 6.4.3. Rotor Assembly Study 2 – bottom prop clevis, FEA stress plot.

STRESS SAFETY FACTOR: 70.4

MAXIMUM DEFLECTION [inches]: 1.02×10^{-7}

UPDATE: This part is no longer used in the assembly.

ROTOR ASSEMBLY STUDY 3: Custom linear actuator mount - right

MATERIALS: 17-4PH H900 – Yield Strength of 155 ksi.

APPLIED LOADS: 75 pound downward load:
145 pounds from worse-case load + 5 pounds from weight of actuator,
divided by 2 = 75-pounds downward load on circular face where custom
mount holds the linear actuator

FIXTURES: Fixed at two mounting holes on back face.

NOTE: The yield strength is less for this material because that is what was
available in the shop. Mesh refined at holes. Maximum stress is a stress
singularity from Solidworks simulation.
Analysis is the same for the right and left sides.

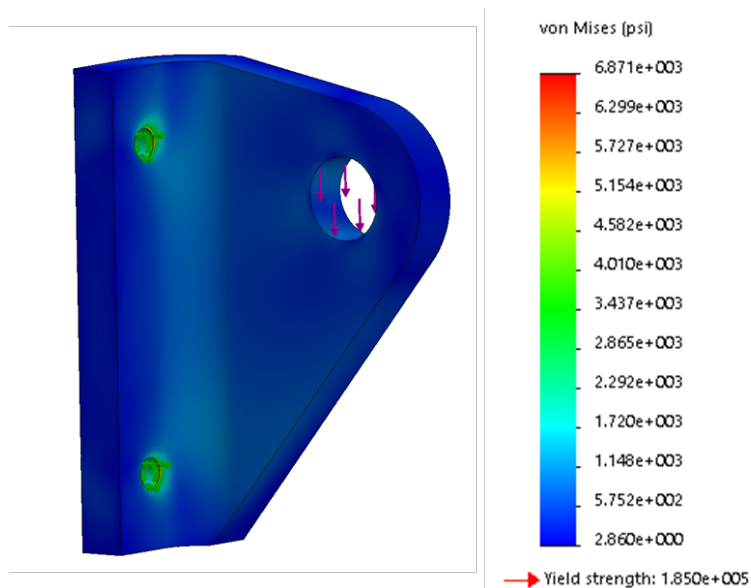


Figure 6.4.4. Rotor Assembly Study 3 – custom linear actuator mount, right, FEA stress plot.

STRESS SAFETY FACTOR: 22.55

MAXIMUM DEFLECTION [inches]: $1.47 \cdot 10^{-7}$

ROTOR ASSEMBLY STUDY 4: Linear Actuator Top Clevis

MATERIALS: 17-4PH H900 – Yield Strength of 155 ksi.

APPLIED LOADS: 150-pound downward load applied on circular face where clevis is supported by the shoulder bolt:
145 pounds from worst-case load + 5 pounds from weight of actuator.

FIXTURES: Fixed at bottom mounting hole.

NOTE: The yield strength is less for this material because that is what was available in the shop. Mesh refined at holes.

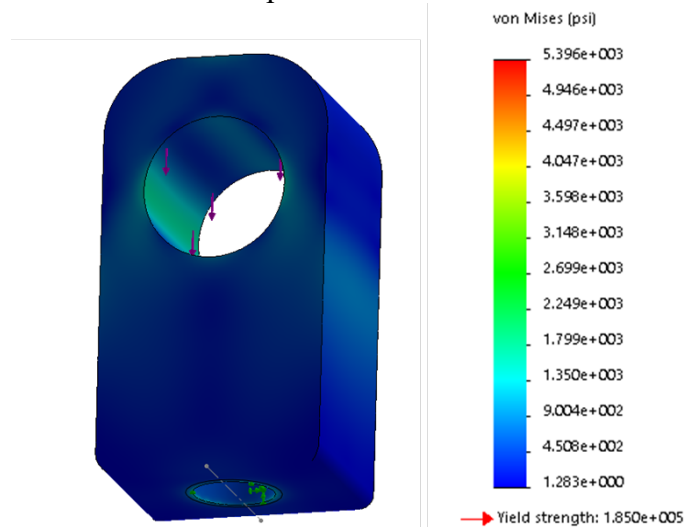


Figure 6.4.5. Rotor Assembly Study 4 – linear actuator top clevis, FEA stress plot.

STRESS SAFETY FACTOR: 28.7

MAXIMUM DEFLECTION [inches]: 2.956×10^{-8}

ROTOR ASSEMBLY STUDY 5: Bottom actuator interface

MATERIALS: 17-4PH H900 – Yield Strength of 155 ksi.

APPLIED LOADS: 150-pound downward load applied on four outside holes at custom mount connections
145 pounds from worst-case load + 5 pounds from weight of actuator.

FIXTURES: Fixed at top and bottom center hole. Roller/sliding fixture at center hole (pin).

NOTE: The yield strength is less for this material because that is what was available in the shop. Mesh refined at holes.

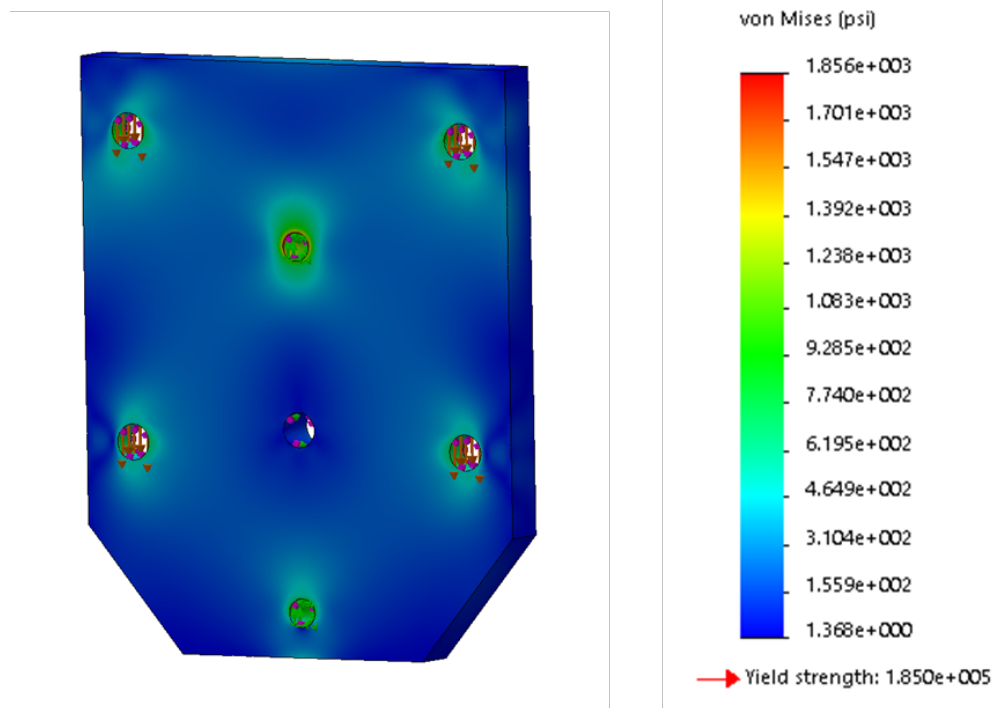


Figure 6.4.6. Rotor Assembly Study 5 – bottom actuator interface, FEA stress plot.

STRESS SAFETY FACTOR: 83.5

MAXIMUM DEFLECTION [inches]: 4.29×10^{-8}

Rotor Assembly Hand Calculations

In this section, the safety factors of off-the-shelf parts were found and additional analyses were performed on some of the manufactured components.

PART: Linear actuator (Ultra Motion, model A1)

PLACEMENT WITHIN ASSEMBLY: Rotates the rotor assembly. Connected to the linear actuator top clevis, custom linear actuator mounts, and bottom actuator interface.

RATED LOAD: 850 pounds is the maximum static load (confirmed with manufacturer)

SF CALCULATION: $SF = 850/145 = 5.86$

PART: Bearing, McMaster # 60695K21 [OLD DESIGN, NO LONGER USED]

PLACEMENT WITHIN ASSEMBLY: Press fit into bottom clevis in the rotor assembly. Two used on each side hole in the bottom clevis.

RATED LOAD: 600 pounds at 120 rpm

SF CALCULATION: $600/(110/2) = 10.9$

NOTES: The load rating given is for the dynamic radial load capacity, which means that the bearing can withstand a maximum load of 600 when going 120 rpm. Since in this application, the bearing will have an extremely small rpm, the maximum load will likely be higher.

PART: Oil-embedded flanged sleeve bearing, McMaster # 6338K566

PLACEMENT WITHIN ASSEMBLY: Two holding up linear actuator

RATED LOAD: 250 pounds at 120 rpm

SF CALCULATION: $250/(150/2) = 3.33$

NOTES: The load rating given is for the dynamic radial load capacity, which means that the bearing can withstand a maximum load of 250 when going 120 rpm. Since for this application, the bearing will have an extremely small rpm, the maximum load will likely be higher.

PART: Flanged sleeve bearing, McMaster # 2938T500

PLACEMENT WITHIN ASSEMBLY: Press fit into the top holes in the vertical support beam. These bearings are at the point of rotation of the rotor assembly.

RATED LOAD: 410 pounds at 120 rpm

SF CALCULATION: Maximum thrust from propellers = 30 pounds, weight of rotor assembly = 4.6 lbs. Load on each bearing = $(30-4.6)/2 = 12.7$. SF = $410/(12.7) = 32.3$

NOTES: The load rating given is for the dynamic radial load capacity.

PART: 5/16" shoulder screw, alloy steel, McMaster # 91259A589 [OLD DESIGN, NO LONGER USED]

PLACEMENT WITHIN ASSEMBLY: Press fit into the bearings in the bottom prop clevis.

RATED TENSILE STRENGTH: 140 ksi

RATED SHEAR STRENGTH: 84 ksi

SHEAR TEAROUT FROM BENDING CALCULATION:

$$\text{Max Bending Moment} = M_{max} = \frac{P}{2} \left(a + \frac{l}{4} \right) \quad (7.23)$$

Where P was the maximum load, a was half of the clevis thickness, and l was the distance between the clevis arms.

$$M_{max} = 75/2(0.39566929/2 + 0.83366142/4)$$

$$M_{max} = 15.23 \text{ in} - \text{lbs}$$

The stress due to bending was then calculated using:

$$\sigma_B = \frac{Mc}{I} \quad \text{where} \quad I = \frac{1}{64} \pi D^4 \quad (7.24)$$

$$\sigma_B = \frac{15.23 \text{ in} - \text{lbs} * 32}{\pi(0.3125 \text{ in})^3}$$

$$\sigma_B = 5083 \text{ psi}$$

SF CALCULATION: SF = $84000/5083 = 16.5$ (ultimate)

PART: 5/16" shoulder screw, alloy steel, McMaster # 91259A108

PLACEMENT WITHIN ASSEMBLY: Press fit into the bearings in the clevis interface.

RATED TENSILE STRENGTH: 140 ksi

RATED SHEAR STRENGTH: 84 ksi

SHEAR TEAROUT FROM BENDING CALCULATION:

Use equation 7.21 and 7.22

$$M_{max} = 150/2(0.6063/2 + 0.9124/4)$$

$$M_{max} = 39.8 \text{ in} - \text{lbs}$$

The stress due to bending was then calculated using:

$$\sigma_B = \frac{Mc}{I} \quad \text{where } I = \frac{1}{64}\pi D^4 \quad (7.25)$$

$$\sigma_B = \frac{39.8 \text{ in} - \text{lbs} * 32}{\pi(0.3125 \text{ in})^3}$$

$$\sigma_B = 13284 \text{ psi}$$

SF CALCULATION: SF = 84000/6642 = 6.3 (ultimate)

PART: High-load oil-embedded 863 sleeve bearing, McMaster # 2868T55

PLACEMENT WITHIN ASSEMBLY: Holding up linear actuator at top

RATED LOAD: 550 pounds at 120 rpm

SF CALCULATION: For 150-pound operational load – SF = 550/150 = 3.67

NOTES: The load rating is the maximum load condition at maximum rpm. Since we will be operating at near zero rpm our SF is actually significantly higher.

PART: 10-32 thread 1/2” long screw, low profile, McMaster # 90665A136

PLACEMENT WITHIN ASSEMBLY: Two holding each custom linear actuator mount, four total, to the bottom actuator interface

TENSILE STRENGTH: 140 ksi

APPLIED LOADS: 150 pounds total, divided by 4 = 37.5 pounds

CALCULATION: See below. (See Definitions and Acronyms Section.)

SF: 107.7

Variable	Value
Number of bolts	4
Shear force (lb)	150
Moment (in-lb)	0
Tensile Force	0
Resultant (in)	0
Bolt Diameter (in)	0.19
Threads per inch	32
Length of Engagement	0.25
Ultimate Tensile Strength	140000
Breaking Strength	
Tensile Area (in ²)	0.019984
Shear Area (in ²)	0.066608
Direct Load (lb/bolt)	37.5
Moment Load (lb/bolt)	0
Total Shear Load (lb)	37.5
Shear Stress (psi)	750.658
Tensile Stress (psi)	0
Von Mises Stress (psi)	1300.178
SF	107.6776

PART: Bottom clevis (rotor assembly) [OLD DESIGN, NO LONGER USED]

PLACEMENT WITHIN ASSEMBLY: Connects the linear actuator to the vertical support beam.

MATERIAL: AISI 4130 steel heat treated – Yield Strength of 160 ksi.

SHEAR TEAROUT CALCULATION: AISC allowable shear stress = 0.4*160 ksi = 64 ksi

Use Equation 7.15:

$$A_s = 2 * 0.39566929 * (0.35 - 0.376 / 2) = 0.1282 \text{in}^2$$

Total load on the bottom clevis was the 75-pound load derived in Calculation 4, plus the weight of the linear actuator and rotor assembly, 7.05 pounds. The total load was 82.05 pounds. Using Equation 7.16 the total stress was calculated.

$$\sigma_s = \frac{F/2}{A_s} = \frac{82.05 \text{lbs}/2}{0.1282 \text{in}^2} = 320 \text{psi}$$

SF CALCULATION: $SF = 64000/320 = 200$

NOTES: The FEA had a lower SF.

6.5 Installation Assembly

FEA was done in SolidWorks on the different components of the installation assembly to determine the maximum stress. Hand calculations were also performed to ensure components had reasonable safety factors.

Installation Assembly FEA

The installation assembly consists of the MTB strut assembly, large screws, mounting block (a.k.a. pillow block), gearbox-pillow block interface, gearbox, motor-gearbox interface, stepper motor, and smaller screws. These parts were subjected to various FEA for all the different possible configurations of the MTB. The worst cases are shown in this section.

INSTALLATION ASSEMBLY STUDY 1: Gearbox-pillow block interface

MATERIALS: 17-4PH H900 – Yield Strength of 155 ksi.

APPLIED LOADS: 50-pound downward load: weight of the gearbox, motor, and interfaces, plus additional handling load

FIXTURES: Fixed at the four corners.

NOTES: The yield strength is less for this material because that is what was available in the shop. Mesh refined at holes.

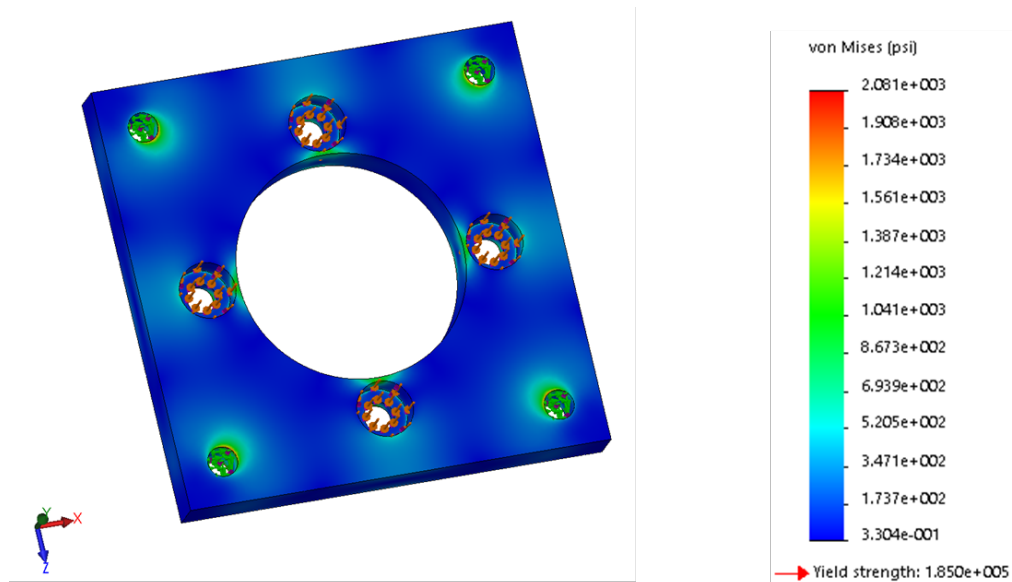


Figure 6.5.1. Installation Assembly Study 1 – gearbox-pillow block interface, FEA stress plot.

STRESS SAFETY FACTOR: 74.5

MAXIMUM DEFLECTION [inches]: 4.45×10^{-8}

INSTALLATION ASSEMBLY STUDY 2: Pillow block

MATERIALS: Unknown steel, set to A36 – Yield Strength of 36 ksi.

APPLIED LOADS: 500-pound downward load (weight of entire assembly +) applied to top face, 107 in-lb moment applied at tapped holes on bottom, 100-pound downward load applied to tapped holes on bottom (weight of components + handling).
Weight of the gearbox, motor, and interfaces, plus additional handling load.

FIXTURES: Fixed at top eight holes, roller/slider fixture on bottom rail cutouts.

NOTES: Mesh refined at holes.

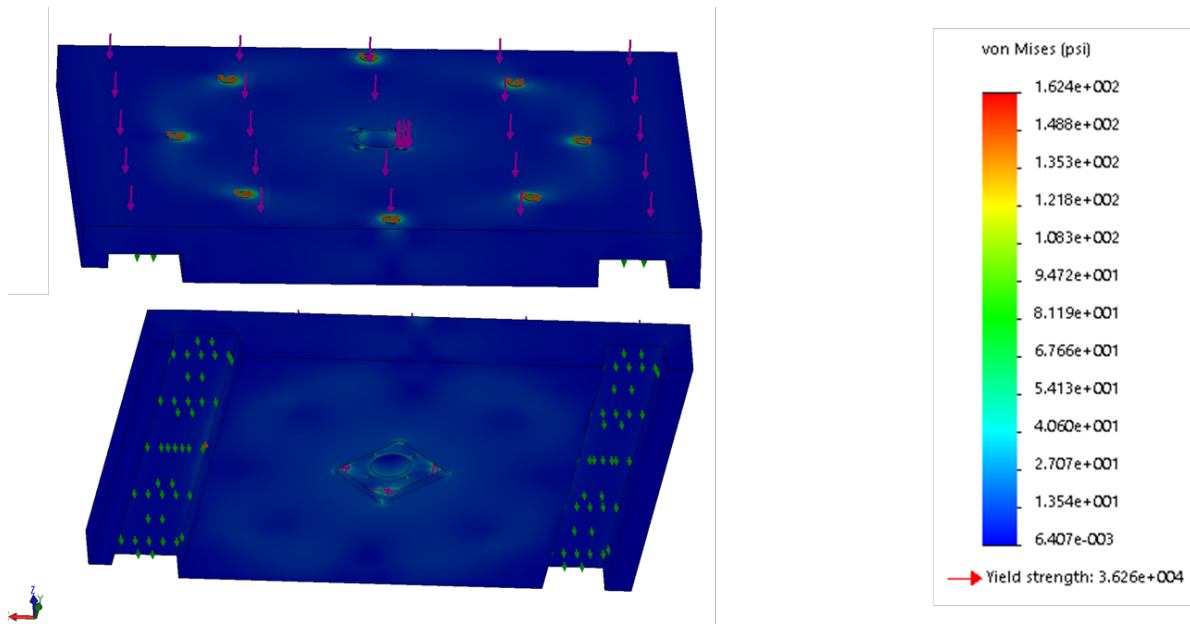


Figure 6.5.2. Installation Assembly Study 2 – pillow block, FEA stress plot.

STRESS SAFETY FACTOR: 222

MAXIMUM DEFLECTION [inches]: 7.5×10^{-6}

Installation Assembly Hand Calculations

In this section, the safety factors of off-the-shelf parts were found and additional analyses were performed on some of the manufactured components.

PART: Screw, 1/4-20 thread 5/8 long, McMaster # 91274A156

PLACEMENT WITHIN ASSEMBLY: Four holding gearbox-motor assembly to the bottom of the pillow block

RATED TENSILE STRENGTH: 170 ksi

APPLIED LOADS: 11.88 in-lb motor, 9:1 gearbox

Total torque = 11.88 in-lb * 9 = 107 in-lb

Added additional 100-pound downward force for the weight of the gearbox-motor assembly (10pounds) + additional handling loads. Conservative estimate.

SF CALCULATION: SF = 200 (See Definitions and Acronyms Section for formulas.)

Variable	Value
Number of bolts	4
Shear force (lb)	0
Moment (in-lb)	106.92
Tensile Force	100
X-Offset (in)	
Y-Offset (in)	
Resultant (in)	1.7
Bolt Diameter (in)	0.25
Threads per inch	20
Length of Engagement	0.325
Ultimate Tensile Strength	170000
Breaking Strength	
Tensile Area (in ²)	0.031805
Shear Area (in ²)	0.110992
Direct Load (lb/bolt)	0
Moment Load (lb/bolt)	15.72353
Total Shear Load (lb)	15.72353
Shear Stress (psi)	188.8855
Tensile Stress (psi)	786.0452
Von Mises Stress (psi)	851.4107
SF	199.6686

6.6 Blade Out FEA

Blade out occurs when one of the propeller blades suddenly comes off the rotor. The single blade would continue to rotate until power was cut off, but the single rotating blade would generate a problematic force. This force was derived using the center of mass of the single blade at specific speeds. This force would be in the plane of the rotor. At 4,000 rpm the maximum alternating in-plane load would be 142 pounds. At 6,000 rpm the maximum alternating in-plane load would be 320 pounds. Although the rotors should not be operating at speeds higher than 4,000 rpm, they are individually capable of going up to 6,000 rpm. So, the load used for the blade out analysis was the 320 pounds alternating in-plane load. Because this situation is very unlikely, the analysis only needs to show a SF of greater than 1 on yield. This would prove that, should blade out occur, the parts would not yield. Deflection is not considered in these studies. A refined mesh was used on these studies to ensure accurate results.

BLADE OUT STUDY 1: Vertical support beam – helicopter – forward load

MATERIALS: 17-4PH H900 – Yield Strength of 185 ksi.

APPLIED LOADS: Offset load applied at the two top holes – 320 pounds forward.
Gravitational load of component.
Weight from rotor assembly and linear actuator applied at top two holes and bottom two holes respectively.

FIXTURES: Slider/roller fixtures were applied along the faces of the beam towards the bottom, where the support beam would interface with the adjusting beam. Fixed at the bottom two holes.

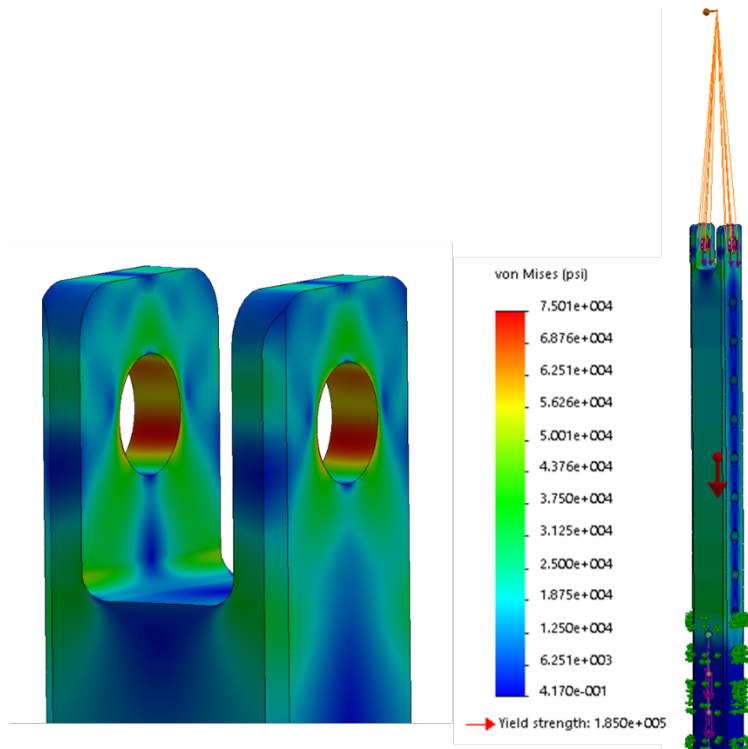


Figure 6.6.1. Blade Out Study 1 – vertical support beam, helicopter, FEA stress plot.

STRESS SAFETY FACTOR: 2.47

BLADE OUT STUDY 2: Vertical support beam – helicopter – side load

MATERIALS: 17-4PH H900 – Yield Strength of 185 ksi.

APPLIED LOADS: Offset load applied at the two top holes - 320 pounds towards the left.
Gravitational load of component.
Weight from rotor assembly and linear actuator applied at top two holes and bottom two holes respectively.

FIXTURES: Slider/roller fixtures were applied along the faces of the beam towards the bottom, where the support beam would interface with the adjusting beam. Fixed at the bottom two holes.

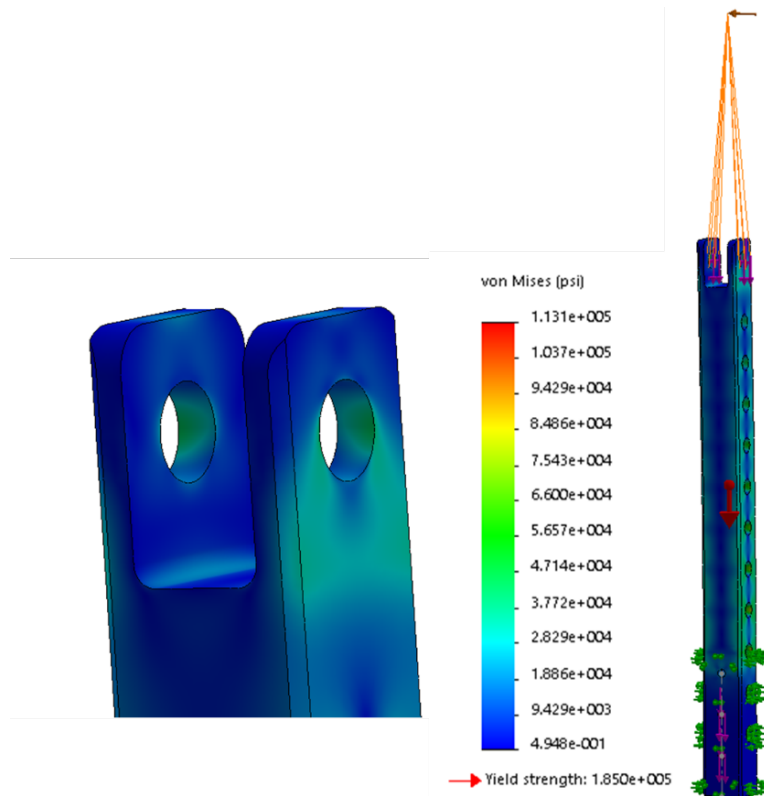


Figure 6.6.2. Blade Out Study 2 – vertical support beam, helicopter, FEA stress plot.

STRESS SAFETY FACTOR: 1.64

NOTES: For this study, there was a stress concentration at the point of application of the slider/roller fixture. It is very likely that this was a stress singularity and can be ignored. Even so, the SF is greater than 1.

BLADE OUT STUDY 3: Vertical support beam – airplane – downward load

MATERIALS: 17-4PH H900 – Yield Strength of 185 ksi.

APPLIED LOADS: Offset load applied at the two top holes – 320 pounds downward.
Gravitational load of component.
Weight from rotor assembly and linear actuator applied at top two holes and bottom two holes respectively.

FIXTURES: Slider/roller fixtures were applied along the faces of the beam towards the bottom, where the support beam would interface with the adjusting beam. Fixed at the bottom two holes.

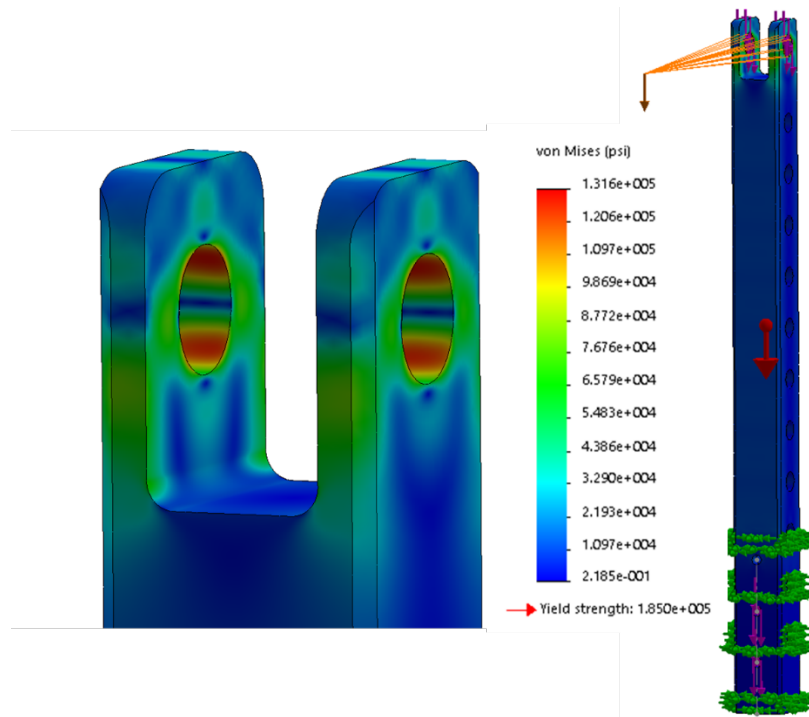


Figure 6.6.3. Blade Out Study 3 – vertical support beam, airplane, FEA stress plot.

STRESS SAFETY FACTOR: 1.4

BLADE OUT STUDY 4: Vertical support beam – airplane – side load

MATERIALS: 17-4PH H900 – Yield Strength of 185 ksi.

APPLIED LOADS: Offset load applied at the two top holes – 320 pounds left.
Gravitational load of component.
Weight from rotor assembly and linear actuator applied at top two holes and bottom two holes respectively.

FIXTURES: Slider/roller fixtures were applied along the faces of the beam towards the bottom, where the support beam would interface with the adjusting beam. Fixed at the bottom two holes.

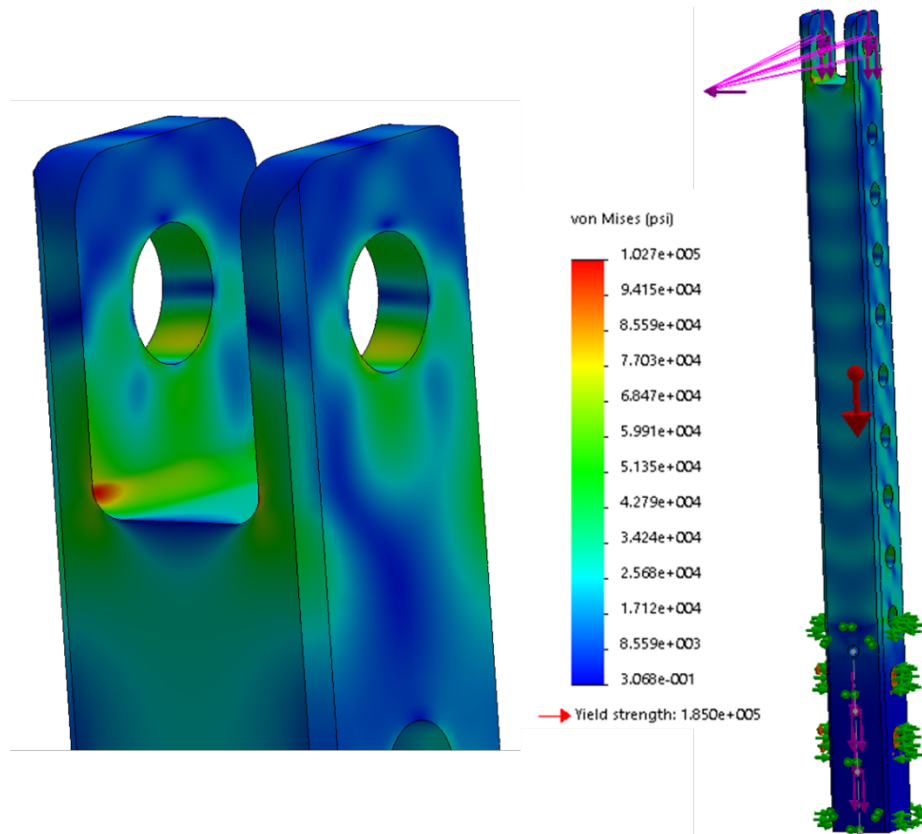


Figure 6.6.4. Blade Out Study 4 – vertical support beam, airplane, FEA stress plot.

STRESS SAFETY FACTOR: 1.8

BLADE OUT STUDY 5: Adjusting L-bracket – airplane – downward load

MATERIALS: 17-4PH H900 – Yield Strength of 185 ksi.

APPLIED LOADS: Offset load applied at the four top holes – 320 pounds downward.
Gravitational load of component.
Weight from rotor assembly, vertical support beam, and linear actuator applied at top four holes (10.57 pounds).

FIXTURES: Slider/roller fixtures were applied inside the L-bracket along the side where the L-bracket would interface with the lateral support beam. Does not account for vertical support beam that would also act as a slider fixture (thus a more conservative study).
Fixed at the two holes on the right side.

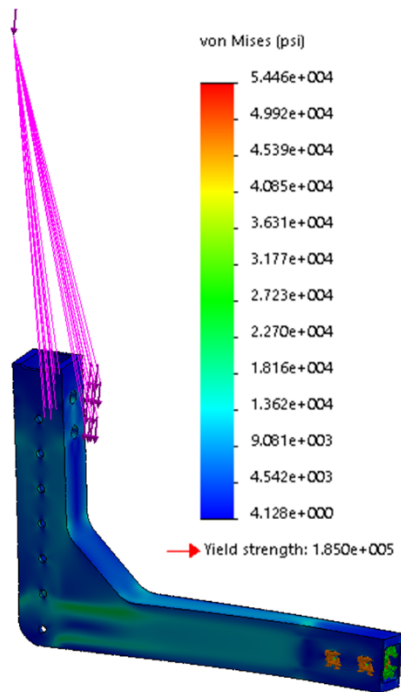


Figure 6.6.5. Blade Out Study 5 – adjusting L-bracket, airplane, stress plot.

STRESS SAFETY FACTOR: 3.4

NOTES: The case for an upward load yielded similar results with a SF of 3.4.

BLADE OUT STUDY 6: Adjusting L-bracket – airplane – side load

MATERIALS: 17-4PH H900 – Yield Strength of 185 ksi.

APPLIED LOADS: Offset load applied at the four top holes – 320 pounds left.
Gravitational load of component.
Weight from rotor assembly, vertical support beam, and linear actuator applied at top four holes.

FIXTURES: Slider/roller fixtures were applied inside the L-bracket along the side where the L-bracket would interface with the lateral support beam. Does not account for vertical support beam that would also act as a slider fixture (thus a more conservative study).
Fixed at the two holes on the right side.

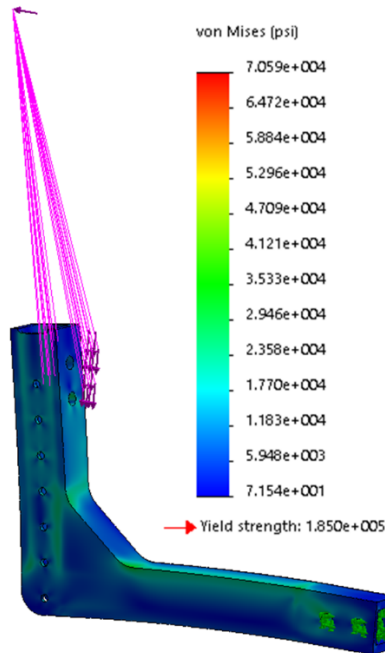


Figure 6.6.6. Blade Out Study 6 – adjusting L-bracket, airplane, stress plot.

STRESS SAFETY FACTOR: 2.62

NOTES: The case for the load going towards the right yielded the same SF of 2.62.

BLADE OUT STUDY 7: Adjusting L-bracket – helicopter – backward load

MATERIALS: 17-4PH H900 – Yield Strength of 185 ksi.

APPLIED LOADS: Offset load applied at the four top holes – 320 pounds backward.
Gravitational load of component.
Weight from rotor assembly, vertical support beam, and linear actuator applied at top four holes.

FIXTURES: Slider/roller fixtures were applied inside the L-bracket along the side where the L-bracket would interface with the lateral support beam. Does not account for vertical support beam that would also act as a slider fixture (thus a more conservative study).
Fixed at the two holes on the right side.

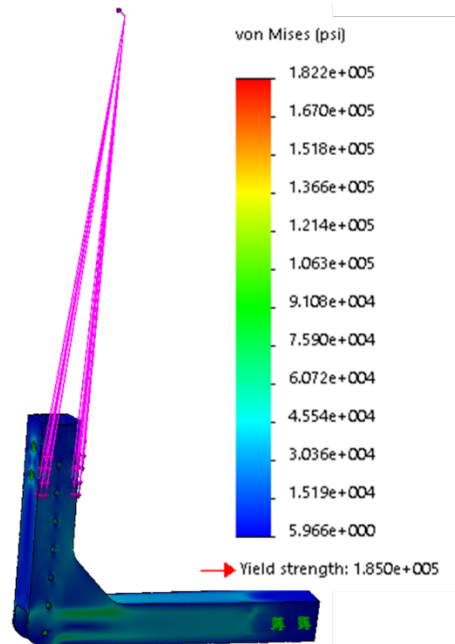


Figure 6.6.7. Blade Out Study 7 – adjusting L-bracket, helicopter, stress plot.

STRESS SAFETY FACTOR: 1.02

NOTES: The case for the load going towards the right yielded the same SF of 1.02. Recall that the fixtures do not include the vertical support beams. It should also be noted that the vertical support beams are more flexible than the L-brackets and will be taking more of the load.

BLADE OUT STUDY 8: Adjusting L-bracket – helicopter – left load

MATERIALS: 17-4PH H900 – Yield Strength of 185 ksi.

APPLIED LOADS: Offset load applied at the 4 top holes – 320 pounds left.
Gravitational load of component.
Weight from rotor assembly, vertical support beam, and linear actuator applied at top four holes.

FIXTURES: Slider/roller fixtures were applied inside the L-bracket along the side where the L-bracket would interface with the lateral support beam. Does not account for vertical support beam that would also act as a slider fixture (thus a more conservative study).
Fixed at the two holes on the right side.

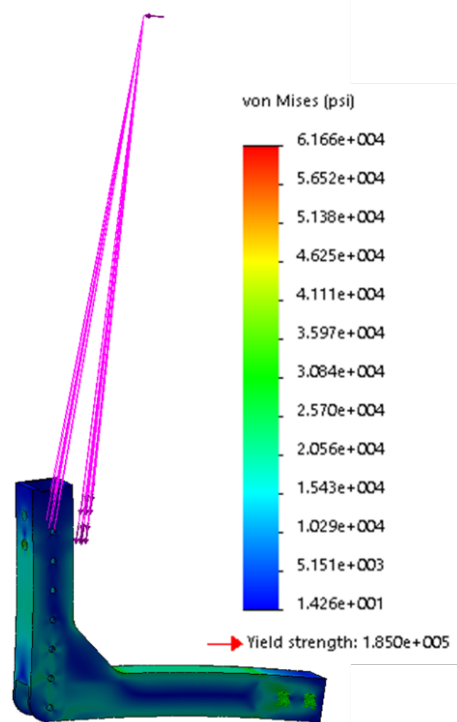


Figure 6.6.8. Blade Out Study 8 – adjusting L-bracket, helicopter, stress plot.

STRESS SAFETY FACTOR: 3.0

NOTES: The case for the load going towards the right yielded the same SF of 3.

Of all of the blade out scenarios, the worst cases were when the rotors were in helicopter mode with the load going backward, and with the rotors in airplane mode with the load going downward.